15 Simplest Extensions of the SM

15.1 Minimal Flavor Violation

15.1.1 Constrained Minimal Flavor Violation (CMFV)

Formulation

This is possibly the simplest class of extensions of the SM. It is defined pragmatically as follows [520]:

- The only source of flavor and CP violation is the CKM matrix. This implies that the only CP-violating phase is the KM phase. Moreover, it is assumed that CP-violating flavor blind phases, to be discussed later on, are absent.
- The only relevant operators in the effective Hamiltonian *below* the electroweak scale are the ones present within the SM.

Detailed expositions of phenomenological consequences of this NP scenario have been given already a long time ago in [521, 697, 870] and more recently in [388]. Here we will collect most important properties of this class of models and summarize their status.

We have seen in Chapter 6 that an elegant formulation of FCNC processes within the SM is the PBE in which the basic object is the set of seven gauge independent master functions in (6.29). They result from calculations of penguin and box diagrams within the SM and depend only on the top quark mass. This description of FCNC processes can be generalized in a straightforward manner to CMFV models by simply replacing in all SM formulas the master functions in (6.29) by the following seven master functions [521]

$$\boxed{S(\omega),\ X(\omega),\ Y(\omega),\ Z(\omega),\ E(\omega),\ D'(\omega),\ E'(\omega),} \tag{15.1}$$

where the variable ω collects the parameters of a given model. Two properties of these functions should be emphasized.

- They are *real* valued as the only complex phases reside in CKM factors that multiply these functions in effective Hamiltonians and flavor observables.
- They are flavor universal, as the full flavor dependence comes from the CKM factors.

These properties imply relations between various observables not only within a given meson system but also in particular between observables in different meson systems that are valid for the whole class of CMFV models and most importantly do not depend on any NP parameters. These relations are in fact the same as in the SM and as such do not

Downloaded from https://www.cambridge.org/core. UNIVERSIDAD AUTONOMA METROPOLITANA, on 17 Nov 2026 at 22:50:50, subject to the Cambridge Core terms of use, available at https://www.cambridge.org/core/terms. https://doi.org/10.1017/9781139524100.021

allow the distinction between various CMFV models that is only possible by means of observables that explicitly depend on the functions in (15.1). On the other hand violation of any of these relations by experimental data would automatically signal new sources of flavor and CP violation beyond CMFV framework and would be a problem for all models of this class.

As the SM contributions are included in the functions in (15.1) it is often useful to write

$$\boxed{S(\omega) = S_0(x_t) + \Delta S, \qquad X(\omega) = X_0(x_t) + \Delta X, \qquad Y(\omega) = Y_0 + \Delta Y,} \tag{15.2}$$

with analogous decomposition for the remaining four functions. The shifts ΔS, ΔX, and ΔY summarize the modifications of SM master functions by NP contributions.

This formulation tells us right away which master functions contribute to a given decay. We have, similar to the SM, the following correspondence between the most interesting FCNC processes and the master functions in the CMFV models

$K^0 - \bar{K}^0$-mixing (ε_K)	$S(\omega)$
$B^0_{d,s} - \bar{B}^0_{d,s}$-mixing ($\Delta M_{s,d}$)	$S(\omega)$
$K \to \pi\nu\bar{\nu}$, $B \to X_{d,s}\nu\bar{\nu}$	$X(\omega)$
$K_L \to \mu\bar{\mu}$, $B_{d,s} \to \ell^+\ell^-$	$Y(\omega)$
$K_L \to \pi^0 e^+ e^-$	$Y(\omega)$, $Z(\omega)$, $E(\omega)$
ε', Nonleptonic $\Delta B = 1$, $\Delta S = 1$	$X(\omega)$, $Y(\omega)$, $Z(\omega)$, $E(\omega)$
$B \to X_s\gamma$	$D'(\omega)$, $E'(\omega)$
$B \to X_s$ gluon	$E'(\omega)$
$B \to X_s\ell^+\ell^-$	$Y(\omega)$, $Z(\omega)$, $E(\omega)$, $D'(\omega)$, $E'(\omega)$

At this point, the impact of QCD corrections on this formulation should be mentioned. As the operator structure is the same as in the SM, the renormalization group evolution from scale $O(m_t)$ down to low energies is precisely the same as in the SM. That is, the functions in (15.1) enter the Wilson coefficients at the matching scale $\mu = O(\mu_{ew})$ with μ_{ew} being any scale like m_t, M_W, or M_Z. But the QCD corrections to the shifts in (15.2) at the matching scale and at all scales above it differ from the ones in the SM and vary from model to model. This model dependence of QCD corrections can be significant between models in which NP enters at vastly different scales as then the size of renormalization group effects in these models is different. But the important feature of these QCD corrections is that they are flavor blind. Therefore, even if the effect of QCD corrections on the shifts in (15.2), as the shifts themselves, is model dependent, the flavor universality of these functions is retained. The breakdown of flavor universality of the master functions could be caused in principle by electroweak corrections and Yukawa couplings that are not flavor blind. But these corrections are not considered in [521, 697, 870] and will be assumed to be small until we discuss the formulation of MFV as an effective theory that is based on flavor symmetries and that goes beyond CMFV.

Under these assumptions the preceding table means that the observables like branching ratios for various decays of K and $B_{s,d}$ mesons, mass differences $\Delta M_{d,s}$ in $B^0_{d,s} - \bar{B}^0_{d,s}$-mixing, and the CP violation parameters ε and ε' within CMFV models, all can be to a

Downloaded from https://www.cambridge.org/core. UNIVERSIDAD AUTONOMA METROPOLITANA, on 17 Nov 2026 at 22:50:50, subject to the Cambridge Core terms of use, available at https://www.cambridge.org/core/terms. https://doi.org/10.1017/9781139524100.021

very good approximation entirely expressed in terms of the corresponding master functions and the relevant CKM factors.

CMFV Relations as Standard Candles of Flavor Physics

The implications of this framework are so stringent that they could be considered as standard candles of flavor physics. Of particular importance are the relations that do not depend on the master functions and involve only CKM parameters and nonperturbative parameters. A review of these relations is given in [521]. Some of them appeared already in previous chapters but it is useful to collect them here at one place. We will see that several more involved NP scenarios violate these relations.

We have:

1. $S_{\psi K_S}$ and $S_{\psi\phi}$ are as in the SM and therefore given by

$$\boxed{S_{\psi K_S} = \sin(2\beta), \qquad S_{\psi\phi} = \sin(2|\beta_s|),} \tag{15.3}$$

with

$$V_{td} = |V_{td}|e^{-i\beta}, \qquad V_{ts} = -|V_{ts}|e^{-i\beta_s}. \tag{15.4}$$

2. While ΔM_d and ΔM_s can differ from the SM values, their ratio is as in the SM

$$\boxed{\left(\frac{\Delta M_d}{\Delta M_s}\right)_{\rm CMFV} = \left(\frac{\Delta M_d}{\Delta M_s}\right)_{\rm SM}.} \tag{15.5}$$

Moreover, this ratio is given entirely in terms of CKM parameters and the nonperturbative parameter ξ:

$$\boxed{\frac{\Delta M_d}{\Delta M_s} = \frac{m_{B_d}}{m_{B_s}}\frac{1}{\xi^2}\left|\frac{V_{td}}{V_{ts}}\right|^2, \qquad \xi = \frac{\sqrt{\hat{B}_s}F_{B_s}}{\sqrt{\hat{B}_d}F_{B_d}}.} \tag{15.6}$$

3. These two properties allow the construction of the *Universal Unitarity Triangle* (UUT) of models with CMFV that uses as inputs the measured values of $S_{\psi K_S}$ and $\Delta M_s/\Delta M_d$ [520]. We will present this construction later. In this manner the angle γ and the ratio $|V_{ub}|/|V_{cb}|$ can be determined and compared with their tree-level determinations.
4. The flavor universality of $S(\omega)$ allows to derive universal relations between ε_K and $\Delta M_{s,d}$ that depend only on $|V_{us}|$, $|V_{cb}|$, known from tree-level decays, and nonperturbative parameters entering the evaluation of ε_K and $\Delta M_{s,d}$ [27, 697, 871].
5. For fixed CKM parameters determined in tree-level decays, $|\varepsilon_K|$, ΔM_s and ΔM_d, if modified, can only be *enhanced* relative to SM predictions [872]. Moreover, this happens in a correlated manner [871]. This follows from the lower bound [872]

$$\boxed{S(\omega) \geq S_0(x_t) = 2.32} \tag{15.7}$$

Downloaded from https://www.cambridge.org/core. UNIVERSIDAD AUTONOMA METROPOLITANA, on 17 Nov 2026 at 22:50:50, subject to the Cambridge Core terms of use, available at https://www.cambridge.org/core/terms. https://doi.org/10.1017/9781139524100.021

with $S_0(x_t)$ given in (6.17). We will see later that this particular correlation between ε_K, ΔM_s, and ΔM_d, appears to be in variance with the data hinting at the presence of NP beyond the CMFV framework in $\Delta F = 2$ transitions.

6. Two other interesting universal relations in models with CMFV are

$$\boxed{\frac{\mathcal{B}(B \to X_d \nu\bar{\nu})}{\mathcal{B}(B \to X_s \nu\bar{\nu})} = \left|\frac{V_{td}}{V_{ts}}\right|^2,} \tag{15.8}$$

$$\boxed{\frac{\mathcal{B}(B_d \to \mu^+\mu^-)}{\mathcal{B}(B_s \to \mu^+\mu^-)} = \frac{\tau(B_d)}{\tau(B_s)} \frac{m_{B_d}}{m_{B_s}} \frac{F_{B_d}^2}{F_{B_s}^2} \left|\frac{V_{td}}{V_{ts}}\right|^2.} \tag{15.9}$$

7. Eliminating $|V_{td}/V_{ts}|$ from (15.6) and (15.9) allows to obtain another universal relation within the CMFV models [503]

$$\boxed{\frac{\mathcal{B}(B_s \to \mu^+\mu^-)}{\mathcal{B}(B_d \to \mu^+\mu^-)} = \frac{\hat{B}_d}{\hat{B}_s} \frac{\tau(B_s)}{\tau(B_d)} \frac{\Delta M_s}{\Delta M_d}} \tag{15.10}$$

that does not involve F_{B_q} and CKM parameters and consequently contains smaller hadronic and parametric uncertainties than the preceding formulas. It involves only measurable quantities except for the ratio $\hat{B}_s/\hat{B}_d$ that is known from lattice calculations already with precision of roughly ±1% [522]. Consequently the r.h.s. of this equation is already very precisely known. This should allow to identify possible NP in $B_{s,d} \to \mu^+\mu^-$ decays and also in $\Delta M_{s,d}$ beyond the CMFV framework even if it was only at the level of 20% of the SM contributions. Therefore the relation (15.10) should allow a precision test of the CMFV framework. Unfortunately, because of difficulties in measuring precisely $\mathcal{B}(B_d \to \mu^+\mu^-)$ it could take even a decade to perform this test.

8. The fact that all amplitudes for FCNC processes within the CMFV framework can be expressed in terms of seven *real* and *universal* master loop functions listed in (15.1) implies numerous correlations between various observables. See Chapter 19.

Construction of the UUT

There are many ways to construct UT but the construction of the UUT must make sure that it does not involve any NP parameters. This is achieved by using

$$\frac{\Delta M_d}{\Delta M_s}, \qquad S_{\psi K_S}. \tag{15.11}$$

We present here the most recent construction of the UUT, which is an update of the one in [388]. From (15.6) we obtain first

$$\frac{|V_{td}|}{|V_{ts}|} = \xi \sqrt{\frac{m_{B_s}}{m_{B_d}}} \sqrt{\frac{\Delta M_d}{\Delta M_s}} = 0.2046 \pm 0.0033, \tag{15.12}$$

where we have used [873]

$$\xi = 1.206 \pm 0.019. \tag{15.13}$$

Downloaded from https://www.cambridge.org/core. UNIVERSIDAD AUTONOMA METROPOLITANA, on 17 Nov 2026 at 22:50:50, subject to the Cambridge Core terms of use, available at https://www.cambridge.org/core/terms. https://doi.org/10.1017/9781139524100.021

On the other hand, from

$$S_{\psi K_S} = \sin 2\beta = 0.699 \pm 0.017, \tag{15.14}$$

we find

$$\beta = (22.17 \pm 0.67)^\circ. \tag{15.15}$$

Now, precisely as in the SM

$$|V_{td}| = |V_{us}||V_{cb}|R_t, \qquad |V_{ts}| = \eta_R |V_{cb}| \tag{15.16}$$

with R_t being one of the sides of the unitarity triangle (see Figure 2.4) and

$$\eta_R = 1 - |V_{us}|\xi \sqrt{\frac{\Delta M_d}{\Delta M_s}} \sqrt{\frac{m_{B_s}}{m_{B_d}}} \cos\beta + \frac{\lambda^2}{2} + O(\lambda^4) = 0.9826, \tag{15.17}$$

where we have used the value of β in (15.15). Thus using (15.12) and (15.16) we determine very precisely

$$R_t = 0.741\, \xi = 0.893 \pm 0.013. \tag{15.18}$$

Having determined β and R_t, we can construct the UUT with

$$\bar{\rho} = 0.172 \pm 0.013, \qquad \bar{\eta} = 0.332 \pm 0.011. \tag{15.19}$$

We observe that these values differ somewhat from the UT obtained in global fits [397, 398], with the latter exhibiting smaller $\bar{\rho}$ and larger $\bar{\eta}$ values. See Table 8.1. Subsequently, using the relation

$$R_b = \left(1 - \frac{\lambda^2}{2}\right) \frac{1}{\lambda} \left|\frac{V_{ub}}{V_{cb}}\right| = \sqrt{1 + R_t^2 - 2R_t \cos\beta} \tag{15.20}$$

allows a very precise determination of the ratio

$$\frac{|V_{ub}|}{|V_{cb}|} = 0.0864 \pm 0.0025. \tag{15.21}$$

This implies a strict correlation between $|V_{ub}|$ and $|V_{cb}|$ that can be compared with the tree-level determinations of both CKM elements once the extraction of $|V_{ub}|$ improves. For our nominal values of $|V_{ub}|$ and $|V_{cb}|$ in (8.154) we obtain 0.088 in good agreement with (15.21). This does not mean that CMFV is in good shape as we will see soon.

We can also determine the angle γ in the UUT using the relation

$$\cot\gamma = \frac{1 - R_t \cos\beta}{R_t \sin\beta}. \tag{15.22}$$

We extract

$$\gamma = (63.0 \pm 2.1)^\circ, \tag{15.23}$$

which is by 2σ below the tree-level value in (8.155). Using instead of ξ in (15.13) the recent RBC-UKQCD result $\xi = 1.1853 \pm 0.0054^{+0.0116}_{-0.0156}$ [522], one obtains $\gamma = (60.7 \pm 1.5)^\circ$. On the other hand, with the recent value from QCD sum rules of $\xi = 1.2014^{+0.0065}_{-0.0072}$ [523] one finds $\gamma = (62.5 \pm 0.9)^\circ$.

Downloaded from https://www.cambridge.org/core. UNIVERSIDAD AUTONOMA METROPOLITANA, on 17 Nov 2026 at 22:50:50, subject to the Cambridge Core terms of use, available at https://www.cambridge.org/core/terms. https://doi.org/10.1017/9781139524100.021

Finally, from (15.15) and (15.23) we determine the angle α in the unitarity triangle

$$\alpha = (95.5 \pm 2.2)^\circ. \tag{15.24}$$

It should be emphasized that the results in (15.15), (15.18), (15.21), (15.23), and (15.24) are independent of $S(\omega)$ and therefore valid for all CMFV models.

Tension between $\Delta M_{s,d}$ and ε_K

The only CKM parameter left is $|V_{cb}|$. Following [388] we can use two strategies to find it:

S_1: ΔM_s strategy in which the experimental value of ΔM_s is used to determine $|V_{cb}|$ as a function of $S(\omega)$, and ε_K is then a derived quantity.

S_2: ε_K strategy in which the experimental value of ε_K is used, while ΔM_s is then a derived quantity, and ΔM_d follows from the determined UUT.

If the concept of CMFV works $|V_{cb}|$ and other elements of the CKM matrix obtained from these two strategies should be equal to each other. But their values will depend on $S(\omega)$, which is bounded from below in (15.7). One finds then:

- The lower bound in (15.7) implies in S_1 *upper bounds* on $|V_{ts}|$, $|V_{td}|$, $|V_{ub}|$, and $|V_{cb}|$, which are saturated in the SM, and in turn allows to derive an *upper bound* on ε_K in CMFV models that is saturated in the SM but turns out to be significantly *below* the data

$$|\varepsilon_K| \le (1.61 \pm 0.25) \cdot 10^{-3}. \tag{15.25}$$

- The lower bound in (15.7) implies in S_2 also *upper bounds* on $|V_{ts}|$, $|V_{td}|$, $|V_{ub}|$, and $|V_{cb}|$, which are saturated in the SM. However, the $S(\omega)$ dependence of these elements determined in this manner differs from the one obtained in S_1, which in turn allows to derive *lower bounds* on $\Delta M_{s,d}$ in CMFV models that are reached in the SM but turn out to be significantly *above* the data

$$\Delta M_s \ge (21.4 \pm 1.8)\,\text{ps}^{-1}, \qquad \Delta M_d \ge (0.608 \pm 0.062)\,\text{ps}^{-1}. \tag{15.26}$$

The implications on the CKM parameters are exhibited in Table 15.1. We observe that the results obtained using strategies S_1 and S_2 are rather different. Whether these tensions remain when the lattice results become very precise remains to be seen. But also the inclusion of $|V_{ub}|$, $|V_{cb}|$, and γ from tree-level decays will help in identifying possible NP at work.

Table 15.1 Upper bounds on CKM elements in units of 10^{-3} and of λ_t in units of 10^{-4} obtained using strategies S_1 and S_2 as explained in the text. We set $S(v) = S_0(x_t)$.

S_i	$\lvert V_{ts}\rvert$	$\lvert V_{td}\rvert$	$\lvert V_{cb}\rvert$	$\lvert V_{ub}\rvert$	$\text{Im}\lambda_t$	$\text{Re}\lambda_t$
S_1	38.9(13)	7.95(29)	39.5(1.3)	3.41(15)	1.20(8)	−2.85(19)
S_2	42.7(12)	8.74(27)	43.4(1.2)	3.75(15)	1.44(8)	−3.44(19)

Downloaded from https://www.cambridge.org/core. UNIVERSIDAD AUTONOMA METROPOLITANA, on 17 Nov 2026 at 22:50:50, subject to the Cambridge Core terms of use, available at https://www.cambridge.org/core/terms. https://doi.org/10.1017/9781139524100.021

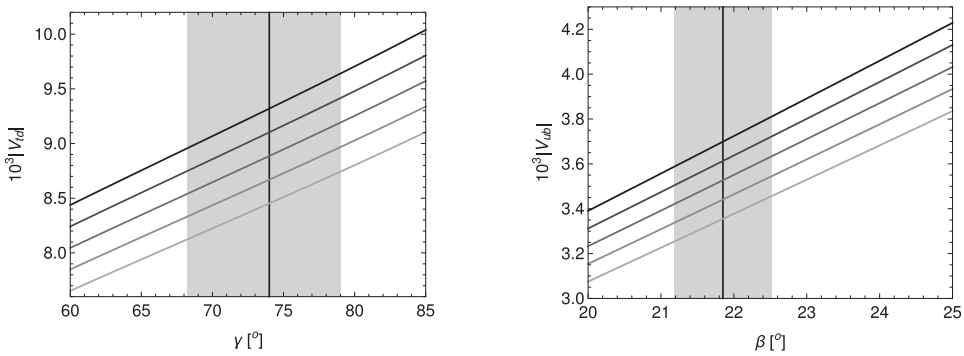


Figure 15.1 Left: $|V_{td}|$ as function of γ, for different values of $|V_{cb}|$. Right: $|V_{ub}|$ as function of β, for different values of $|V_{cb}|$. From bottom to top: $|V_{cb}| = 39 \cdot 10^{-3}, 40 \cdot 10^{-3}, 41 \cdot 10^{-3}, 42 \cdot 10^{-3}, 43 \cdot 10^{-3}$. From [874].

Emerging ΔM_d-Anomaly, the Angle γ, and $|V_{cb}|$

As we discussed already in Chapter 3, most recent tree-level measurements of $|V_{cb}|$ favor its high value and consequently no ε_K anomaly. As then NP is expected in $\Delta M_{s,d}$, it appears as a better strategy to replace their ratio by the angle γ and instead treat $\Delta M_{s,d}$ as outputs being functions of γ, β, and $|V_{cb}|$ [874]. The four fundamental CKM parameters used to determine the remaining entries in the CKM matrix are then

$$\boxed{|V_{us}|, \qquad |V_{cb}|, \qquad \gamma, \qquad \beta.} \tag{15.27}$$

In Figure 15.1 we show $|V_{td}|$ as a function of γ and $|V_{ub}|$ as a function of β for different values of $|V_{cb}|$. The dependences of $|V_{td}|$ on β and of $|V_{ub}|$ on γ are very small. These plots will allow to monitor the values of $|V_{td}|$ and $|V_{ub}|$ that enter various observables as the uncertainties of γ, β, and $|V_{cb}|$ will shrink with time.

In Figure 15.2 we show in the left panel ΔM_d and ΔM_s normalized to their experimental values. Evidently, for central values of all parameters, ΔM_d differs by roughly 30% from the data while in the case of ΔM_s the corresponding difference amounts only to 12%. But the uncertainties in other parameters like $|V_{cb}|$ and the hadronic parameters are still significant. However, we expect that in the coming years these uncertainties will be reduced by much so that a possible ΔM_d anomaly will be better seen.

In the right panel of Figure 15.2 we show the ratio $\Delta M_s/\Delta M_d$ as a function of γ. The dependence on $|V_{cb}|$ cancels in this ratio, and the error on ξ in (15.13) is much smaller than the hadronic uncertainties affecting the plot in the left panel of Figure 15.2. Consequently the disagreement of the ratio in question with the data, shown as a horizontal line at 35.1, is clearly visible and expresses the problem of CMFV models and those based on the $U(2)^3$ symmetry as discussed later in this book.

As discussed in [874], in the presence of only left-handed currents, the required suppression of ΔM_d and to a lesser extent ΔM_s implies large new CP-violating phases and significant deviations from the SM in CP-asymmetries of radiative and rare $b \to d$ and $b \to s$ decays.

Downloaded from https://www.cambridge.org/core. UNIVERSIDAD AUTONOMA METROPOLITANA, on 17 Nov 2026 at 22:50:50, subject to the Cambridge Core terms of use, available at https://www.cambridge.org/core/terms. https://doi.org/10.1017/9781139524100.021

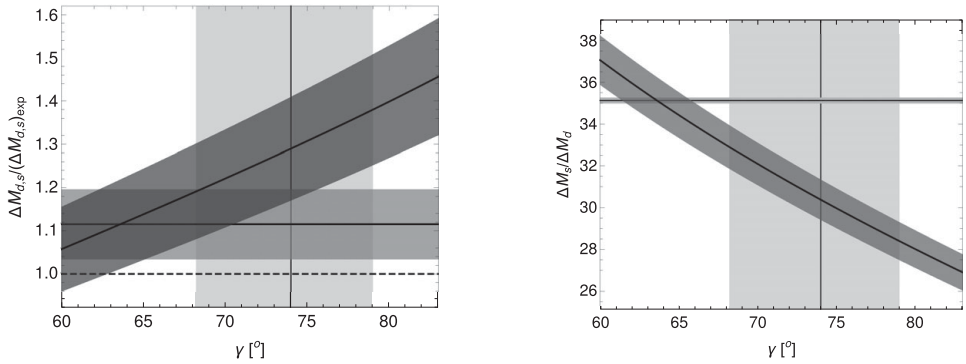


Figure 15.2 Left: ΔM_d (dark gray) and ΔM_s (light gray) as functions of γ, normalized to their experimental values. The 1σ-band includes all other uncertainties. Right: $\Delta M_s/\Delta M_d$ as function of γ. From [874].

In the presence of both left- and right-handed couplings, on the other hand, the suppression of ΔM_d is much easier to achieve without introducing large CP-violating phases. In this context probably most interesting are models in which the SMEFT operator O_{Hd} involving right-handed flavor-violating couplings to down-quarks is generated at the NP scale, that is the Scenario I discussed in Section 14.4.1. We saw there that the renormalization group evolution to low-energy scales involving also left-handed currents present already within the SM generates left-right $\Delta F = 2$ operators representing FCNC mediated by the Z boson.

An explicit realization of such an NP scenario is provided by models with vector-like quarks with an additional U(1) gauge symmetry so that both tree-level Z and Z' exchanges are present, and in some models of this type also box diagram contributions with vector-like quarks, Higgs and other scalar and pseudoscalar exchanges are important [666]. We will discuss models with vector-like quarks in Section 16.3.2.

In any case, this anomaly, if confirmed by improved measurements of the angle γ, will have implications for observables sensitive to $b \to d$ transitions like $b \to d\ell^+\ell^-$ and $b \to d\nu\bar{\nu}$ which will be explored by Belle II. It will open a new oasis of NP, analogous to the one related to the recent anomalies in $b \to s\ell^+\ell^-$ and their implications for $b \to s\nu\bar{\nu}$ transitions. Depending on the NP flavor structure, it could also have implications for $K^+ \to \pi^+\nu\bar{\nu}$ and $K_{\rm L} \to \pi^0\nu\bar{\nu}$.

New Physics in $\Delta\Gamma_{d,s}$

In this book, as far as particle-antiparticle mixing is concerned we will mainly discuss NP contributions to ΔM_K and $\Delta M_{d,s}$ but NP could also affect $\Delta\Gamma_{d,s}$. Good references here are [387, 393], where collection of references to earlier papers can be found. One finds that NP can affect $\Delta\Gamma_d$ by even 100%, as pointed out in [875] and analyzed in detail in [393]. NP related to the violation of CKM unitarity and automatically beyond the MFV framework could be responsible for sizable modifications of $\Delta\Gamma_d$ that could be measured through semileptonic CP asymmetries in B_d^0 decays. Also effective operators of the form

Downloaded from https://www.cambridge.org/core. UNIVERSIDAD AUTONOMA METROPOLITANA, on 17 Nov 2026 at 22:50:50, subject to the Cambridge Core terms of use, available at https://www.cambridge.org/core/terms. https://doi.org/10.1017/9781139524100.021

$(\bar{d}b)(\tau^+\tau^-)$ could be important here with implications for rare B_d^0 decays with $(\tau^+\tau^-)$ in the final state. Much smaller NP effects are expected in $\Delta\Gamma_s$ because of various constraints from flavor observables. Improved data from LHCb and Belle II will certainly shed light on this issue.

15.1.2 Minimal Flavor Violation as an Effective Field Theory (MFV)

Preliminaries

More generally the formulation of MFV with the help of global symmetries present in the limit of vanishing Yukawa couplings as formulated in [624] is elegant and useful. See also [876] for a similar formulation that goes beyond the MFV. Other profound discussions of various aspects of MFV can be found in [877–882]. Excellent compact formulations of MFV as an effective theory has been given by Isidori [883] and Nir [884]. We also recommend the reviews in [623, 885], where phenomenological aspects of MFV are summarized. In what follows we will first make general comments on this framework. Subsequently we will provide very brief mathematical formulation of MFV following [883, 884].

In short the hypothesis of MFV amounts to assuming that the Yukawa couplings are the only sources of the flavor violation and of CP-violation. The phenomenological implications of the MFV hypothesis formulated in this grander manner than the CMFV formulation given earlier can be found model independently by using an effective field theory approach (EFT) [624] in the spirit of SMEFT but more constrained that the latter. In this framework the SM Lagrangian is supplemented by all higher-dimension operators consistent with the MFV hypothesis, built using the Yukawa couplings as spurion fields. The NP effects in this framework are then parametrized in terms of a few *flavor-blind* free parameters and SM Yukawa couplings that are solely responsible for flavor violation and also CP violation if these flavor-blind parameters are chosen to be *real* quantities as done in [624]. This approach naturally suppresses FCNC processes to the level observed experimentally even in the presence of new particles with masses of a few hundred GeV. It also implies specific correlations between various observables, which in many cases are identical to the CMFV ones that we listed earlier. Some differences will be mentioned later.

Yet, it should be stressed that the MFV symmetry principle in itself does not forbid the presence of *flavor-blind* CP-violating sources [877, 879–882, 886–890] that make effectively the flavor-blind free parameters *complex* quantities having flavor-blind phases (FBPs). These phases can in turn enhance the electric dipole moments (EDMs) of various particles and atoms and in the interplay with the CKM matrix can have also profound impact on flavor-violating observables, in particular the CP-violating ones. In the context of the so-called aligned 2HDM model such effects have also been emphasized in [891].

The introduction of flavor-blind CPV phases compatible with the MFV symmetry principle turns out to be a very interesting setup [877, 879, 881, 882, 889]. Moreover, it was very popular around 2007–2009 when experiments at Tevatron indicated a large new CP phase in B_s^0–$\bar{B}_s^0$ mixing, in contradiction with very small phase β_s in the CKM matrix. In particular, as noted in [881], a large new phase in B_s^0–$\bar{B}_s^0$ mixing could in principle be

Downloaded from https://www.cambridge.org/core. UNIVERSIDAD AUTONOMA METROPOLITANA, on 17 Nov 2026 at 22:50:50, subject to the Cambridge Core terms of use, available at https://www.cambridge.org/core/terms. https://doi.org/10.1017/9781139524100.021

obtained in a MFV framework if additional FBPs are present. This is so-called General MFV (MFV).

As of 2020 we know from the LHCb experiment that the new phases in B_s^0–$\bar{B}_s^0$ mixing, if present, must be rather small. See Section 8.5.3. Consequently, also the role of flavor-blind phases in describing data decreased significantly relative to the one they played ten years ago. However, the full assessment of the importance of these phases will only be possible when the CP-violation in B_s^0–$\bar{B}_s^0$ mixing will be precisely measured and also the bounds on electric dipole moments improve. Therefore, we just briefly summarize some lessons from past studies that could turn out to be useful in the future.

In a sense small new CP phases in B_s^0–$\bar{B}_s^0$ mixing were expected in the ordinary MSSM with MFV, as shown in [529, 892]. This is due to the suppression in the MSSM of effective operators with several Yukawa insertions. Sizable couplings for these operators are necessary both to have an effective large CP-violating phase in B_s^0–$\bar{B}_s^0$ mixing and, at the same time, to evade bounds from other observables, such as $B_s \to \mu^+\mu^-$ and $B \to X_s\gamma$. However, it could be realized in different underlying models, such as the uplifted MSSM, as pointed out in [893], in the so-called beyond-MSSM scenarios [894, 895] and in the 2HDM with MFV and FBPs, the so-called 2HDM$_{\overline{\text{MFV}}}$ [896], which we will briefly describe in Section 15.2. The interested reader should look up these papers even if presently they do not play such an important role as they played around the year 2010. But they could come back when the size of new CP phases, not only in B physics, will be precisely known. An excellent review of 2HDMs can be found in [897].

Basic Structure

To be more explicit let us recall the gauge part of the SM Lagrangian

$$\boxed{\mathcal{L}^{\text{SM}}_{\text{gauge}} = \sum_{i=1\ldots3} \sum_{\psi=Q_L^i\ldots E_R^i} \bar{\psi} i \not{D} \psi - \frac{1}{4} \sum_{a=1\ldots8} G^a_{\mu\nu} G^a_{\mu\nu} - \frac{1}{4} \sum_{a=1\ldots3} W^a_{\mu\nu} W^a_{\mu\nu} - \frac{1}{4} B_{\mu\nu} B_{\mu\nu}} \tag{15.28}$$

and the fermion content consisting of five fields with different quantum numbers under the gauge group:

$$Q_L^i(3,2)_{+1/6}\,,\quad U_R^i(3,1)_{+2/3}\,,\quad D_R^i(3,1)_{-1/3}\,,\quad L_L^i(1,2)_{-1/2}\,,\quad E_R^i(1,1)_{-1}\,, \tag{15.29}$$

with $(i = 1, 2, 3)$ denoting different generations. The different numbers in parentheses indicate how SM fermions transform under $\text{SU}(3)_C$ and $\text{SU}(2)_L$ groups. The last numbers represent Y of $\text{U}(1)_Y$.

In the absence of the Higgs and Yukawa interactions, the Lagrangian in (15.28) has large global flavor symmetry $\text{U}(3)^5$ group or equivalently

$$\boxed{\mathcal{G}_{\text{flavor}} = \text{U}(1)^5 \times \mathcal{G}_q \times \mathcal{G}_\ell\,,} \tag{15.30}$$

Downloaded from https://www.cambridge.org/core. UNIVERSIDAD AUTONOMA METROPOLITANA, on 17 Nov 2026 at 22:50:50, subject to the Cambridge Core terms of use, available at https://www.cambridge.org/core/terms. https://doi.org/10.1017/9781139524100.021

corresponding to the independent unitary rotations in flavor space of the five fermion fields in (15.29). The nonabelian factors are

$$\mathcal{G}_q = \mathrm{SU}(3)_{Q_L} \times \mathrm{SU}(3)_{U_R} \times \mathrm{SU}(3)_{D_R}, \qquad \mathcal{G}_\ell = \mathrm{SU}(3)_{L_L} \otimes \mathrm{SU}(3)_{E_R} \ . \tag{15.31}$$

The five U(1) subgroups can be identified as follows

$$\mathrm{U}(1)^5 = \mathrm{U}(1)_B \times \mathrm{U}(1)_L \times \mathrm{U}(1)_Y \times \mathrm{U}(1)_{\mathrm{PQ}} \times \mathrm{U}(1)_E \tag{15.32}$$

that is with baryon number (B), lepton number (L), and hypercharge (Y), which are respected by the Yukawa interactions. The two remaining U(1) groups can be identified with the Peccei-Quinn symmetry whereby the Higgs and D_R, E_R fields have opposite charges, and with a global rotation of E_R only.

While $\mathrm{U}(1)_B$, $\mathrm{U}(1)_L$, and $\mathrm{U}(1)_Y$ are unaffected by Yukawa interactions, the nonabelian groups $\mathcal{G}_q$ and $\mathcal{G}_\ell$ are explicitly broken by them. Indeed

$$-\mathcal{L}^{\mathrm{SM}}_{\mathrm{Yukawa}} = Y_d^{ij} \bar{Q}^i_L \phi D^j_R + Y_u^{ij} \bar{Q}^i_L \tilde{\phi} U^j_R + Y_e^{ij} \bar{L}^i_L \phi E^j_R + \mathrm{h.c.} \qquad (\tilde{\phi} = i\tau_2 \phi^\dagger) \tag{15.33}$$

breaks explicitly $\mathcal{G}_q$ and $\mathcal{G}_\ell$ because the Yukawa couplings $Y_{d,u,e}$ are not proportional to a unit matrix because of the known mass spectrum of quarks and leptons.

The MFV hypothesis as formulated in [624] is then based on the assumption that Y_d and Y_u are the only sources of flavor symmetry breaking not only in the SM but also beyond it. On the technical side to implement this hypothesis in a consistent manner, one assumes that $\mathcal{G}_q$ is a good symmetry and promotes first $Y_{u,d}$ to be nondynamical fields (*spurions*) with nontrivial transformation properties under $\mathcal{G}_q$:

$$Y_u \sim (3, \bar{3}, 1) \ , \qquad Y_d \sim (3, 1, \bar{3}) \ . \tag{15.34}$$

In this manner also the Yukawa Lagrangian is invariant under $\mathcal{G}_q$. Once these Yukawas take their background values, that is their SM values, the symmetry $\mathcal{G}_q$ is broken.

Within an effective-theory approach to physics beyond the SM, an effective theory satisfies the criterion of MFV in the quark sector if all higher-dimensional operators, constructed from SM and Y fields, are invariant under CP and (formally) under the flavor group $\mathcal{G}_q$ [624].

Strictly speaking one should then consider operators with arbitrary powers of the (dimensionless) Yukawa fields. But fortunately except for top Yukawa coupling all the eigenvalues of the Yukawa matrices are small and also off-diagonal elements of the CKM matrix are strongly suppressed so that

$$\left[Y_u (Y_u)^\dagger\right]^n_{i \neq j} \ \approx \ y_t^n V^*_{it} V_{tj} \ . \tag{15.35}$$

Then, in the limit where we neglect light quark masses, the leading $\Delta F = 2$ and $\Delta F = 1$ FCNC amplitudes get exactly the same CKM suppression as in the SM [883]:

$$\mathcal{A}(d^i \to d^j)_{\mathrm{MFV}} = (V^*_{tj} V_{ti}) \ \mathcal{A}^{(\Delta F=1)}_{\mathrm{SM}} \left[1 + a_1 \frac{16\pi^2 M_W^2}{\Lambda^2}\right] , \tag{15.36}$$

$$\mathcal{A}(M_{ij} - \bar{M}_{ij})_{\mathrm{MFV}} = (V^*_{tj} V_{ti})^2 \mathcal{A}^{(\Delta F=2)}_{\mathrm{SM}} \left[1 + a_2 \frac{16\pi^2 M_W^2}{\Lambda^2}\right] , \tag{15.37}$$

Downloaded from https://www.cambridge.org/core. UNIVERSIDAD AUTONOMA METROPOLITANA, on 17 Nov 2026 at 22:50:50, subject to the Cambridge Core terms of use, available at https://www.cambridge.org/core/terms. https://doi.org/10.1017/9781139524100.021

where the $\mathcal{A}_{\rm SM}^{(i)}$ are the SM loop amplitudes and the a_i are $O(1)$ *real* parameters. The a_i depend on the specific operator considered but are *flavor independent.* This implies the same relative correction in $s \to d$, $b \to d$, and $b \to s$ transitions, and the structure is very similar to the one in CMFV models.

Yet, one should stress that MFV as formulated here is, in contrast to CMFV, based on a renormalization-group-invariant symmetry argument, which can easily be extended above the electroweak scale where new degrees of freedoms, such as extra Higgs doublets or SUSY partners of the SM fields are included. It can also be extended to strongly coupled gauge theories, although in this case the expansion in powers of the Yukawa spurions is not necessarily a rapidly convergent series. In this case, a resummation of the terms involving the top-quark Yukawa coupling needs to be performed [898]

This model-independent structure does not hold in CMFV in which one assumes that the effective FCNC operators playing a significant role within the SM are the only relevant ones also beyond the SM. This condition is realized only in weakly coupled theories at the TeV scale with only one light Higgs doublet. In the MSSM, where two Higgs doublets are present, it still works for small $\tan\beta$ but does not work for large $\tan\beta$ as then new scalar operators become important. A very nice summary of this situation can be found in [883], and further details are presented in [624].

Despite these differences between CMFV and MFV, many phenomenological implications listed by us in the CMFV section are the same. In particular the CP asymmetries $S_{\psi K_S}$ and $S_{\psi\phi}$ are the same, and this applies also to relations (15.8) and (15.9). But (15.10) could be violated in MFV if new operators to $B_{s,d} \to \mu^+\mu^-$ and $\Delta M_{s,d}$ become important.

Personally, I think that CMFV relations being more stringent than the MFV ones are a useful starting point. If one day significant violation of them will be found, one can then see whether they can be accommodated within MFV.

15.1.3 Further Implications of CMFV for Weak Decays

$B^+ \to \tau^+\nu_\tau$

Let us then see what MFV can tell us about this simple decay. Here we would like to point out that in this class of models the branching ratio for this decay is enhanced (suppressed) for the same (opposite) sign of the lepton coupling of the new charged gauge boson relative to the SM one. Indeed, the only possibility to modify the SM result up to loop corrections in CMFV is through a tree-level exchange of a new charged gauge boson, whose flavor interactions with quarks are governed by the CKM matrix. In particular the operator structure is the same.

Denoting this gauge boson by $\tilde{W}$ and the corresponding gauge coupling by $\tilde{g}_2$, one has

$$\frac{\mathcal{B}(B^+ \to \tau^+\nu)}{\mathcal{B}(B^+ \to \tau^+\nu)^{\rm SM}} = \left(1 + r\frac{\tilde{g}_2^2}{g_2^2}\frac{M_W^2}{M_{\tilde{W}}^2}\right)^2, \tag{15.38}$$

where we introduced a factor r allowing a modification in the lepton couplings relative to the SM ones, in particular of its sign. Which sign is favored will be known once the data and SM prediction improve.

Downloaded from https://www.cambridge.org/core. UNIVERSIDAD AUTONOMA METROPOLITANA, on 17 Nov 2026 at 22:50:50, subject to the Cambridge Core terms of use, available at https://www.cambridge.org/core/terms. https://doi.org/10.1017/9781139524100.021

If $\tilde{W}$ with these properties is absent, the branching ratio in this framework is not modified with respect to the SM up to loop corrections that could involve new particles but are expected to be small. A $H^{\pm}$ exchange generates new operators and is outside this framework. The same comment applies to gauge bosons with right-handed couplings (W') that we will discuss later.

15.1.4 Comparison with Other Suppressions of FCNC

Still in the context of natural flavor conservation, as present in the MFV framework, one should mention that FCNC can be avoided at tree-level without fine-tuning through a special arrangement of the couplings of the Higgs system with two or more doublets to SM fermions [899, 900], so that there are no FCNC mediated by neutral scalars at tree-level. This is, for instance, the case of the MSSM and many 2HDM models in which one Higgs doublet is responsible for the up-quark masses and a second for down-quark ones.

However, there are still other ways of suppressing FCNC proposed in the literature, discussed in in the context of two-Higgs doublet models in [891, 896, 901–903]. They have been compared critically with the MFV framework in [896]. We describe here briefly only some of these models.

In the so-called BGL models [901], six models in total, the strength of FCNCs in the up- or down-type sector, is unambiguously related to the off-diagonal elements of the CKM matrix. While all the six BGL models are interesting, only one of them is compatible with the MFV principle. It is the one in which $d_i \to d_j$ FCNC transitions are proportional to $V_{3j}^* V_{3i}$. Recently, motivated by the $b \to s\mu^+\mu^-$ anomalies, these ideas have been used in the context of Z' models in which Z' couples flavor nonuniversally to SM quarks [904]. Other recent analyses of FCNC processes in this framework can be found in [905, 906].

On the other hand, the *Yukawa alignment model* [891] is a limiting case of the general MFV construction, where the higher-order powers in Y_u and Y_d are not included. It includes also flavor-blind CP-violating phases mentioned earlier. Neutral-Higgs phenomenology of this model is presented in [891] and the one for charged Higgs in [907]. Electric dipole moments are discussed in [908].

15.2 2HDM$_{\overline{\text{MFV}}}$

15.2.1 Preliminaries

We will next discuss a specific 2HDM model, namely 2HDM with MFV accompanied by flavor-blind CP phases that is called for short 2HDM$_{\overline{\text{MFV}}}$ [896] with the "bar" on MFV indicating the presence of FBPs. We present this model mainly to illustrate how flavor-blind phases can affect various observables.

Let us first list a few important points of the 2HDM$_{\overline{\text{MFV}}}$ framework.

- The presence of FBPs in this MFV framework modifies through their interplay with the standard CKM flavor violation the usual characteristic relations of the MFV framework.

Downloaded from https://www.cambridge.org/core. UNIVERSIDAD AUTONOMA METROPOLITANA, on 17 Nov 2026 at 22:50:50, subject to the Cambridge Core terms of use, available at https://www.cambridge.org/core/terms. https://doi.org/10.1017/9781139524100.021

In particular the mixing induced CP asymmetries in $B_d^0 \to \psi K_S$ and $B_s^0 \to \psi\phi$ take the form known from non-MFV frameworks like LHT, RSc, and in particular Z' models discussed later

$$\boxed{S_{\psi K_S} = \sin(2\beta + 2\varphi_{B_d}), \qquad S_{\psi\phi} = \sin(2|\beta_s| - 2\varphi_{B_s}),} \tag{15.39}$$

where φ_{B_q} are NP phases in $B_q^0 - \bar{B}_q^0$ mixings. Thus in the presence of nonvanishing φ_{B_d} and φ_{B_s}, originating here in nonvanishing FBPs, these two asymmetries do not measure β and β_s but $(\beta + \varphi_{B_d})$ and $(|\beta_s| - \varphi_{B_s})$, respectively.

- The FBPs in the 2HDM$_{\overline{\text{MFV}}}$ can appear both in Yukawa interactions and in the Higgs potential. While in [896] only the case of FBPs in Yukawa interactions has been considered, in [909] these considerations have been extended to include also the FBPs in the Higgs potential. The two flavor-blind CPV mechanisms can be distinguished through the correlation between $S_{\psi K_S}$ and $S_{\psi\phi}$ that is strikingly different if only one of them is relevant. In fact the relations between generated new phases are very different in each case:

$$\varphi_{B_d} = \frac{m_d}{m_s}\varphi_{B_s} \qquad \text{and} \quad \varphi_{B_d} = \varphi_{B_s} \tag{15.40}$$

  for FBPs in Yukawa couplings and Higgs potential, respectively.
- The heavy Higgs contributions to ε_K are negligible, and consequently this model, similar to CMFV, favors the high value of $|V_{cb}|$ for which the SM is consistent with the data on ε_K. But in contrast to CMFV if one day $|V_{ub}|$ will turn out to be high, the presence of a negative phase φ_{B_d} will allow in principle to remove the tension with the experimental value of $S_{\psi K_S}$. Simultaneously $S_{\psi\phi}$ will be enhanced over its SM value with the size of enhancement depending on whether FBPs in Yukawas or Higgs potential are at work.
- The selection of the large value of $|V_{ub}|$ would improve the agreement between the experimental value of $\mathcal{B}(B \to \tau^+\nu_\tau)$ and its SM value that is somewhat lower than experimentally found, see Section 9.3.
- Further implications of this NP scenario, in particular in connection with EDMs, can be found in [896, 909].

What is nice about this model is that while having new sources of CP violation it has a small number of free parameters and a number of definite predictions and correlations between various flavor observables that provide very important tests of this model. The question then arises how this simple model would face the $\Delta F = 2$ tensions and related anomalies if they turned out more significant than presently known. The lessons listed next are based on [909] and updates that happened in this decade.

1. The removal of the $|V_{ub}| - S_{\psi K_S}$ anomaly, in case of a large $|V_{ub}|$, which is achieved through the negative phase φ_{B_d}, is only possible with the help of FBPs in the Higgs potential so that optimally $\varphi_{B_s} = \varphi_{B_d}$ implying the full dominance of the $Q_{1,2}^{\text{SLL}}$ operators as far as CP-violating contributions are concerned.

2. The negative value of φ_{B_d} would through (15.39) automatically increase $S_{\psi\phi}$ relative to the SM value. Finding in the future that nature chooses a *negative* value of $S_{\psi\phi}$ and simultaneously large value of $|V_{ub}|$ would practically rule out 2HDM$_{\overline{\text{MFV}}}$.

Downloaded from https://www.cambridge.org/core. UNIVERSIDAD AUTONOMA METROPOLITANA, on 17 Nov 2026 at 22:50:50, subject to the Cambridge Core terms of use, available at https://www.cambridge.org/core/terms. https://doi.org/10.1017/9781139524100.021

3. In the case of the full dominance of NP effects from the Higgs potential, represented by the operators $Q_{1,2}^{\text{SLL}}$,[1] also in the case of $\Delta M_{s,d}$ the CMFV relation in (15.6) is valid. Yet, the CMFV correlation between ε_K and $\Delta M_{s,d}$ is absent, and $\Delta M_{s,d}$ can be both suppressed and enhanced if necessary. In view of the tension discussed in Section 15.1.1 this could be a problem. The presence of large contributions of operators $Q_{1,2}^{\text{LR}}$ would not help. They suppress ΔM_s with basically no effect on ΔM_d.

15.3 Beyond MFV: Models with U(2)^3 Symmetry

Possibly the simplest solution to the possible tensions between ε_K and $\Delta M_{s,d}$ in models with MFV is to reduce the flavor symmetry U(3)^3 down to U(2)^3 [910–916]. As pointed out in [917], in this case NP effects in ε_K and $B_{s,d}^0 - \bar{B}_{s,d}^0$ are not correlated with each other so that the enhancement of ε_K and suppression of $\Delta M_{s,d}$ can be achieved if necessary for the values of $|V_{cb}|$, $F_{B_s}\sqrt{\hat{B}_{B_s}}$, and $F_{B_d}\sqrt{\hat{B}_{B_d}}$ for which MFV has problems as discussed in Section 15.1.1.

A pragmatic definition of these models in the case of $\Delta F = 2$ transitions could be as follows:

- Flavor and CP-violation in $K^0 - \bar{K}^0$ mixing is governed by CMFV.
- The dominant source of flavor and CP violation in $B_{d,s} - \bar{B}_{d,s}$ mixings is the CKM matrix. Yet, new universal, with respect to B_d and B_s, flavor-violating and CP-violating effects in these transitions are possible. The universality in question is a direct consequence of the U(2)^3 symmetry imposed on the quark doublets of the first two generations. Moreover, only SM operators are relevant in $B_{d,s} - \bar{B}_{d,s}$ mixings. We comment on the possible small nonuniversal corrections and contributions of new operators later.
- Very importantly NP effects in K physics and $B_{d,s}$ observables are uncorrelated with each other, although in specific models such correlation could be forced by the underlying theory and the data.

In the grander formulation by means of the effective theory [910], these models are governed by a global flavor symmetry

$$\boxed{G_F = \text{U}(2)_Q \times \text{U}(2)_u \times \text{U}(2)_d} \tag{15.41}$$

broken *minimally*[2] by three spurions transforming under G_F as follows

$$\Delta Y_u = (2, \bar{2}, 1), \quad \Delta Y_d = (2, 1, \bar{2}), \quad V = (2, 1, 1). \tag{15.42}$$

As demonstrated by means of a spurion analysis in section 5 of [910], the phenomenological consequences of this framework for $\Delta F = 2$ transitions as summarized in the pragmatic definition are general consequences of U(2)^3 symmetry and its breaking pattern.

[1] Not a likely situation because these operators are forbidden by SMEFT.
[2] More complicated breakdown is discussed in [910].

Downloaded from https://www.cambridge.org/core. UNIVERSIDAD AUTONOMA METROPOLITANA, on 17 Nov 2026 at 22:50:50, subject to the Cambridge Core terms of use, available at https://www.cambridge.org/core/terms. https://doi.org/10.1017/9781139524100.021

In particular, if one considers leading flavor-changing amplitudes no assumption of the dominance of SM operators has to be made. Moreover, the universality of NP effects in $B_{d,s} - \bar{B}_{d,s}$ systems, up to the overall usual CKM factors and the hermicity of the $\Delta F = 2$ Hamiltonian implies that the function S_K is real [910]. This result in combination with the dominance of SM operators in this framework implies the CMFV structure of $\Delta S = 2$ transitions.

In this context the following remark should be made. As in the MFV case the leading flavor-changing amplitudes in the framework of [910] are of a left-handed type and to a very good approximation can be evaluated neglecting the effects of light-quark masses. To generate dimension-6 LR operators contributing to $\Delta F = 2$ transitions, one needs at least two extra insertions of the down-type spurion ΔY_d, which implies an extra suppression of amplitudes proportional to down-quark masses. Such effects being proportional to light quark masses ($m_{s,d}$) break the flavor universality between B_d and B_s systems. They can be at best relevant for B_s-mixing, for instance in 2HDM models or supersymmetric models. However, unless one goes to a specific regime of large $\tan\beta$ and small Higgs masses, such effects are always subleading, and we will neglect them.

Let us compare then the general properties of the $\Delta F = 2$ functions S_i $(i = K, d, s)$ in this scenario with the ones in CMFV models.

1. In CMFV we have

$$S_K = S_d = S_s \geq S_0(x_t), \qquad \varphi_K = \varphi_{B_d} = \varphi_{B_s} = 0 \qquad \text{(CMFV)}, \tag{15.43}$$

Consequently,

$$S_{\psi K_S} = \sin(2\beta), \qquad S_{\psi\phi} = \sin(2|\beta_s|) \qquad \text{(CMFV)}. \tag{15.44}$$

$|\varepsilon_K|$, ΔM_d and ΔM_s can only be enhanced in CMFV models. Moreover, this happens in a correlated manner. The enhancement of one of these observables implies automatically and uniquely the enhancement of the other two observables [697, 871].

2. On the other hand in U(2)^3 models in question (15.43) and (15.3) are replaced by

$$S_K = r_K S_0(x_t), \quad |S_d| = |S_s| = r_B S_0(x_t), \quad \varphi_K = 0, \quad \varphi_{B_d} = \varphi_{B_s} \equiv \varphi_{\rm new}, \quad \text{(MU(2)}^3\text{)} \tag{15.45}$$

with r_K and r_B unrelated to each other. The last equality implies

$$S_{\psi K_S} = \sin(2\beta + 2\varphi_{\rm new}), \qquad S_{\psi\phi} = \sin(2|\beta_s| - 2\varphi_{\rm new}), \qquad \text{(U(2)}^3\text{)}, \tag{15.46}$$

that is an anticorrelation between these two asymmetries. As there is no relation of $S_d = S_s$ to S_K in these models, ΔM_d and ΔM_s can be suppressed or enhanced with respect to the SM values, and there is no direct correlation between $|\varepsilon_K|$ and $\Delta M_{s,d}$.

In short, with respect to $\Delta F = 2$ processes there are only three new parameters in this class of models

$$r_K \geq 1, \qquad r_B, \qquad \varphi_{\rm new}, \tag{15.47}$$

with r_K and r_B being real and positive definite.

The first inequality in (15.47) is a direct consequence of the CMFV structure in the $\Delta S = 2$ transitions in this framework [872]. Therefore in the U(2)^3 framework $|\varepsilon_K|$ can only

Downloaded from https://www.cambridge.org/core. UNIVERSIDAD AUTONOMA METROPOLITANA, on 17 Nov 2026 at 22:50:50, subject to the Cambridge Core terms of use, available at https://www.cambridge.org/core/terms. https://doi.org/10.1017/9781139524100.021

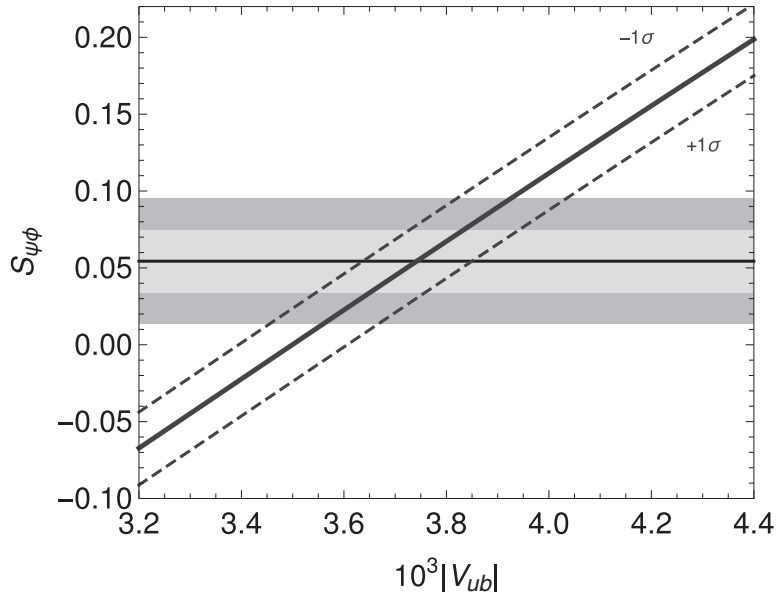


Figure 15.3 $S_{\psi\phi}$ vs. $|V_{ub}|$ in models with $U(2)^3$ symmetry for different values of $|V_{ub}|$. From top to bottom: $S_{\psi K_S} = 0.682,\ 0.699,\ 0.716$. Light/dark gray: experimental $1\sigma/2\sigma$ region.

be increased over the SM value, but as stated here, this property is generally uncorrelated with $B_{s,d}$ systems.

3. Flavor universality of the functions S_q in CMFV and $U(2)^3$ models implies

$$\left(\frac{\Delta M_d}{\Delta M_s}\right)_{\rm CMFV} = \left(\frac{\Delta M_d}{\Delta M_s}\right)_{U(2)^3} = \left(\frac{\Delta M_d}{\Delta M_s}\right)_{\rm SM} = \frac{m_{B_d}}{m_{B_s}}\frac{\hat{B}_d}{\hat{B}_s}\frac{F_{B_d}^2}{F_{B_s}^2}\left|\frac{V_{td}}{V_{ts}}\right|^2 \equiv \frac{m_{B_d}}{m_{B_s}}\frac{1}{\xi^2}\left|\frac{V_{td}}{V_{ts}}\right|^2 . \tag{15.48}$$

This could be problematic in view of tensions between ΔM_d and ΔM_s and γ pointed out in [874] and discussed in Section 15.1.

4. As pointed out in [917] the relation $\varphi_{B_d} = \varphi_{B_s}$ implies for fixed $|V_{cb}|$ and γ a triple $S_{\psi K_S} - S_{\psi\phi} - |V_{ub}|$ correlation that constitutes an important test of this NP scenario. The dependence of $S_{\psi K_S}$ on $S_{\psi\phi}$ for different $|V_{ub}|$ can be found in figure 1 of [917]. In view of the precise experimental value of $S_{\psi K_S}$ we show this time in Figure 15.3 only $S_{\psi\phi}$ as a function of $|V_{ub}|$ for three values of $S_{\psi K_S}$ which is an update of figure 2 in [917].[3] It is a good exercise to check this plot, which was obtained for $\gamma = 74^\circ$ and $|V_{cb}| = 42.0 \times 10^{-3}$. The γ dependence is fully negligible. The value of $|V_{ub}|$ is proportional to $|V_{cb}|$ as one can check performing the standard construction of the UT. Note that this correlation is independent of the values of $F_{B_s}\sqrt{\hat{B}_{B_s}}$ and $F_{B_d}\sqrt{\hat{B}_{B_d}}$. As seen in this figure the important

[3] The author thanks Monika Blanke for providing this plot.

Downloaded from https://www.cambridge.org/core. UNIVERSIDAD AUTONOMA METROPOLITANA, on 17 Nov 2026 at 22:50:50, subject to the Cambridge Core terms of use, available at https://www.cambridge.org/core/terms. https://doi.org/10.1017/9781139524100.021

advantage of $U(2)^3$ models over $2HDM_{\overline{MFV}}$ is that in the case of $S_{\psi\phi}$ being very small or even having opposite sign to SM prediction, this framework can survive with concrete prediction for $|V_{ub}|$. Other implications of this NP scenario that could turn out to be relevant when the data improve can be found in [917]. In particular the impact of $U(2)^3$ symmetry on tree-level FCNC due to gauge boson and scalar exchanges has been analyzed in [611] and [504], respectively.

15.4 Beyond MFV: Z' Boson

15.4.1 Preliminaries

In the following sections we will generalize the discussion of the previous section to NP models, which go beyond the framework of MFV. In these models new sources of flavor violation are present, and in some of them new operators strongly suppressed in the SM become important. Even if on the fundamental level the WCs are the ones that play the crucial role, it turns out that also in this case the formulation of FCNC processes in terms of master functions is useful, simply because then the effects of non-MFV interactions are transparently seen. Indeed, we will see that beyond MFV

- The master functions become complex quantities.
- Their flavor universality is broken.
- The presence of right-handed neutral and charged vector currents will require the introduction of new master functions.
- The presence of scalar and pseudoscalar interactions will require the introduction of still other master functions.

In this section we will first introduce the notation for the master functions in this more general framework. Subsequently we will calculate them in a number of very simple NP models:

- A model with an additional $U(1)'$ gauge symmetry and related heavy neutral gauge boson Z' with flavor-violating couplings and implied tree-level contributions to FCNC processes. This scenario is very useful for the illustration of the new formulas in explicit terms. Reviews of these models can be found in [918, 919], and more references will be given later.
- A model in which the SM Z boson mediates FCNC already at tree level. We will see that the pattern of flavor violation in this case differs significantly from the one caused by tree-level Z' exchanges. We mentioned it already at the end of Section 14.5.
- A model with tree-level FCNC mediated by heavy scalars and pseudoscalars. The pattern of flavor violation in this case will not only differ from the Z' and Z cases, but will also depend on whether a scalar or pseudoscalar is considered.
- While Z' and the heavy scalars and pseudoscalars just mentioned will be colorless, it will be of interest to consider in a separate section simple models with heavy gauge

Downloaded from https://www.cambridge.org/core. UNIVERSIDAD AUTONOMA METROPOLITANA, on 17 Nov 2026 at 22:50:50, subject to the Cambridge Core terms of use, available at https://www.cambridge.org/core/terms. https://doi.org/10.1017/9781139524100.021

bosons, scalars, and pseudoscalars that carry color as in these cases the patterns of flavor violation will still be different from the ones encountered in models with new colorless gauge bosons, scalars, and pseudoscalars.

The different NP scenarios just listed and presented in this chapter can be considered as *simplified models* because in concrete NP models that we will discuss subsequently in the next chapter, several of these tree-level exchanges can contribute to a given flavor observable simultaneously. Moreover, in certain models also new one-loop diagrams will turn out to be important. But the technology developed in the context of the simplified models in question will turn out to be very useful for the discussion of more complicated NP scenarios. We will also see that although some of these specific models will contain more free parameters than a single simplified model, the couplings of the gauge bosons, scalars, and pseudoscalars, rather arbitrary in simplified models, will be given in terms of fundamental parameters of a given model. This will imply correlations between observables in different meson systems and also the correlations with flavor-conserving processes studied both at high-energy colliders and low-energy facilities. Moreover, it will be possible to find out whether the contributions from tree-level diagrams or one-loop diagrams to a given observable are most important.

15.4.2 Introducing Generalized Master Functions

The formulation given next in the case of models having the same operator structure as the SM but including new sources of flavor violation has been first presented in the context of the Littlest Higgs model with T-parity in [700]. It has been generalized to include in addition to left-handed (LH) currents also the right-handed (RH) ones in an analysis of Randall–Sundrum models in [920]. While in the latter paper it turned out to be useful to work with $V-A$ and V currents, we will here follow the formulation in terms of L, R, V, and A currents presented in [611]. The indices L and R in the functions following correspond to LH and RH currents, respectively.

For our purposes it will be sufficient to consider the following functions:

- For $\Delta F = 2$ processes

$$\boxed{S(K), \qquad S(B_d), \qquad S(B_s),} \tag{15.49}$$

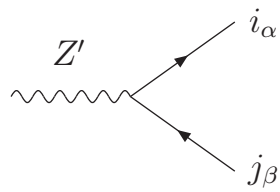
  where we will include in the definitions of these functions the contributions of operators with LL, RR, and LR Dirac structures.
- For decays with a meson and $\nu\bar{\nu}$ in the final state

$$\boxed{X_{L,R}(K), \qquad X_{L,R}(B_d), \qquad X_{L,R}(B_s).} \tag{15.50}$$

- For decays with $\mu\bar{\mu}$ or generally $\ell^+\ell^-$ in the final state

$$\boxed{Y_A(K), \qquad Y_A(B_d), \qquad Y_A(B_s).} \tag{15.51}$$

Downloaded from https://www.cambridge.org/core. UNIVERSIDAD AUTONOMA METROPOLITANA, on 17 Nov 2026 at 22:50:50, subject to the Cambridge Core terms of use, available at https://www.cambridge.org/core/terms. https://doi.org/10.1017/9781139524100.021



$$i\gamma_\mu \delta_{\alpha\beta}[\Delta_L^{ij}(Z')P_L + \Delta_R^{ij}(Z')P_R]$$

Figure 15.4 Feynman rule for the coupling of a colorless neutral gauge boson Z' to quarks, where i, j denote different quark flavors and α, β the colors. $P_{L,R} = (1 \mp \gamma_5)/2$.

- For decays with $P\ell^+\ell^-$ in the final state, where $P = K, B_{s,d}$

$$\boxed{Z_V(K), \qquad Z_V(B_d), \qquad Z_V(B_s).} \tag{15.52}$$

All these functions, in contrast to the SM and more generally CMFV models, depend on the meson considered and moreover are complex valued. In the absence of new sources of flavor violation and the absence of RH currents, the functions with the index R vanish and the remaining ones reduce to S_0, X_0, Y_0, and Z_0 within the SM and to S, X, Y, and Z within MFV models.

15.4.3 Master Functions in Z′ Models

We will next illustrate how these functions look like in Z' models with arbitrary LH and RH complex quark couplings

$$\boxed{\Delta_L^{sd}(Z'), \qquad \Delta_R^{sd}(Z')} \tag{15.53}$$

that are defined in Figure 15.4.

Moreover, we will also work with real lepton couplings

$$\Delta_V^{\mu\bar{\mu}}(Z') = \Delta_R^{\mu\bar{\mu}}(Z') + \Delta_L^{\mu\bar{\mu}}(Z'), \qquad \Delta_A^{\mu\bar{\mu}}(Z') = \Delta_R^{\mu\bar{\mu}}(Z') - \Delta_L^{\mu\bar{\mu}}(Z'). \tag{15.54}$$

We recall the relevant CKM factors

$$\lambda_i^{(K)} = V_{is}^* V_{id}, \qquad \lambda_t^{(d)} = V_{tb}^* V_{td}, \qquad \lambda_t^{(s)} = V_{tb}^* V_{ts}, \tag{15.55}$$

which will be kept as overall factors in front of the master functions to have a better comparison with MFV scenario. We also introduce

$$g_{\rm SM}^2 = 4\frac{G_F}{\sqrt{2}}\frac{\alpha}{2\pi \sin^2\theta_W} = 4\frac{G_F^2 M_W^2}{2\pi^2} = 1.78137 \times 10^{-7}\,\text{GeV}^{-2}. \tag{15.56}$$

Downloaded from https://www.cambridge.org/core. UNIVERSIDAD AUTONOMA METROPOLITANA, on 17 Nov 2026 at 22:50:50, subject to the Cambridge Core terms of use, available at https://www.cambridge.org/core/terms. https://doi.org/10.1017/9781139524100.021

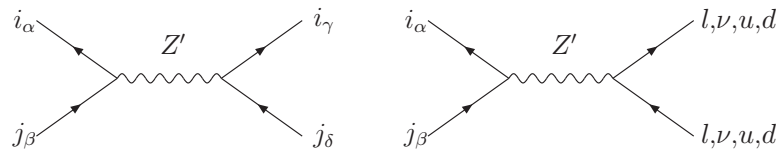


Figure 15.5 Tree-level Z' contribution to $\Delta F = 2$ (left) and $\Delta F = 1$ (right) processes. Labels are explained in Figure 15.4.

This relation is only valid in the leading order of electroweak interactions but for the time being this is sufficient for our purposes.

$\Delta F = 2$ Master Functions

The $\Delta F = 2$ master functions for $M = K, B_q$ are given as follows

$$S(M) = S_0(x_t) + \Delta S(M) \equiv |S(M)|e^{i\theta_S^M}, \tag{15.57}$$

with $\Delta S(M)$ receiving contributions from various operators so that it is useful to write

$$\Delta S(M) = [\Delta S(M)]_{\rm VLL} + [\Delta S(M)]_{\rm VRR} + [\Delta S(M)]_{\rm LR}. \tag{15.58}$$

The contributing operators are defined for the K system as follows [746, 749]

$$Q_1^{\rm VLL} = \left(\bar{s}\gamma_\mu P_L d\right)\left(\bar{s}\gamma^\mu P_L d\right), \tag{15.59a}$$

$$Q_1^{\rm VRR} = \left(\bar{s}\gamma_\mu P_R d\right)\left(\bar{s}\gamma^\mu P_R d\right), \tag{15.59b}$$

$$Q_1^{\rm LR} = \left(\bar{s}\gamma_\mu P_L d\right)\left(\bar{s}\gamma^\mu P_R d\right), \tag{15.59c}$$

$$Q_2^{\rm LR} = \left(\bar{s}P_L d\right)\left(\bar{s}P_R d\right), \tag{15.59d}$$

with analogous expressions for $B_{s,d}$ systems, given already explicitly in Section 13.2. For instance, in the B_s system $Q_1^{\rm VLL} = \left(\bar{b}\gamma_\mu P_L s\right)\left(\bar{b}\gamma^\mu P_L s\right)$. We suppress color indices as they are summed up in each factor. For instance, $\bar{s}\gamma_\mu P_L d$ stands for $\bar{s}_\alpha\gamma_\mu P_L d_\alpha$ and similarly for other factors.

The formulas for $[\Delta S(M)]_{\rm VLL}$ and $[\Delta S(M)]_{\rm VRR}$ are very simple as there is only one operator in each case. Calculating the left diagram in Figure 15.5, multiplying it by i, and dividing by the combinatoric factor of 2, we find first the shift in the effective Hamiltonian in the VLL case. Comparing this shift with the SM Hamiltonian and taking care of modified QCD corrections we find [611, 613]:

$$[\Delta S(B_q)]_{\rm VLL} = \left[\frac{\Delta_L^{bq}(Z')}{\lambda_t^{(q)}}\right]^2 \frac{4\tilde{r}(\mu_{Z'})}{M_{Z'}^2 g_{\rm SM}^2}, \qquad [\Delta S(K)]_{\rm VLL} = \left[\frac{\Delta_L^{sd}(Z')}{\lambda_t^{(K)}}\right]^2 \frac{4\tilde{r}(\mu_{Z'})}{M_{Z'}^2 g_{\rm SM}^2}, \tag{15.60}$$

Downloaded from https://www.cambridge.org/core. UNIVERSIDAD AUTONOMA METROPOLITANA, on 17 Nov 2026 at 22:50:50, subject to the Cambridge Core terms of use, available at https://www.cambridge.org/core/terms. https://doi.org/10.1017/9781139524100.021

where

$$\tilde{r}(\mu_{Z'}) = \frac{C_1^{\rm VLL}(\mu_{Z'})}{0.985}\eta_6^{6/21}\left[1 + 1.371\frac{\alpha_s^{(6)}(m_t)}{4\pi}(1-\eta_6)\right]. \tag{15.61}$$

Here $\mu_{Z'} = O(M_{Z'})$, and

$$C_1^{\rm VLL}(\mu_{Z'}) = 1 + \frac{\alpha_s}{4\pi}\left(-2\log\frac{M_{Z'}^2}{\mu_{Z'}^2} + \frac{11}{3}\right) \tag{15.62}$$

represents $O(\alpha_s)$ QCD corrections to Z' tree-level exchange [749]. The two factors involving

$$\eta_6 = \frac{\alpha_s^{(6)}(\mu_{Z'})}{\alpha_s^{(6)}(m_t)} \tag{15.63}$$

represent together NLO QCD renormalization group evolution from m_t to $\mu_{Z'} = O(M_{Z'})$ as given in [746]. The renormalization scheme dependence of this evolution is canceled by the one of $C_1^{\rm VLL}(\mu_{Z'})$.

Even if $\tilde{r}$ will turn out to be close to unity, it is instructive to discuss its origin. As the VLL operator is the one of the SM, the $\hat{B}_q$ and $\hat{B}_K$ parameters that have been factored out are the same as in the SM. The same applies to the renormalization group evolution between low-energy scales relevant for hadronic matrix elements and $\mu_t = O(m_t)$ entering the evaluation of η_2 and η_B [137] that have also been factored out. Therefore, the departure of $\tilde{r}$ from unity is governed by the renormalization group effects between μ_t and $\mu_{Z'} = O(M_{Z'})$, absent in the SM, and the difference in matching conditions between full and effective theories, involving tree diagrams with Z' exchanges but box diagrams in the SM. These are represented by $C_1^{\rm VLL}(M_{Z'})$ and the numerical factor 0.985 [137], respectively. The latter factor describes flavor universal QCD correction to $S_0(x_t)$ in the SM and is usually included in η_B and η_2 [137]. The coefficient 1.371, calculated in [746], corresponds to the effective theory with six flavors $f = 6$. We assume tacitly that there are no new fermions lighter than Z'. Their inclusion into this formula would have a very small impact on $\tilde{r}$ anyway. Note that $\tilde{r}$ is free from hadronic uncertainties. It is also flavor universal, as all the flavor dependence is already included in η_2, η_B, $\hat{B}_q$, and $\hat{B}_K$ that have been factored out.

We find then

$$\tilde{r}(M_{Z'} = 1\,\text{TeV}) = 0.985, \quad \tilde{r}(M_{Z'} = 3\,\text{TeV}) = 0.9534. \tag{15.64}$$

$[\Delta S(M)]_{\rm VRR}$ is obtained from (15.60) by simply replacing L by R.

To calculate the LR contributions, we introduce quantities familiar from SM expressions for mixing amplitudes

Downloaded from https://www.cambridge.org/core. UNIVERSIDAD AUTONOMA METROPOLITANA, on 17 Nov 2026 at 22:50:50, subject to the Cambridge Core terms of use, available at https://www.cambridge.org/core/terms. https://doi.org/10.1017/9781139524100.021

$$T(B_q) = \frac{G_F^2}{12\pi^2} F_{B_q}^2 \hat{B}_{B_q} m_{B_q} M_W^2 \left(\lambda_t^{(q)}\right)^2 \eta_B, \tag{15.65}$$

$$T(K) = \frac{G_F^2}{12\pi^2} F_K^2 \hat{B}_K m_K M_W^2 \left(\lambda_t^{(K)}\right)^2 \eta_2, \tag{15.66}$$

where η_i are QCD corrections and $\hat{B}_i$ known SM nonperturbative factors.

The first difference from VLL and VRR cases is the appearance of two operators that mix with each other under renormalization, but even more important is the increased size of hadronic matrix elements of these new operators and the increased role of renormalization group effects due to the presence of large anomalous dimensions of these operators. We have seen this already in Section 13.2.

When constructing the effective Hamiltonian one has to remember that with two different currents, two different diagrams giving the same result can be constructed so that the combinatorial factor 1/2 included in VLL and VRR cases is canceled. We have then

$$T(K)[\Delta S(K)]_{\rm LR} = \frac{\Delta_L^{sd}(Z')\Delta_R^{sd}(Z')}{M_{Z'}^2}\left[C_1^{\rm LR}(\mu_{Z'})\langle Q_1^{\rm LR}(\mu_{Z'},K)\rangle + C_2^{\rm LR}(\mu_{Z'})\langle Q_2^{\rm LR}(\mu_{Z'},K)\rangle\right]. \tag{15.67}$$

To expose NP present in the couplings $\Delta_{L,R}^{sd}(Z')$, we have chosen as the renormalization scale, not the low-energy scale at which hadronic matrix elements of $Q_{1,2}^{\rm LR}$ are evaluated by LQCD, but a high scale $\mu_{Z'} = O(M_{Z'})$ at which Z' is integrated out. These matrix elements are given by

$$\langle Q_i^{\rm LR}(\mu_{Z'},K)\rangle \equiv \frac{m_K F_K^2}{3} P_i^{\rm LR}(\mu_{Z'},K) \tag{15.68}$$

with the coefficients $P_i^{\rm LR}$, introduced in [746], relating these matrix elements to the ones calculated by LQCD. Including NLO QCD corrections [749] the Wilson coefficients of LR operators are given by

$$C_1^{\rm LR}(\mu_{Z'}) = 1 + \frac{\alpha_s}{4\pi}\left(-\log\frac{M_{Z'}^2}{\mu_{Z'}^2} - \frac{1}{6}\right), \qquad C_2^{\rm LR}(\mu_{Z'}) = \frac{\alpha_s}{4\pi}\left(-6\log\frac{M_{Z'}^2}{\mu_{Z'}^2} - 1\right). \tag{15.69}$$

The $\mu_{Z'}$ dependence of $C_i^a(\mu_{Z'})$ cancels the one of $P_i^a(\mu_{Z'})$ so that $\Delta S(K)$ does not depend on $\mu_{Z'}$. Similarly for B_q systems we have

$$T(B_q)[\Delta S(B_q)]_{\rm LR} = \frac{\Delta_L^{bq}(Z')\Delta_R^{bq}(Z')}{M_{Z'}^2}\left[C_1^{\rm LR}(\mu_{Z'})\langle Q_1^{\rm LR}(\mu_{Z'},B_q)\rangle + C_2^{\rm LR}(\mu_{Z'})\langle Q_2^{\rm LR}(\mu_{Z'},B_q)\rangle\right], \tag{15.70}$$

Downloaded from https://www.cambridge.org/core. UNIVERSIDAD AUTONOMA METROPOLITANA, on 17 Nov 2026 at 22:50:50, subject to the Cambridge Core terms of use, available at https://www.cambridge.org/core/terms. https://doi.org/10.1017/9781139524100.021

where the Wilson coefficients $C_i^a(\mu_{Z'})$ are as in the K system. Information on hadronic matrix elements has been given in Section 13.2, in particular in Table 13.2.

Combinatoric Factors in $\Delta F = 2$ Calculations

In calculating the box diagrams in the SM, MFV, and Z' models, we argued that combinatoric factor of 1/2 has to be included in the VLL and VRR cases but none in the LR case. While this rule can be derived diagrammatically, it is much faster to find it by integrating out Z' by means of equations of motion given in (1.2) with ϕ replaced by Z'.

Consider then the Lagrangian

$$\mathcal{L}(Z') = \frac{1}{2} M_{Z'}^2 Z'^{,\mu} Z'_\mu + \Delta_L^{sd}(Z') \bar{s}_L \gamma^\mu d_L Z'_\mu + \Delta_R^{sd}(Z') \bar{s}_R \gamma^\mu d_R Z'_\mu. \tag{15.71}$$

Inserting it into the Euler–Lagrange equation in (1.2), we find

$$Z'_\mu = -\frac{1}{M_{Z'}^2} \left[\Delta_L^{sd}(Z') \bar{s}_L \gamma_\mu d_L + \Delta_R^{sd}(Z') \bar{s}_R \gamma_\mu d_R \right]. \tag{15.72}$$

Inserting it back into (15.71) and reversing the overall sign to obtain the Hamiltonian, a simple algebra convinces us that our rule for combinatoric factors is correct.

$\Delta F = 1$ Master Functions ($\nu\bar{\nu}$ and $\mu\bar{\mu}$)

Proceeding in the same manner for $\Delta F = 1$ transitions and calculating the diagrams in Figure 15.5 with leptons in the final state, we readily find[4]

$$X_{\rm L}(K) = \eta_X X_0(x_t) + \frac{\Delta_L^{\nu\bar{\nu}}(Z')}{g_{\rm SM}^2 M_{Z'}^2} \frac{\Delta_L^{sd}(Z')}{V_{ts}^* V_{td}} \equiv |X_L(K)| e^{i\theta_X^K}, \tag{15.73}$$

$$X_{\rm R}(K) = \frac{\Delta_L^{\nu\bar{\nu}}(Z')}{g_{\rm SM}^2 M_{Z'}^2} \frac{\Delta_R^{sd}(Z')}{V_{ts}^* V_{td}}, \tag{15.74}$$

$$X_{\rm L}(B_q) = \eta_X X_0(x_t) + \left[\frac{\Delta_L^{\nu\nu}(Z')}{M_{Z'}^2 g_{\rm SM}^2} \right] \frac{\Delta_L^{qb}(Z')}{V_{tq}^* V_{tb}} \equiv |X_L(B_q)| e^{i\theta_X^{B_q}}, \tag{15.75}$$

$$X_{\rm R}(B_q) = \left[\frac{\Delta_L^{\nu\nu}(Z')}{M_{Z'}^2 g_{\rm SM}^2} \right] \frac{\Delta_R^{qb}(Z')}{V_{tq}^* V_{tb}}, \tag{15.76}$$

[4] Obviously no combinatoric factors are present in $\Delta F = 1$ transitions.

Downloaded from https://www.cambridge.org/core. UNIVERSIDAD AUTONOMA METROPOLITANA, on 17 Nov 2026 at 22:50:50, subject to the Cambridge Core terms of use, available at https://www.cambridge.org/core/terms. https://doi.org/10.1017/9781139524100.021

$$Y_{\rm A}(K) = \eta_Y Y_0(x_t) + \frac{\left[\Delta_A^{\mu\bar{\mu}}(Z')\right]}{M_{Z'}^2 g_{\rm SM}^2}\left[\frac{\Delta_L^{sd}(Z') - \Delta_R^{sd}(Z')}{V_{ts}^* V_{td}}\right] \equiv |Y_A(K)|e^{i\theta_Y^K}, \tag{15.77}$$

$$Y_{\rm A}(B_q) = \eta_Y Y_0(x_t) + \frac{\left[\Delta_A^{\mu\bar{\mu}}(Z')\right]}{M_{Z'}^2 g_{\rm SM}^2}\left[\frac{\Delta_L^{qb}(Z') - \Delta_R^{qb}(Z')}{V_{tq}^* V_{tb}}\right] \equiv |Y_A(B_q)|e^{i\theta_Y^{Bq}}. \tag{15.78}$$

Here $\eta_{X,Y}$ are QCD factors, which for $m_t = m_t(m_t)$ are close to unity [181, 182]. In 2019 after the inclusion of electroweak NLO corrections and NNLO QCD corrections they read [187, 203]

$$\eta_X = 0.994, \qquad \eta_Y = 0.988\,. \tag{15.79}$$

15.4.4 Effective Hamiltonian for $b \to s\ell^+\ell^-$ and $d \to s\ell^+\ell^-$

In the case of $b \to s\ell^+\ell^-$ and $d \to s\ell^+\ell^-$ transitions, the functions $Y_{\rm A}$ describe only axial-vector couplings, and it is necessary to look at the general effective Hamiltonian given in (9.1). In the case of Z' models this Hamiltonian involves only the Wilson coefficients

$$\boxed{C_9, \qquad C_{10}, \qquad C_9', \qquad C_{10}'} \tag{15.80}$$

with only the first two present in the SM. The new coefficients signal the presence of flavor-violating right-handed currents. The effective Hamiltonian for Z' models reads then

$$\mathcal{H}_{\rm eff}(b \to s\ell\bar{\ell}) = \mathcal{H}_{\rm eff}(b \to s\gamma) - \frac{4G_{\rm F}}{\sqrt{2}}\frac{\alpha}{4\pi}V_{ts}^* V_{tb}\sum_{i=9,10}[C_i(\mu)Q_i(\mu) + C_i'(\mu)Q_i'(\mu)], \tag{15.81}$$

where

$$Q_9 = (\bar{s}\gamma_\mu P_L b)(\bar{\ell}\gamma^\mu \ell), \qquad Q_{10} = (\bar{s}\gamma_\mu P_L b)(\bar{\ell}\gamma^\mu\gamma_5 \ell), \tag{15.82}$$

$$Q_9' = (\bar{s}\gamma_\mu P_R b)(\bar{\ell}\gamma^\mu \ell), \qquad Q_{10}' = (\bar{s}\gamma_\mu P_R b)(\bar{\ell}\gamma^\mu\gamma_5 \ell). \tag{15.83}$$

Here $\mathcal{H}_{\rm eff}(b \to s\gamma)$ stands for the effective Hamiltonian for the $b \to s\gamma$ transition that involves the dipole operators. In the SM this Hamiltonian is given in (6.273). An explicit formula for this Hamiltonian in the presence of Z' contributions can be found in [611], but as NP contributions to this part turn out to be negligible, we do not present them here.

Downloaded from https://www.cambridge.org/core. UNIVERSIDAD AUTONOMA METROPOLITANA, on 17 Nov 2026 at 22:50:50, subject to the Cambridge Core terms of use, available at https://www.cambridge.org/core/terms. https://doi.org/10.1017/9781139524100.021

The Wilson coefficients (15.80) in Z' models are found in the case of $\mu\bar{\mu}$ to be

$$\sin^2\vartheta_W C_9 = [\eta_Y Y_0(x_t) - 4\sin^2\vartheta_W Z_0(x_t)] - \frac{1}{g_{\rm SM}^2}\frac{1}{M_{Z'}^2}\frac{\Delta_L^{sb}(Z')\Delta_V^{\mu\bar{\mu}}(Z')}{V_{ts}^* V_{tb}}, \tag{15.84}$$

$$\sin^2\vartheta_W C_{10} = -\eta_Y Y_0(x_t) - \frac{1}{g_{\rm SM}^2}\frac{1}{M_{Z'}^2}\frac{\Delta_L^{sb}(Z')\Delta_A^{\mu\bar{\mu}}(Z')}{V_{ts}^* V_{tb}}, \tag{15.85}$$

$$\sin^2\vartheta_W C_9' = -\frac{1}{g_{\rm SM}^2}\frac{1}{M_{Z'}^2}\frac{\Delta_R^{sb}(Z')\Delta_V^{\mu\bar{\mu}}(Z')}{V_{ts}^* V_{tb}}, \tag{15.86}$$

$$\sin^2\vartheta_W C_{10}' = -\frac{1}{g_{\rm SM}^2}\frac{1}{M_{Z'}^2}\frac{\Delta_R^{sb}(Z')\Delta_A^{\mu\bar{\mu}}(Z')}{V_{ts}^* V_{tb}}, \tag{15.87}$$

with $\Delta_{V,A}^{\mu\bar{\mu}}(Z')$ defined in (15.54) and explicit expressions for the SM one-loop functions X_0, Y_0, and Z_0 given in Chapter 6.

The presence of several couplings introduces new parameters and consequently significant freedom in phenomenological analyses of general Z' scenarios. But as we will see later on, in concrete models these couplings are given in terms of fundamental parameters of a given theory implying more stringent constraints.

It should be stressed that the preceding formulas do not include QCD renormalization group effects, which influence only C_9 and C_9'. As Z' is integrated out at a scale $O(M_{Z'})$, the RG QCD evolution has to be performed in the Z' part down to EW scale. Strictly speaking, also other RG effects present in the SMEFT have to be included to obtain the full picture. Such a complete analysis should be available in 2020.

15.4.5 Basic Formulas for Observables

We will next generalize the formulas for various observables presented already for the SM and models with MFV in the previous sections. The formulation of NP effects as modifications of the master functions makes this generalization straightforward. The main changes originate in the presence of new phases, and consequently one has to remember that the master functions are now complex quantities. The presence of new operators induced by the right-handed currents is another modification that forces us to distinguish functions with indices L and R and take care of the related minus sign in certain decays, but this is straightforward as well.

$\Delta F = 2$ Observables

The $\Delta B = 2$ mass differences are given as follows:

$$\boxed{\Delta M_d = \frac{G_F^2}{6\pi^2} M_W^2 m_{B_d} |\lambda_t^{(d)}|^2 F_{B_d}^2 \hat{B}_{B_d}\eta_B |S(B_d)|,} \tag{15.88}$$

Downloaded from https://www.cambridge.org/core. UNIVERSIDAD AUTONOMA METROPOLITANA, on 17 Nov 2026 at 22:50:50, subject to the Cambridge Core terms of use, available at https://www.cambridge.org/core/terms. https://doi.org/10.1017/9781139524100.021

$$\boxed{\Delta M_s = \frac{G_F^2}{6\pi^2} M_W^2 m_{B_s} |\lambda_t^{(s)}|^2 F_{B_s}^2 \hat{B}_{B_s} \eta_B |S(B_s)|.} \tag{15.89}$$

The absolute values of $S(B_q)$ should be noticed.

The corresponding mixing induced CP-asymmetries are modified with respect to the ones in MFV models because $S(B_q)$ carry now nonvanishing phases. We have

$$\boxed{S_{\psi K_S} = \sin(2\beta + 2\varphi_{B_d}), \qquad S_{\psi\phi} = \sin(2|\beta_s| - 2\varphi_{B_s}),} \tag{15.90}$$

where the phases β and β_s are defined in (15.4) and $\beta_s \simeq -1^\circ$. The new phases φ_{B_q} are directly related to the phases of the functions $S(B_q)$ defined in (15.57)

$$2\varphi_{B_q} = -\theta_S^{B_q}. \tag{15.91}$$

Our phase conventions have been summarized in Section 8.1. Different signs in front of new phases in $S_{\psi K_S}$ and $S_{\psi\phi}$ in (15.90) should be noticed. This difference becomes important in concrete NP models.

For the CP-violating parameter ε_K and ΔM_K, we have, respectively,

$$\boxed{\varepsilon_K = \frac{\kappa_\varepsilon e^{i\varphi_\varepsilon}}{\sqrt{2}(\Delta M_K)_{\rm exp}} \left[{\rm Im}\left(M_{12}^K\right)\right], \qquad \Delta M_K = 2{\rm Re}\left(M_{12}^K\right),} \tag{15.92}$$

where

$$\left(M_{12}^K\right)^* = \frac{G_F^2}{12\pi^2} F_K^2 \hat{B}_K m_K M_W^2 \left[\lambda_c^2 \eta_1 x_c + \lambda_t^2 \eta_2 S(K) + 2\lambda_c\lambda_t \eta_3 S_0(x_c, x_t)\right]. \tag{15.93}$$

Relative to the SM the only difference is the new function $S(K)$, which has been evaluated including QCD corrections few pages before.

$B_{d,s} \to \mu^+\mu^-$

With the assumption that the CKM parameters have been determined independent of NP and are therefore the same in all models considered, we find

$$\boxed{\frac{\overline{\mathcal{B}}(B_s \to \mu^+\mu^-)}{\overline{\mathcal{B}}(B_s \to \mu^+\mu^-)^{\rm SM}} = \frac{r^{\rm SM}(y_s)}{r(y_s)} \left|\frac{Y_A(B_s)}{\eta_Y Y_0(x_t)}\right|^2,} \tag{15.94}$$

and

$$\boxed{\frac{\mathcal{B}(B_d \to \mu^+\mu^-)}{\mathcal{B}(B_d \to \mu^+\mu^-)^{\rm SM}} = \left|\frac{Y_A(B_d)}{\eta_Y Y_0(x_t)}\right|^2,} \tag{15.95}$$

where $Y_A(B_q)$ is given in (15.78) and in (15.94), following the discussion in Section 9.2, we included $\Delta\Gamma_s$ effects, which are summarized in

$$r(y_s) \equiv \frac{1 - y_s^2}{1 + \mathcal{A}_{\Delta\Gamma}^\lambda y_s} \approx 1 - \mathcal{A}_{\Delta\Gamma}^\lambda y_s \tag{15.96}$$

Downloaded from https://www.cambridge.org/core. UNIVERSIDAD AUTONOMA METROPOLITANA, on 17 Nov 2026 at 22:50:50, subject to the Cambridge Core terms of use, available at https://www.cambridge.org/core/terms. https://doi.org/10.1017/9781139524100.021

with

$$y_s \equiv \tau_{B_s} \frac{\Delta\Gamma_s}{2} = 0.065 \pm 0.005 \tag{15.97}$$

and general formula for $\mathcal{A}^{\lambda}_{\Delta\Gamma}$ given in (9.122). Of particular interest now is also the CP-asymmetry $\mathcal{S}_{\mu^+\mu^-}$ for which general formula in terms of Wilson coefficients is given in (9.115). Using these formulas we find in Z' models very simple expressions

$$\mathcal{A}^{\lambda}_{\Delta\Gamma} = \cos(2\theta_Y^{B_s} - 2\varphi_{B_s}), \quad \mathcal{S}_{\mu^+\mu^-} = \sin(2\theta_Y^{B_s} - 2\varphi_{B_s}) \tag{15.98}$$

$\theta_Y^{B_s}$ is defined in (15.78). Both $\mathcal{A}^{\lambda}_{\Delta\Gamma}$ and $S^s_{\mu^+\mu^-}$ are theoretically clean observables.

We stress again the presence of new phases in the $B_q - \bar{B}_q$ mixings as we deal here with the mixing-induced CP violation. Their presence is also required to cancel any phase convention dependences. The SM phases cancel in this asymmetry [507, 508], and in the SM and CMFV models one has

$$\mathcal{A}^{\lambda}_{\Delta\Gamma} = 1, \quad \mathcal{S}_{\mu^+\mu^-} = 0, \quad r(y_s) = 0.935 \pm 0.007 \tag{15.99}$$

independent of NP parameters.

While $\Delta\Gamma_d$ is very small and y_d can be set to zero, in the case of $B_d \to \mu^+\mu^-$ one can still consider the CP asymmetry $\mathcal{S}^d_{\mu^+\mu^-}$ [508], for which in the case of Z' models we simply find

$$\mathcal{S}^d_{\mu^+\mu^-} = \sin(2\theta_Y^{B_d} - 2\varphi_{B_d}). \tag{15.100}$$

$K_L \to \mu^+\mu^-$

As discussed in Section 9.7.1 only the so-called short-distance (SD) part of the dispersive contribution to $K_L \to \mu^+\mu^-$ can be reliably calculated. Therefore usually this decay is treated only as an additional constraint with the rough upper bound given in (9.268). The relevant formula in the models considered is easily found by simply taking into account that $Y_A(K)$ is complex. We find then ($\lambda = 0.2252$)

$$\boxed{\mathcal{B}(K_L \to \mu^+\mu^-)_{\rm SD} = 2.01 \cdot 10^{-9} \left[\frac{{\rm Re}Y_{\rm eff}}{\lambda^5} + \frac{{\rm Re}\lambda_c}{\lambda} P_c\,(Y(K))\right]^2,} \tag{15.101}$$

where $P_c\,(Y(K)) = 0.115 \pm 0.017$ [625] and

$$Y_{\rm eff} = V_{ts}^* V_{td} Y_A(K). \tag{15.102}$$

As LH and RH couplings in $Y_A(K)$ in (15.77) enter with opposite signs, the impact of the upper bound in (9.268) on the observables in which these signs are equal is markedly different. This is the case of decays $K^+ \to \pi^+\nu\bar{\nu}$ and $K_{\rm L} \to \pi^0\nu\bar{\nu}$, which we will discuss next.

Downloaded from https://www.cambridge.org/core. UNIVERSIDAD AUTONOMA METROPOLITANA, on 17 Nov 2026 at 22:50:50, subject to the Cambridge Core terms of use, available at https://www.cambridge.org/core/terms. https://doi.org/10.1017/9781139524100.021

$K^+ \to \pi^+ \nu\bar{\nu}$ and $K_L \to \pi^0 \nu\bar{\nu}$

Generalizing SM expressions for these two branching ratios to the case at hand, we obtain

$$\boxed{\mathcal{B}(K^+ \to \pi^+ \nu\bar{\nu}) = \kappa_+ \left[\left(\frac{\mathrm{Im}X_{\mathrm{eff}}}{\lambda^5}\right)^2 + \left(\frac{\mathrm{Re}X_{\mathrm{eff}}}{\lambda^5} + \frac{\mathrm{Re}\lambda_c}{\lambda} P_c(X)\right)^2\right],} \tag{15.103}$$

$$\boxed{\mathcal{B}(K_L \to \pi^0 \nu\bar{\nu}) = \kappa_L \left(\frac{\mathrm{Im}X_{\mathrm{eff}}}{\lambda^5}\right)^2,} \tag{15.104}$$

with $\kappa_{+,L}$ and $P_c(X)$ unchanged and given in (9.184) and (9.186), respectively.

The short-distance contributions are described by

$$X_{\mathrm{eff}} = V_{ts}^* V_{td} (X_L(K) + X_R(K)), \tag{15.105}$$

where $X_{L,R}(K)$ are given in (15.73) and (15.74). As mentioned earlier the signs in LH and RH contributions are now the same, making the identification of RH currents on the basis of these decays difficult. However, such an identification is possible when $K^+ \to \pi^+ \nu\bar{\nu}$ and $K_L \to \mu^+\mu^-$ are considered simultaneously. We will discuss this later.

$K_S \to \mu\bar{\mu}$

In addition to $K_{\mathrm{L}} \to \pi^0 \nu\bar{\nu}$, the decay $K_S \to \mu\bar{\mu}$ provides another sensitive probe of imaginary parts of short-distance couplings. Its branching fraction receives long-distance (LD) and short-distance (SD) contributions, which are added incoherently in the total rate [626, 630]. This is in contrast to the decay $K_L \to \mu\bar{\mu}$, where LD and SD amplitudes interfere, and moreover as seen in (15.101) $\mathcal{B}(K_L \to \mu\bar{\mu})$ is sensitive to real parts of couplings. The SD part of $\mathcal{B}(K_S \to \mu\bar{\mu})$ is given as

$$\boxed{\mathcal{B}(K_S \to \mu\bar{\mu})_{\mathrm{SD}} = \tau_{K_S} \frac{G_F^2 \alpha_e^2}{8\pi^3} m_K f_K^2 \beta_\mu m_\mu^2 \,\mathrm{Im}^2 \left[\lambda_t^{sd} C_{10,\mathrm{SM}} + \frac{\pi}{\alpha_e} v^2 \left(C_{10,\mathrm{NP}}^{\mu\mu sd} - C_{10',\mathrm{NP}}^{\mu\mu sd}\right)\right],} \tag{15.106}$$

where $v = 246\,\mathrm{GeV}$ and relative to the SM expression in (9.270), we have included NP contributions from Z' exchanges. Recall that in K decays also the notation $C_{10} = C_{7A}$ is used. The experimental status of this decay and the SM prediction are given in (9.271) and (9.272), respectively.

$B \to \{X_s, K, K^*\} \nu\bar{\nu}$

In Section 9.6.7 we have expressed the branching ratios of these decays in terms of the parameters ϵ and η. In Z' models they are given by

$$\boxed{\epsilon^2 = \frac{|X_{\mathrm{L}}(B_s)|^2 + |X_{\mathrm{R}}(B_s)|^2}{|\eta_X X_0(x_t)|^2}, \qquad \eta = \frac{-\mathrm{Re}\left(X_{\mathrm{L}}(B_s) X_{\mathrm{R}}^*(B_s)\right)}{|X_{\mathrm{L}}(B_s)|^2 + |X_{\mathrm{R}}(B_s)|^2},} \tag{15.107}$$

with $X_{L,R}(B_s)$ defined in (15.75) and (15.76).

Downloaded from https://www.cambridge.org/core. UNIVERSIDAD AUTONOMA METROPOLITANA, on 17 Nov 2026 at 22:50:50, subject to the Cambridge Core terms of use, available at https://www.cambridge.org/core/terms. https://doi.org/10.1017/9781139524100.021

$K_L \to \pi^0 \ell^+ \ell^-$

The rare decays $K_L \to \pi^0 e^+ e^-$ and $K_L \to \pi^0 \mu^+ \mu^-$ are dominated by CP-violating contributions, and we discussed them already within the SM in Sections 6.6.2 and 9.7.3. The numerical analysis in [611] demonstrated that the present experimental upper bounds on $K_L \to \pi^0 e^+ e^-$ and $K_L \to \pi^0 \mu^+ \mu^-$ have no impact on $K^+ \to \pi^+ \nu\bar{\nu}$ and $K_L \to \pi^0 \nu\bar{\nu}$ decays, and the present data on $K^+ \to \pi^+ \nu\bar{\nu}$ do not allow to reach the bounds in the Z' scenarios considered. The same applies to Z scenarios considered in the next section. Before presenting explicit formulas for $K_L \to \pi^0 \ell^+ \ell^-$ in Z' models, let us make a few comments that will facilitate their derivation.

Detailed studies in concrete models show the following. In the LHT model the branching ratios for both decays can be enhanced at most by a factor of 1.5 [700, 921]. Slightly larger effects are still allowed in Randall–Sundrum models with custodial protection (RSc) for left-handed couplings [920]. Larger effects are found if the custodial protection is absent [922].

Probably the most extensive model-independent analysis of decays in question has been performed in [637], where formulas for branching ratios for both decays in the presence of new operators have been presented. These formulas have been already used in [700, 923] for the LHT model and in [920] in the case of RSc. In the LHT model, where only SM operators are present, the effects of NP can be compactly summarized by generalization of the real SM functions $Y_0(x_t)$ and $Z_0(x_t)$ to two complex functions $Y(K)$ and $Z(K)$, respectively. As demonstrated in the context of the corresponding analysis within RSc [920], also in the presence of RH currents two complex functions $\tilde{Y}(K)$ and $\tilde{Z}(K)$ are sufficient to describe jointly the SM and NP contributions. But as indicated with a "tilde," their structure differs from the one used in the LHT model because of RH current contributions.

Consequently, the LHT formulas (8.1)–(8.8) of [700] with $\tilde{Y}(K)$ and $\tilde{Z}(K)$ given on next page can be used in the context of tree-level neutral gauge boson exchanges like Z' and Z ones. The original papers behind these formulas can be found in [131, 634–637]. Here we recall these formulas for completeness.

We have then

$$\boxed{\mathcal{B}(K_L \to \pi^0 \ell^+ \ell^-) = \left(C^\ell_{\rm dir} \pm C^\ell_{\rm int} |a_s| + C^\ell_{\rm mix} |a_s|^2 + C^\ell_{\rm CPC}\right) \cdot 10^{-12},} \tag{15.108}$$

where

$$C^e_{\rm dir} = (4.62 \pm 0.24)(\omega^2_{7V} + \omega^2_{7A}), \qquad C^\mu_{\rm dir} = (1.09 \pm 0.05)(\omega^2_{7V} + 2.32\omega^2_{7A}), \tag{15.109}$$

$$C^e_{\rm int} = (11.3 \pm 0.3)\omega_{7V}, \qquad C^\mu_{\rm int} = (2.63 \pm 0.06)\omega_{7V}, \tag{15.110}$$

$$C^e_{\rm mix} = 14.5 \pm 0.05, \qquad C^\mu_{\rm mix} = 3.36 \pm 0.20, \tag{15.111}$$

$$C^e_{\rm CPC} \simeq 0, \qquad C^\mu_{\rm CPC} = 5.2 \pm 1.6, \tag{15.112}$$

$$|a_s| = 1.2 \pm 0.2, \tag{15.113}$$

Downloaded from https://www.cambridge.org/core. UNIVERSIDAD AUTONOMA METROPOLITANA, on 17 Nov 2026 at 22:50:50, subject to the Cambridge Core terms of use, available at https://www.cambridge.org/core/terms. https://doi.org/10.1017/9781139524100.021

with

$$\omega_{7V} = \frac{1}{2\pi}\left[P_0 + \frac{|\tilde{Y}(K)|}{\sin^2\theta_W}\frac{\sin\beta_Y^K}{\sin(\beta-\beta_s)} - 4|\tilde{Z}(K)|\frac{\sin\beta_Z^K}{\sin(\beta-\beta_s)}\right]\left[\frac{\mathrm{Im}\,\lambda_t}{1.4\cdot 10^{-4}}\right], \quad (15.114)$$

$$\omega_{7A} = -\frac{1}{2\pi}\frac{|\tilde{Y}(K)|}{\sin^2\theta_W}\frac{\sin\beta_Y^K}{\sin(\beta-\beta_s)}\left[\frac{\mathrm{Im}\,\lambda_t}{1.4\cdot 10^{-4}}\right], \quad (15.115)$$

where $P_0 = 2.88 \pm 0.06$

$$\beta_Y^K = \beta - \beta_s - \theta_Y^K, \qquad \beta_Z^K = \beta - \beta_s - \theta_Z^K. \quad (15.116)$$

The expressions for ω_{7V} and ω_{7A} in terms of WC of the SMEFT can be found in [667].

Finally, as derived in [611] from the formulas in [920],

$$\tilde{Y}(K) = \eta_Y Y_0(x_t) + \left[\frac{\Delta_A^{\mu\bar{\mu}}(Z')}{M_{Z'}^2 g_{\rm SM}^2}\right]\frac{\Delta_V^{sd}(Z')}{V_{ts}^* V_{td}}, \quad (15.117)$$

$$\tilde{Z}(K) = Z_0(x_t) + \frac{1}{4\sin^2\vartheta_W}\left[\frac{2\Delta_R^{\mu\bar{\mu}}(Z')}{M_{Z'}^2 g_{\rm SM}^2}\right]\frac{\Delta_V^{sd}(Z')}{V_{ts}^* V_{td}}. \quad (15.118)$$

$\Delta_{V,A}^{sd}(Z')$ are defined in (15.54). We indeed observe that $\tilde{Y}(K)$ differs from $Y(K)$ in (15.77).

The presence of additional coupling $\Delta_R^{\mu\bar{\mu}}(Z')$, in addition to $\Delta_A^{\mu\bar{\mu}}(Z')$, introduces as in $B \to K^*\ell^+\ell^-$, $B \to K\ell^+\ell^-$ and $B \to X_s\ell^+\ell^-$ two new parameters and allows thereby to avoid present constraints if necessary. In the case of FCNC processes mediated by Z, which will be discussed in Section 15.5, all leptonic couplings are known, and the predictions for $K_L \to \pi^0 e^+e^-$ and $K_L \to \pi^0\mu^+\mu^-$ are more specific.

15.4.6 Lessons on NP Patterns in Z' Scenarios

A detailed phenomenology of tree-level Z' exchanges has been presented in [601, 611, 851]. We will now summarize the highlights of these papers in the form of lessons gained through these analyses. Numerous plots related to these lessons can be found in these papers.

We begin with the K-meson system and concentrate on the results obtained in [851]. The summary of the lessons is rather brief. On the other hand, the presentation in [851] is very detailed with numerous analytic expressions that could be useful for nonexperts who want to understand the details of the patterns of various effects. In the latter paper the main goal was to investigate what are the implications of the ε'/ε anomaly discussed in Chapter 10 on rare decays $K^+ \to \pi^+\nu\bar{\nu}$ and $K_{\rm L} \to \pi^0\nu\bar{\nu}$ in various scenarios for the Z' couplings to quarks.

We begin with the K-meson system. Z' models exhibit quite different pattern of NP effects in the K-meson system than the Z scenarios discussed later in Section 15.5. In Z scenarios only electroweak penguin (EWP) Q_8 and Q_8' operators can contribute in an

Downloaded from https://www.cambridge.org/core. UNIVERSIDAD AUTONOMA METROPOLITANA, on 17 Nov 2026 at 22:50:50, subject to the Cambridge Core terms of use, available at https://www.cambridge.org/core/terms. https://doi.org/10.1017/9781139524100.021

important manner to ε'/ε because of flavor-dependent diagonal Z coupling to quarks. But in Z' models the diagonal quark couplings can be flavor universal so that QCD penguin operators (QCDP) (Q_6, Q_6') can dominate NP contributions to ε'/ε. Interestingly, the pattern of NP in rare K decays depends on whether NP in ε'/ε is dominated by QCDP or EWP operators [851]. Let us discuss this briefly.

In the strategy in [851] the central role is played by ε'/ε and ε_K for which in the presence of NP contributions we have

$$\frac{\varepsilon'}{\varepsilon} = \left(\frac{\varepsilon'}{\varepsilon}\right)^{\rm SM} + \left(\frac{\varepsilon'}{\varepsilon}\right)^{\rm NP}, \qquad \varepsilon_K \equiv e^{i\varphi_\varepsilon}\left[\varepsilon_K^{\rm SM} + \varepsilon_K^{\rm NP}\right]. \tag{15.119}$$

As the size of NP contributions is presently not precisely known, the strategy of [851] is to parametrize this contributions as

$$\left(\frac{\varepsilon'}{\varepsilon}\right)^{\rm NP} = \kappa_{\varepsilon'} \cdot 10^{-3}, \qquad 0.5 \le \kappa_{\varepsilon'} \le 1.5 \tag{15.120}$$

and

$$(\varepsilon_K)^{\rm NP} = \kappa_\varepsilon \cdot 10^{-3}, \qquad 0.1 \le \kappa_\varepsilon \le 0.4. \tag{15.121}$$

The ranges for $\kappa_{\varepsilon'}$ and κ_ε only indicate possible size of NP contributions as argued in [851] in 2016. In 2019 κ_ε is more likely in the range $-0.2 \le \kappa_\varepsilon \le 0.2$ [874]. Anyway, using the formulas in [851] $\kappa_{\varepsilon'}$ and κ_ε can also be treated as free parameters. Once $|V_{cb}|$ will be precisely known the size and sign of the latter will be determined. The results summarized following are based on (15.121).

To simplify the discussion we assume that only LH flavor-violating coupling of Z' are nonvanishing. The first general findings of [851] are then as follows:

- For a given κ_ε that determines the imaginary part of $\Delta_L^{sd}(Z')$, the real part of this coupling is determined for a not too large κ_ε from the ε_K.
- There is a large hierarchy between real and imaginary parts of the flavor-violating couplings implied by anomalies in QCDP and EWP scenarios. As shown in [851] in the case of QCDP imaginary parts dominate over the real ones, while in the case of EWP this hierarchy is opposite unless the κ_ε is very small. This is related to the fact that strong suppression of QCDP to ε'/ε by the factor 1/22 coming from $\Delta I = 1/2$ rule requires a large imaginary coupling in QCDP scenario to enhance significantly this ratio. This suppression is absent in the case of EWP, and this coupling can be smaller.

Because of this important difference in the manner QCDP and EWP enter ε'/ε, there are striking differences in the implications for the correlation between $K^+ \to \pi^+\nu\bar{\nu}$ and $K_{\rm L} \to \pi^0\nu\bar{\nu}$ in these two NP scenarios if significant NP contributions to ε'/ε are required. Various plots in [851] show clearly the differences between QCDP and EWP scenarios. We refer to [851] for more details, in particular analytic derivation of all these results. We extract from these results the following lessons:

Lesson 1: In the case of QCDP scenario the correlation between $\mathcal{B}(K_{\rm L} \to \pi^0\nu\bar{\nu})$ and $\mathcal{B}(K^+ \to \pi^+\nu\bar{\nu})$ takes place along the branch parallel to the Grossman–Nir (GN) bound

Downloaded from https://www.cambridge.org/core. UNIVERSIDAD AUTONOMA METROPOLITANA, on 17 Nov 2026 at 22:50:50, subject to the Cambridge Core terms of use, available at https://www.cambridge.org/core/terms. https://doi.org/10.1017/9781139524100.021

[602] in (9.218) that is illustrated in Figure 15.6. Moreover, this feature is independent of $M_{Z'}$. Also the dependence on κ_ε is negligible.

Lesson 2: In the EWP scenario the correlation between $\mathcal{B}(K_L \to \pi^0\nu\bar{\nu})$ and $\mathcal{B}(K^+ \to \pi^+\nu\bar{\nu})$ proceeds away from this branch for diagonal quark couplings $O(1)$ if NP in ε_K is present and it is very different from the one of the QCDP case as seen in the plots in [851]. NP effects are also much smaller than in QCDP scenario.

Lesson 3: For fixed values of the neutrino and diagonal quark couplings in ε'/ε, the predicted enhancements of $\mathcal{B}(K_L \to \pi^0\nu\bar{\nu})$ and $\mathcal{B}(K^+ \to \pi^+\nu\bar{\nu})$ are much larger when NP in QCDP is required to remove the ε'/ε anomaly than it is in the case of EWP. This is simply related to the fact, as mentioned earlier, that the $\Delta I = 1/2$ rule suppresses QCDP contributions to ε'/ε so that QCDP operators are less efficient in enhancing ε'/ε than EWP operators. Consequently, the imaginary parts of the flavor-violating couplings are required to be larger, implying then larger effects in rare K decays. Only for the diagonal quark couplings $O(10^{-2})$ the requirement of shifting upwards ε'/ε implies large effects in $K^+ \to \pi^+\nu\bar{\nu}$ and $K_L \to \pi^0\nu\bar{\nu}$ in EWP scenario. See [851] for a detail discussion of this point and a more detailed analysis to appear in 2020.

Lesson 4: In QCDP scenario ΔM_K is *suppressed*, and this effect increases with increasing $M_{Z'}$ whereas in the EWP scenario ΔM_K is *enhanced*, and this effect decreases with increasing $M_{Z'}$ as long as real couplings dominate. Already on the basis of this property one could differentiate between these two scenarios when the SM prediction for ΔM_K improves. Interestingly, the recent RBC-UKQCD result in (8.18), if confirmed, would then at first sight favor QCDP scenario. Yet, this conclusion is only true if the $Z'\bar{q}q$ couplings are $O(1)$ and RH FCNC couplings are absent. In LH scenario with couplings $Z'\bar{q}q = O(10^{-2})$ also EWP scenario would lead to the suppression of ΔM_K due to enhanced imaginary parts of FCNC couplings required for the explanation of the ε'/ε anomaly. This is clearly seen in the relevant formulas in [851]. But the presence of both LH and RH FCNC couplings, introducing more parameters, would enrich the analysis and only correlations with other observables, in particular with the branching ratios for $K^+ \to \pi^+\nu\bar{\nu}$ and $K_L \to \pi^0\nu\bar{\nu}$ could lead to clear cut conclusions.

In summary once the results from NA62 and KOPIO are available, it should be possible to select between various scenarios just presented.

Yet, one should realize that the analysis in [851] included only QCD evolution, and it would be of interest to see how the lessons just listed are modified when the full machinery of the SMEFT is switched on. In particular the effects of Yukawa couplings could play here a significant role. We expect that this issue should be clarified in 2020.

15.4.7 $K_L \to \pi^0\nu\bar{\nu}, K^+ \to \pi^+\nu\bar{\nu}$ and ε_K beyond the SM

It should be stressed that the correlation between $K_L \to \pi^0\nu\bar{\nu}$ with $K^+ \to \pi^+\nu\bar{\nu}$ gives us generally more information about NP than the correlation between these two decays and ε'/ε. The reason is very simple. While the flavor-violating couplings in $K_L \to \pi^0\nu\bar{\nu}$, $K^+ \to \pi^+\nu\bar{\nu}$, and ε'/ε are the same in a given model, the flavor conserving ones in ε'/ε involving quarks are generally different from neutrino ones, and some assumptions about them have

Downloaded from https://www.cambridge.org/core. UNIVERSIDAD AUTONOMA METROPOLITANA, on 17 Nov 2026 at 22:50:50, subject to the Cambridge Core terms of use, available at https://www.cambridge.org/core/terms. https://doi.org/10.1017/9781139524100.021

to be made as done in [851] and also in a number of simplified scenarios considered in [601]. Table 3 in [851] illustrates this point.

However, as pointed out by Monika Blanke [924], more information about the nature of NP can be obtained by looking simultaneously at $K_L \to \pi^0\nu\bar{\nu}$, $K^+ \to \pi^+\nu\bar{\nu}$, and ε_K, simply because the latter depends only on the flavor-violating couplings, which equal to those in $K_L \to \pi^0\nu\bar{\nu}$ and $K^+ \to \pi^+\nu\bar{\nu}$. We will now summarize the insight gained from [924] that have been verified in Z' models considered in [611] and also in [601].

To this end let us parametrize X_{eff} in (15.105) as follows [601]

$$X_{\text{eff}} = V_{ts}^* V_{td}(X_L(K) + X_R(K)) \equiv V_{ts}^* V_{td} X_L^{\text{SM}}(K)(1 + \xi e^{i\theta}), \tag{15.122}$$

so that the short-distance dynamics is encapsulated in two real parameters ξ and θ that vanish in the SM. Measuring these branching ratios one day will allow to determine those parameters and, comparing them with their expectations in concrete models, to obtain insight into the flavor structure of the NP contributions. Those, as we have seen earlier, can be dominated by left-handed currents, by right-handed currents, or by both with similar magnitudes and phases. In general one can then distinguish between three classes of models [924]:

1. Models with a CKM-like structure of flavour interactions. If based on flavor symmetries only, they include MFV and $\text{U}(2)^3$ models. In this case the function $X_L(K)$ is real, and $X_R(K) = 0$. There is then only one variable to our disposal, the value of $X_L(K)$, and the only allowed values of both branching ratios are on the two broad light gray branches in Figure 15.6 that touch the origin of the plot. But due to stringent correlations with other observables present in this class of models, only certain ranges for $\mathcal{B}(K^+ \to \pi^+\nu\bar{\nu})$ and $\mathcal{B}(K_L \to \pi^0\nu\bar{\nu})$ are still allowed, which have been determined in simplified models in [601].
2. Models with new flavor- and CP-violating interactions in which either left-handed currents or right-handed currents fully dominate, implying that left-right operator contributions to ε_K can be neglected. In this case there is a strong correlation between NP contributions to ε_K and $K \to \pi\nu\bar{\nu}$ and the ε_K constraint implies the thin light gray branch structure shown in Figure 15.6. On the horizontal branch NP contribution to $K \to \pi\nu\bar{\nu}$ is real and therefore vanishes in the case of $K_L \to \pi^0\nu\bar{\nu}$. On the second branch NP contribution is purely imaginary, and this branch is parallel to the Grossman–Nir (GN) bound [602] shown in the plot. In practice, due to uncertainties in ε_K, there are moderate deviations from this structure, which is characteristic for the LHT model [921], or Z or Z' FCNC scenarios with either pure LH or RH couplings [211, 611].
3. If left-right operators have significant contribution to ε_K or generally if the correlation between ε_K and $K \to \pi\nu\bar{\nu}$ is weak or absent, the two-branch structure is also absent. Dependent on the values of ξ or θ, any value of $\mathcal{B}(K^+ \to \pi^+\nu\bar{\nu})$ and $\mathcal{B}(K_L \to \pi^0\nu\bar{\nu})$ is in principle possible. The dark gray region in Figure 15.6 shows the resulting structure for a fixed value of ξ and $0 \le \theta \le 2\pi$. Randall–Sundrum models with custodial protection belong to this class of models [920]. However, it should be kept in mind that usually the removal of the correlation with ε_K requires subtle cancellations between different contributions to ε_K and consequently some tuning of parameters [211, 920].

Downloaded from https://www.cambridge.org/core. UNIVERSIDAD AUTONOMA METROPOLITANA, on 17 Nov 2026 at 22:50:50, subject to the Cambridge Core terms of use, available at https://www.cambridge.org/core/terms. https://doi.org/10.1017/9781139524100.021

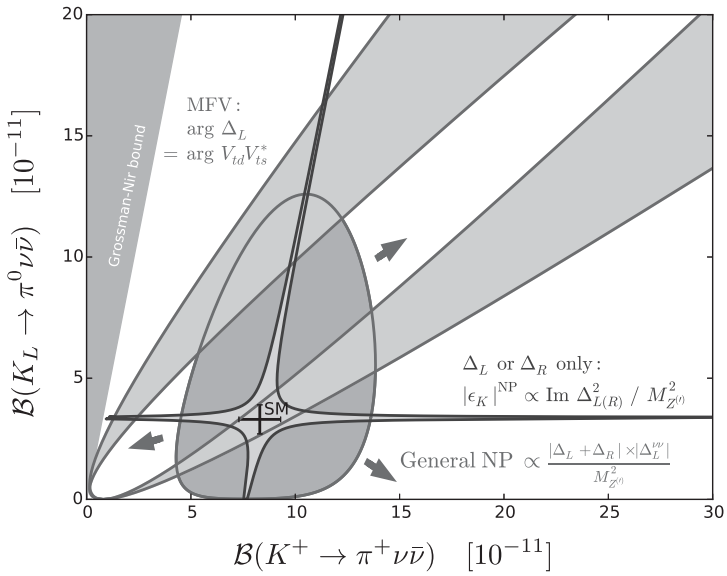


Figure 15.6 Correlations in the $\mathcal{B}(K^+ \to \pi^+\nu\bar{\nu})$ versus $\mathcal{B}(K_L \to \pi^0\nu\bar{\nu})$ plane beyond the SM [601]. See text for explanations.

More details with colorful plots can be found in [601, 924] and also in figure 35 of [208], where the dependence of both branching ratios on ξ for various values of θ is shown.

15.4.8 Z' Facing B Physics Anomalies

In Chapter 12 we mentioned various B physics anomalies, and we will return to them again in Chapter 18, where we will compare various explanations of them. Here we would like to concentrate on Z' models.

In fact, general Z' models can easily explain the $b \to s\ell^+\ell^-$ anomalies but cannot explain the charged current anomalies without the participation of other new particles. Beginning with $b \to s\ell^+\ell^-$ anomalies, the most successful Z' models are the following ones.

i) Z' models with vector couplings to muons are free of gauge anomalies and consequently offer a natural $C_9^{\rm NP}$-like solution. The most extensively studied models of this type are $L_\mu - L_\tau$ models [925–931] in which NP is absent in electron channels. Unfortunately in these models, unless some additional heavy particles are added, only very small NP effects in $B_{s,d} \to \mu^+\mu^-$ and $K \to \pi\nu\bar{\nu}$ transitions are possible. On the other hand, they can explain the $(g-2)_\mu$ anomaly, which will be discussed in Section 17.4.

ii) Besides $L_\mu - L_\tau$, various other combinations of gauged flavor symmetries have been used to construct Z' models that can address the $b \to s\ell^+\ell^-$ anomalies [904, 927, 928, 932–942].

iii) Also models with loop-induced Z' couplings [943] and Z' models with heavy vector-like fermions [933] can work. Yet when choosing properly Z' couplings to explain the

Downloaded from https://www.cambridge.org/core. UNIVERSIDAD AUTONOMA METROPOLITANA, on 17 Nov 2026 at 22:50:50, subject to the Cambridge Core terms of use, available at https://www.cambridge.org/core/terms. https://doi.org/10.1017/9781139524100.021

$b \to s\ell^+\ell^-$ anomalies, one has to be careful that no gauge anomalies are introduced. We will discuss this point soon.

As far as $R(D)$ and $R(D^*)$ anomalies are concerned, they cannot be explained in Z' models without the addition of charged current processes or new particles generating them. Here we briefly describe a few papers that tried to address these anomalies in addition to $b \to s\mu^+\mu^-$ ones. The leptoquarks and vector-like fermions that are mentioned next are discussed in detail in Chapter 16.

In [931] the $R(K^{(*)})$ and $R(D^{(*)})$ anomalies have been addressed in a model with the $U(1)_{L_\mu - L_\tau}$ gauge symmetry. To be able to achieve this goal, one vector-like lepton (VLL) doublet and one singlet scalar leptoquark (LQ) S_1 are considered. The $b \to sZ'$ effective interaction relevant for the $R(K^{(*)})$ is generated at one-loop from VLL and LQ, and $R(D^{(*)})$ is governed by LQ. While this model can, as claimed by the authors, explain $R(K^{(*)})$ and $R(D^{(*)})$ anomalies, it will likely fail in the case of ε'/ε unless it can be generated at tree-level. We will discuss this issue in Section 16.4.

Next models in which the Z' is part of a $SU(2)_L$ triplet have been suggested as a simultaneous explanation of the $b \to s\ell^+\ell^-$ anomalies and of $R(D)$ and $R(D^*)$ ones [719, 769, 777, 933, 934, 944, 945].

In [946] Z' model with MFV has been considered and $b \to s\ell^+\ell^-$ anomalies analyzed. Constraints from $\mu \to e\gamma$, $l_i \to \ell_j\ell_k\ell_l$, $B^0 - \bar{B}^0$ mixing that all appear at tree-level have been taken into account. Results for $\tau \to 3\mu$, $B \to Ke\mu$, $K_L \to e\mu$, $Z \to \ell\ell'$ are found close to the experimental bounds.

In [942] flavor symmetry group $SU(3)_L \times SU(3)_R$ has been considered with the goal to connect NP responsible for the $R(K^{(*)})$ anomalies with the understanding of the origin of flavor. As this symmetry is gauged and broken spontaneously, we are dealing eventually with 16 new heavy gauged bosons, one of them being Z', light enough to explain $R(K^{(*)})$ anomalies.

As far as a light Z' is concerned, it has been considered in [947] with the goal to explain low q^2 region of the $R(K^*)$ anomaly. In [948] the role of Z' in $R(K^{(*)})$ and $(g-2)_\mu$ anomalies has been considered. Finally, in [949, 950] lepton-flavor violating Z' has been used to explain $(g-2)_\mu$ anomaly. A light Z' is again required. See also [951, 952].

One important constraint on Z' explanations of $b \to s\ell^+\ell^-$ anomalies comes from $B_s - \bar{B}_s$-mixing [953–955]. The Z' mass can be at most several TeV; otherwise an explanation of the anomalies requires couplings to leptons that are nonperturbatively large. This constraint will increase in importance, when lattice QCD calculations increase the precision on hadronic matrix elements. Most recent analysis of collider constraints on simple Z' models can be found in [955]. A combination of $B_s - \bar{B}_s$-mixing constraint and collider data implies further reduction of the parameter space in simple Z' models, but the effect is clearly model dependent.

We should also mention that certain concrete models, like 331 models, in which LFUV is absent at tree-level, will be disfavored [612, 956] if LFUV will be confirmed in the future. On the other hand, as discussed in Section 16.2, some of them can explain the suppression of C_9 or C_{10}.

As described in detail in [957], neutrino trident production can provide stringent constraints on Z' models. It is a process by which a neutrino, scattering off the Coulomb

Downloaded from https://www.cambridge.org/core. UNIVERSIDAD AUTONOMA METROPOLITANA, on 17 Nov 2026 at 22:50:50, subject to the Cambridge Core terms of use, available at https://www.cambridge.org/core/terms. https://doi.org/10.1017/9781139524100.021

field of a heavy nucleus, generates a pair of charged leptons: $\nu_\mu \to \nu_\mu \mu^+ \mu^-$. Future measurements of this process at DUNE will be highly sensitive to NP in general. But in particular, as found in this paper, they will cover almost entirely the parameter space of the $L_\mu - L_\tau$ models. Finally in an interesting paper [1327] the ε'/ε anomaly, the $B \to K\pi$ puzzle, and $b \to s\ell^+\ell^-$ anomalies have been addressed simultaneously in an $U(2)^3$ model.

15.4.9 Gauge (triangle) Anomalies and Z'

Preliminaries

One of the important issues often not considered in papers on Z' models is the cancellation of the gauge anomalies, called also triangle anomalies, that naturally are generated in the presence of an additional $U(1)'$ gauge group. This issue has been studied in [730, 904, 935, 938, 958–964] but in most of these papers, exception being [938, 959], flavor universality has been assumed. Also in most of these papers Z' couplings to the first generation have been set to zero and similar for complex phases. For recent studies of anomaly-free models see [1323–1325].

Here we would like to list all anomaly equations without any assumptions on $U(1)'$ charges and present a simple solution that has been found in collaboration with Jason Aebischer, Maria Cerdá-Sevilla, and Fulvia De Fazio. We assume that only SM fermions, except for heavy right-handed neutrinos, are present.

As Z' is a singlet under the SM gauge group, the left-handed leptons in a given doublet ℓ_i with $i = 1, 2, 3$ must have the same $U(1)'$ charges and similar for the members of left-handed quark doublets q_i. On the other hand, the right-handed leptons ν_i and e_i can have different $U(1)'$ charges and the same for right-handed quarks u_i and d_i. We will allow all these charges to be generation dependent. This is required to generate flavor-violating neutral currents after rotating from flavor to mass eigenstate basis. The right-handed neutrinos will sometimes turn out to be relevant for the cancellation of the gauge anomalies.

Denoting by q_i and ℓ_i left-handed doublets and by u_i, d_i, ν_i, and e_i right-handed singlets allows us to drop the subscripts L and R on the fields. For convenience we recall their hypercharges:

$$y_{q_i} = 1/6, \qquad y_{u_i} = 2/3, \qquad y_{d_i} = -1/3, \qquad y_{\ell_i} = -1/2, \qquad y_{e_i} = -1. \tag{15.123}$$

General Formulas

The rules for calculating triangle anomalies can be found in any textbook on QFT. For a left-handed fermion in the loop, one just multiplies the couplings (charges) of this fermion to a given gauge boson in the vertex. For a right-handed fermion an additional overall minus sign is included. This means that for fermions with left-handed and right-handed charges being equal, that is, for vector-like fermions, there are no gauge anomalies. The SM fermions are not vector-like, and the cancellation of gauge anomalies related to the SM gauge group takes place between quarks and leptons. To this end one has to remember that a color factor of 3 has to be introduced when a quark is running in the loop. As the gauge

Downloaded from https://www.cambridge.org/core. UNIVERSIDAD AUTONOMA METROPOLITANA, on 17 Nov 2026 at 22:50:50, subject to the Cambridge Core terms of use, available at https://www.cambridge.org/core/terms. https://doi.org/10.1017/9781139524100.021

anomalies must be cancelled, the values of the gauge couplings, as well as the result of integrating over momentum in the triangle diagram, are irrelevant. Moreover, being mass independent, this integral is universal for all fermions. Only the charges under a given gauge group matter. In the case of U(1)′ we will denote these charges by

$$z_{q_i}, \quad z_{u_i}, \quad z_{d_i}, \quad z_{l_i}, \quad z_{\nu_i}, \quad z_{e_i}, \tag{15.124}$$

with $i = 1, 2, 3$ labeling different generations.

There are six gauge anomalies generated by the presence of Z' [958]. Four of them are linear in U(1)′ charges, one quadratic in them, and one cubic one. It is useful to begin with linear equations as they are simpler and teach us already something.

The structure of the four linear equations can be simplified by defining

$$z_q = z_{q_1} + z_{q_2} + z_{q_3}, \qquad z_u = z_{u_1} + z_{u_2} + z_{u_3}, \qquad z_d = z_{d_1} + z_{d_2} + z_{d_3}, \tag{15.125}$$

$$z_l = z_{l_1} + z_{l_2} + z_{l_3}, \qquad z_\nu = z_{\nu_1} + z_{\nu_2} + z_{\nu_3}, \qquad z_e = z_{e_1} + z_{e_2} + z_{e_3}. \tag{15.126}$$

Then the $[\mathrm{SU}(3)_c]^2\mathrm{U}(1)'$, $[\mathrm{SU}(2)]^2\mathrm{U}(1)'$, and $[\mathrm{U}(1)_Y]^2\mathrm{U}(1)'$ anomaly cancellation conditions can be written, respectively, as

$$\boxed{A_{33z} = 2z_q - z_u - z_d = 0,} \tag{15.127}$$

$$\boxed{A_{22z} = 3z_q + z_l = 0,} \tag{15.128}$$

$$\boxed{A_{11z} = \frac{1}{6}z_q - \frac{4}{3}z_u - \frac{1}{3}z_d + \frac{1}{2}z_l - z_e = 0.} \tag{15.129}$$

The fourth linear condition involves two gravitons and Z' and is given by

$$A_{GGz} = 3[2z_q - z_u - z_d] + 2z_l - z_e - z_\nu = 0, \tag{15.130}$$

but using (15.127) it reduces to

$$\boxed{A_{GGz} = 2z_l - z_e - z_\nu = 0.} \tag{15.131}$$

To write the remaining two anomaly cancellation conditions in a transparent form, we define

$$z_f^{(3)} = \sum_{i=1,2,3} z_{fi}^3, \qquad z_f^{(2)} = \sum_{i=1,2,3} z_{fi}^2. \tag{15.132}$$

Then the $\mathrm{U}(1)_Y[\mathrm{U}(1)']^2$ anomaly cancellation condition is given by

$$\boxed{A_{1zz} = [z_q^{(2)} - 2z_u^{(2)} + z_d^{(2)}] - [z_l^{(2)} - z_e^{(2)}] = 0,} \tag{15.133}$$

and the one for $[\mathrm{U}(1)']^3$ anomaly by

$$\boxed{A_{zzz} = 3[2z_q^{(3)} - z_u^{(3)} - z_d^{(3)}] + [2z_l^{(3)} - z_\nu^{(3)} - z_e^{(3)}] = 0.} \tag{15.134}$$

It is a good exercise to check these equations.

Downloaded from https://www.cambridge.org/core. UNIVERSIDAD AUTONOMA METROPOLITANA, on 17 Nov 2026 at 22:50:50, subject to the Cambridge Core terms of use, available at https://www.cambridge.org/core/terms. https://doi.org/10.1017/9781139524100.021

Solution to Linear Equations

There are four linear equations with six unknowns. This implies that we can express four of the charges in (15.125) and (15.126) in terms of the two remaining ones. We give here two examples:

d-case
We choose as free parameters z_q and z_d, then

$$z_u = 2z_q - z_d, \qquad z_l = -3z_q, \qquad z_e = z_d - 4z_q, \qquad z_\nu = -2z_q - z_d. \tag{15.135}$$

u-case
We choose as free parameters z_q and z_u, then

$$z_d = 2z_q - z_u, \qquad z_l = -3z_q, \qquad z_e = -z_u - 2z_q, \qquad z_\nu = -4z_q + z_u. \tag{15.136}$$

We emphasize that the simple relations (15.135) and (15.136) are model-independent. Moreover, it turns out, that the solutions in both cases solve in the case of flavor universality the quadratic and cubic equations (15.133)–(15.134). Furthermore, the SM case for the hypercharges can be retrieved from these relations. This is not surprising because the same equations as (15.127), (15.128), (15.131), and (15.134) are obtained in the case of the $\mathrm{U}(1)_Y$ gauge boson, by simply replacing $z_f \to y_f$. Indeed, the anomaly equations are solved by choosing $z_{q_i} = 1/6$ independent of i as well as $z_{d_i} = -1/3$ in the d-case and $z_{u_i} = 2/3$ in the u-case.

A Simple Gauge Anomaly Free Model

To obtain phenomenologically interesting scenario we break flavor universality in all four families. But not to end up with many free parameters we break the flavor universality in a rather special manner. This simple model has been constructed by Fulvia De Fazio and analyzed by us four.

To this end let us denote by f one of the following fermions: $f = q, u, d, \ell, e, \nu$, and let us add a generation index: f_i for $i = 1, 2, 3$. We know that the SM hypercharge is generation universal so that $y_{f_i} = y_f \; \forall i = 1, 2, 3$. The solution of all equations is provided by the charges

$$\boxed{z_{f_i} = y_f + \epsilon_i, \qquad \sum_{i=1}^{3} \epsilon_i = 0} \tag{15.137}$$

so that we have

$$\boxed{z_f = \sum_{i=1}^{3} z_{f_i} = \sum_{i=1}^{3} (y_f + \epsilon_i) = 3y_f + \sum_{i=1}^{3} \epsilon_i = 3y_f + \epsilon, \qquad \epsilon = \sum_{i=1}^{3} \epsilon_i.} \tag{15.138}$$

It should be noted that the breakdown of flavor universality has been made in a very special manner:

Downloaded from https://www.cambridge.org/core. UNIVERSIDAD AUTONOMA METROPOLITANA, on 17 Nov 2026 at 22:50:50, subject to the Cambridge Core terms of use, available at https://www.cambridge.org/core/terms. https://doi.org/10.1017/9781139524100.021

- The parameters ϵ_i, while generation dependent, are universal within a given generation. For instance, ϵ_1 is the same not only for the members of the left-handed doublets q_1, ℓ_1 but also for right-handed singlets u_1, d_1, ν_1, and e_1. This implies that cancellation of gauge anomalies involves all generations as opposed to the SM, where it takes place within one generation. See (15.137).
- This implies that the shifts ϵ_i are vector-like, which allows for a straightforward solution of all anomaly cancellation equations. But as hypercharges of left-handed and right-handed fields, as seen in (15.123), differ from each other, the flavor-conserving Z' couplings are not vector-like.

It is a good exercise to check that indeed the charges in (15.137) satisfy six anomaly equations listed earlier. They are only satisfied if $\epsilon = 0$. Having only few parameters, the model implies correlations not only between various quark observables and between various lepton observables, but also in particular quark and lepton observables. The derivation of the relevant couplings proceeds as illustrated in Section 14.3.2. Details of this analysis should appear in 2020.

In [938] an additional $\mathrm{U}(1)_X$ gauge symmetry with $X = B_3 - L_\mu$, has been considered. Unlike other alternative schemes, which typically require the addition of new charged fermions or leptoquarks, all anomalies induced by this gauge symmetry, including gravitational ones, are canceled. This model then can explain $R(K^{(*)})$ anomalies with the help of Z'.

The cancellation of triangle anomalies in the preceding simple example can be verified by hand. In more complicated cases, and in particular when constructing models involving many new particles, computer programs turn out to be very useful. We refer to one recent analysis of this type [965], where references to earlier literature can be found. In particular in [966] the $\mathrm{U}(1)'$ charges of the third generation equal their hypercharges, with the first two generations being uncharged under $\mathrm{U}(1)'$. Even if hypercharge plays a role in this model, the model differs significantly from our model. In particular, ε'/ε and K-meson physics cannot be successfully addressed in the model in [966].

15.5 Beyond MFV: Z Boson with FCNC

15.5.1 Preliminaries

At first sight the discussion of FCNC mediated by Z' in the previous section and the numerous formulas presented there could be used for models in which FCNC are mediated by the SM Z boson already at tree-level. See Figures 15.7 and 15.8. In particular the following changes in all formulas could be made right away

- The flavor-violating couplings $\Delta^{ij}_{L,R}(Z')$ are replaced by $\Delta^{ij}_{L,R}(Z)$.
- Flavor-diagonal couplings of Z to quarks and leptons are replaced by SM ones, which reduces the number of free parameters. Explicit expressions are collected in Appendix B.
- $M_{Z'}$ is replaced by M_Z and $\mu_{Z'}$ by $m_t(m_t)$.

Downloaded from https://www.cambridge.org/core. UNIVERSIDAD AUTONOMA METROPOLITANA, on 17 Nov 2026 at 22:50:50, subject to the Cambridge Core terms of use, available at https://www.cambridge.org/core/terms. https://doi.org/10.1017/9781139524100.021

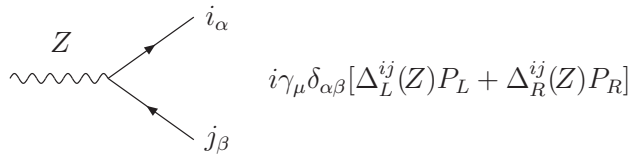


Figure 15.7 Feynman rule for the coupling of the Z to quarks, where i, j denote different quark flavors and α, β the colors. $P_{L,R} = (1 \mp \gamma_5)/2$.

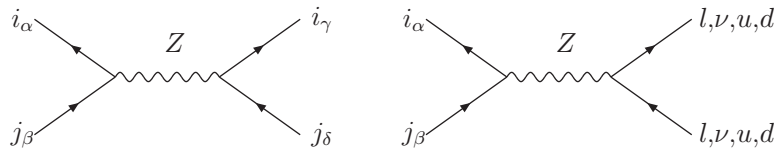


Figure 15.8 Tree-level Z contribution to $\Delta F = 2$ (left) and $\Delta F = 1$ (right) processes. Labels are explained in Figure 15.7.

- The hadronic matrix elements are evaluated at $m_t(m_t)$ as the inclusion of NLO QCD corrections allows us to choose any scale of $O(M_Z)$ without changing physical results. They are collected in Table 13.1.
- The QCD correction $\tilde{r}$ in (15.61) takes now the value $\tilde{r} = 1.068$.

From the point of view of SMEFT, this procedure is correct for $\Delta F = 1$ processes but misses important contributions to $\Delta F = 2$ processes as pointed out in [766] and also analyzed partially in [799]. The present section is based on [766, 851].

We will first address this NP scenario from the point of view of SMEFT, expressing $\Delta_{L,R}^{ij}(Z)$ in terms of Wilson coefficients of SMEFT and identifying the missing contributions. Subsequently we will collect the formulas for the master functions in these NP scenarios. Concrete examples are models with vector-like quarks (VLQs) in which the mixing of SM quarks with these new heavy quarks generates flavor-violating Z couplings. We will discuss these models in Section 16.3.

In should be remarked that in concrete models there could be still other contributions to $\Delta F = 2$ processes that in certain ranges of parameters could be more important than the ones considered here. This is the case of box diagrams with VLQs and Higgs exchanges, which we will discuss in Section 16.3.

15.5.2 The SMEFT View

The operators that induce FC quark couplings of the Z are the ones of Scenarios I and II of the previous chapter. The ones with LH quark currents are[5]

$$\boxed{O_{Hq}^{(1)} = (H^\dagger i\overleftrightarrow{\mathcal{D}}_\mu H)[\bar{q}_L^i\gamma^\mu q_L^j], \qquad O_{Hq}^{(3)} = (H^\dagger i\overleftrightarrow{\mathcal{D}}_\mu^a H)[\bar{q}_L^i\sigma^a\gamma^\mu q_L^j],} \tag{15.139}$$

[5] To simplify notations we suppress flavour indices on the operators.

Downloaded from https://www.cambridge.org/core. UNIVERSIDAD AUTONOMA METROPOLITANA, on 17 Nov 2026 at 22:50:50, subject to the Cambridge Core terms of use, available at https://www.cambridge.org/core/terms. https://doi.org/10.1017/9781139524100.021

including also modified LH $W^\pm$ couplings. The ones with RH quark currents are

$$\boxed{O_{Hd} = (H^\dagger i\overleftrightarrow{\mathcal{D}_\mu} H)[\bar{d}_R^i \gamma^\mu d_R^j], \qquad O_{Hu} = (H^\dagger i\overleftrightarrow{\mathcal{D}_\mu} H)[\bar{u}_R^i \gamma^\mu u_R^j].} \tag{15.140}$$

Finally, there is one operator with charged RH quark currents:

$$\boxed{O_{Hud} = (\widetilde{H}^\dagger i\mathcal{D}_\mu H)[\bar{u}_R^i \gamma^\mu d_R^j].} \tag{15.141}$$

Here $\widetilde{H} \equiv i\sigma_2 H^*$. The complex-valued coefficients of these operators are denoted by

$$[C_{Hq}^{(1)}]_{ij}, \qquad [C_{Hq}^{(3)}]_{ij}, \qquad [C_{Hd}]_{ij}, \qquad [C_{Hu}]_{ij}, \qquad [C_{Hud}]_{ij}, \tag{15.142}$$

where the indices $ij = 1, 2, 3$ denote different generations of up- and down-type quarks.

After EWSB, the transition from a weak to the mass eigenbasis takes place for gauge and quark fields. The quark fields are rotated by 3×3 unitary rotations in flavor space as explicitly shown in Section 14.4.1. We end up then with the important formulas (14.32) and (14.33), which give us Y_u as a function of up-quark masses and the CKM parameters. Y_d are diagonal as explained when deriving formulas (14.32) and (14.33).

The $\psi^2 H^2 D$ operators lead to modifications of the couplings of quarks to the weak gauge bosons ($V = W^\pm, Z$ and $g_Z \equiv \sqrt{g_1^2 + g_2^2}$):

$$\begin{aligned}\mathcal{L}_{\psi\bar{\psi}V}^{\text{dim}-6} = &-\frac{g_Z}{2} v^2 Z_\mu \Big(\left[V_L^{d\dagger}(C_{Hq}^{(1)} + C_{Hq}^{(3)})V_L^d\right]_{ij} [\bar{d}_i \gamma^\mu P_L d_j] + \left[V_R^{d\dagger} C_{Hd} V_R^d\right]_{ij} [\bar{d}_i \gamma^\mu P_R d_j] \\ &+ \left[V_L^{u\dagger}(C_{Hq}^{(1)} - C_{Hq}^{(3)})V_L^u\right]_{ij} [\bar{u}_i \gamma^\mu P_L u_j] + \left[V_R^{u\dagger} C_{Hu} V_R^u\right]_{ij} [\bar{u}_i \gamma^\mu P_R u_j] \Big), \\ &+ \frac{g_2}{\sqrt{2}} v^2 \Big(\left[V_L^{u\dagger} C_{Hq}^{(3)} V_L^d\right]_{ij} [\bar{u}_i \gamma^\mu P_L d_j] W_\mu^+ + \left[V_R^{u\dagger} \frac{C_{Hud}}{2} V_R^d\right]_{ij} [\bar{u}_i \gamma^\mu P_R d_j] W_\mu^+ + \text{h.c.} \Big),\end{aligned} \tag{15.143}$$

where we display all rotation matrices for completeness.

Note that in our notation fermion fields with an index for their handedness correspond to weak eigenstates, whereas mass eigenstates – like in this equation – do not carry this index. The values for v and the gauge couplings $g_{1,2}$ differ from the SM ones by dim-6 contributions. However, because the couplings in (15.143) are already at the level of dim-6, such corrections would count as dim-8 contributions, which is of higher order than considered here. From this equation it is apparent that our definition of the Wilson coefficients $[C_a]_{ij}$ (at μ_{ew}) for our special choice of the weak quark basis – $V_{L,R}^d = \mathbb{1}$ and $V_R^u = \mathbb{1}$ – is particularly convenient for the study of down-type quark $\Delta F = 1, 2$ transitions, see also [563], because additional CKM factors appear only in couplings of operators involving left-handed up-type quarks. Thus the associated Wilson coefficients $C_{Hq}^{(1,3)}$ enter down- *and* up-type-quark processes, leading to correlations between the affected processes that depend on the appearing CKM factors.

If one deals with down-type quark $\Delta F = 1, 2$ processes, it is justified to omit O_{Hu} and O_{Hud} in the phenomenology. This is mainly because their RG flow does not induce leading logarithmic contributions to down-type quark $\Delta F = 1, 2$ processes. The Wilson coefficients

Downloaded from https://www.cambridge.org/core. UNIVERSIDAD AUTONOMA METROPOLITANA, on 17 Nov 2026 at 22:50:50, subject to the Cambridge Core terms of use, available at https://www.cambridge.org/core/terms. https://doi.org/10.1017/9781139524100.021

$C_{Hq}^{(1,3)}$, C_{Hd} (and C_{Hu}) are complex-valued matrices in flavor space with a symmetric real part and antisymmetric imaginary part, such that each contains $6 + 3 = 9$ real degrees of freedom.

We can now express the usual FC quark couplings of the Z in terms of $C_{Hq}^{(1,3)}$, C_{Hd}. We have first

$$\mathcal{L}^{\rm NP}_{\psi\bar{\psi}Z} = Z_\mu \sum_{\psi=u,d} \bar{\psi}_i \, \gamma^\mu \left([\Delta_L^\psi(Z)]_{ij} \, P_L + [\Delta_R^\psi(Z)]_{ij} \, P_R \right) \psi_j, \tag{15.144}$$

with $\psi = u, d$ distinguishing between *up*- and *down*-quark couplings. These complex-valued couplings are related to the WCs of SMEFT operators of Chapter 14 through

$$\boxed{[\Delta_L^u(Z)]_{ij} = -\frac{g_Z}{2} v^2 \left[C_{Hq}^{(1)} - C_{Hq}^{(3)} \right]_{ij}, \qquad [\Delta_R^u(Z)]_{ij} = -\frac{g_Z}{2} v^2 [C_{Hu}]_{ij},} \tag{15.145}$$

$$\boxed{[\Delta_L^d(Z)]_{ij} = -\frac{g_Z}{2} v^2 \left[C_{Hq}^{(1)} + C_{Hq}^{(3)} \right]_{ij}, \qquad [\Delta_R^d(Z)]_{ij} = -\frac{g_Z}{2} v^2 [C_{Hd}]_{ij}.} \tag{15.146}$$

As all these vertices are $O(v^2/\Lambda^2)$, it is evident that a simple tree-level Z exchange with FC couplings corresponds to dimension-6 contribution in the case of $\Delta F = 1$ processes while to dimension-8 in the case of $\Delta F = 2$ transitions. Fortunately our results from Section 14.4 can tell us what the dimension-6 contributions to $\Delta F = 2$ are. In the LO they are simply given by the expressions in (14.39) and (14.43) for RH and LH scenarios, respectively.

A detailed analysis of these contributions has been presented in [766]. As this paper uses our notations and conventions, we will not repeat this analysis here and ask interested readers to consult this paper. Instead we will summarize here the main lessons from this study, which demonstrate that the simplified approach used for Z' contributions cannot be used in Z scenarios for $\Delta F = 2$ contributions. These lessons are as follows.

1. In the presence of right-handed FC Z couplings, i.e., $C_{H_d} \neq 0$ or $[\Delta_R^d(Z)]_{ij}$, the RG analysis of Section 14.4 yields that at $\mu_{\rm ew}$ the left-right $\Delta F = 2$ operators $O_{\rm LR,1}$ in (14.37) are generated, and as seen in (14.39) their contributions are enhanced by the large leading logarithm $\ln \mu_\Lambda/\mu_{\rm ew}$. Such operators are known to provide very important contributions to $\Delta F = 2$ observables because of their enhanced hadronic matrix elements and an additional enhancement from QCD RG effects below $\mu_{\rm ew}$, in particular in the K-meson system. As a result *these* operators – and not $O^{ij}_{\rm VRR}$ in (14.36), as used in [601, 611, 851] – dominate $\Delta F = 2$ processes. The results in [759] allow the calculation of this dominant contribution including only leading logarithms, but this is sufficient for our purposes, and even for scales μ_Λ as high as 20 TeV a good approximation is to keep only leading logarithm.
2. Because of the usual $\mu_{\rm ew}$ scale ambiguity present at leading order (LO) the next-to-leading order (NLO) matching corrections of O_{Hd} to $\Delta F = 2$ processes at $\mu_{\rm ew}$ within SMEFT have to be calculated. One NLO contribution is obtained by replacing the flavor-diagonal lepton vertex in the SM Z-penguin diagram by $[C_{Hd}]_{ij}$, which again generates the operator $O^{ij}_{\rm LR,1}$ simply because the flavor-changing part of the SM penguin

Downloaded from https://www.cambridge.org/core. UNIVERSIDAD AUTONOMA METROPOLITANA, on 17 Nov 2026 at 22:50:50, subject to the Cambridge Core terms of use, available at https://www.cambridge.org/core/terms. https://doi.org/10.1017/9781139524100.021

diagram is LH. In fact, this contribution has been first pointed out in [799]. But such contributions are by themselves gauge dependent, simply because the function $C_0(x_t)$ present in the SM vertex is gauge dependent. In [766] the missing contributions have been calculated using SMEFT, obtaining a gauge-independent contribution, which was later confirmed in [799]. However, the LO contribution is not only more important due to the large logarithm $\ln \mu_\Lambda/\mu_{\rm ew}$, but has also opposite sign to the NLO term, allowing to remove the LO $\mu_{\rm ew}$ dependence. Moreover, being strongly enhanced with respect to the contributions considered in [601, 611, 851], it has a very large impact on phenomenology, in particular as discussed below the correlations between $\Delta F = 2$ and $\Delta F = 1$ observables are drastically changed.

3. The situation for LH FC Z couplings is different from the RH case both qualitatively and quantitatively. The result in (14.43) tells us that the two operators $O_{Hq}^{(1)}$ and $O_{Hq}^{(3)}$ in SMEFT generate only the $\Delta F = 2$-operator $O_{\rm VLL}$ in (14.36) that is dominant already in the SM. The operator structure is then the same as in [611]. The resulting NP effects are then much smaller than in the RH case because no LR operators are present. But now comes an important difference from [611]. The correlations between $\Delta F = 1$ and $\Delta F = 2$ processes are weakened very significantly: While $\Delta F = 1$ transition amplitudes are proportional to the sum $C_{Hq}^{(1)} + C_{Hq}^{(3)}$, the leading RG contribution to $\Delta F = 2$ processes is proportional to the difference of these couplings. Correlations between $\Delta F = 1$ and $\Delta F = 2$ processes are hence only present in specific scenarios, e.g., when the couplings are given in terms of the fundamental parameters of a given model that can be determined in other processes. This is in stark contrast to the contributions considered in [601, 611, 851], where the same couplings enter both classes of processes, and no involvement of specific models was necessary. Of course, correlations remain in each sector separately because both are governed by two complex couplings, but as previously only one complex coupling was present, one needs more observables to determine them model independently. Moreover, in models where $\Delta F = 2$ and $\Delta F = 1$ observables are correlated, the constraints become weaker, allowing for larger NP effects in rare decays.
4. Also for the operators $O_{Hq}^{(1,3)}$ the NLO contributions to $\Delta F = 2$ corresponding to the replacement of the flavor-diagonal lepton vertex in the SM Z-penguin diagram by $C_{Hq}^{(1,3)}$ are gauge dependent. Including the remaining contributions to remove this gauge dependence one finds two gauge-independent functions of x_t, analogous to $X_0(x_t)$, $Y_0(x_t)$, and $Z_0(x_t)$ known from the SM. Because the NLO contributions are different for $C_{Hq}^{(1)}$ and $C_{Hq}^{(3)}$, it is not just their difference contributing to $O_{\rm VLL}$ anymore, but also their sum.
5. At NLO also new gauge-independent contributions are generated that are unrelated to tree-level Z exchanges and only proportional to $C_{Hq}^{(3)}$, analogous to the usual box diagrams with $W^\pm$ and quark exchanges. They turn out to be important for gauge-independence and depend not only on the coefficients for the quark transition under consideration, but also on additional couplings to the possible intermediate quarks in the box diagrams. But when the hierarchies in CKM elements are taken into account, $C_{Hq}^{(3)}$ for the quark transition under consideration is the only free entry in this part.

Downloaded from https://www.cambridge.org/core. UNIVERSIDAD AUTONOMA METROPOLITANA, on 17 Nov 2026 at 22:50:50, subject to the Cambridge Core terms of use, available at https://www.cambridge.org/core/terms. https://doi.org/10.1017/9781139524100.021

It should be stressed in this context that the contributions to $\Delta F = 2$ transitions from FC quark couplings of the Z could be less relevant in NP scenarios with other sources of $\Delta F = 2$ contributions. Most important, $\Delta F = 2$ operators could receive a direct contribution at tree-level at the scale μ_Λ, but also in models where this does not happen Z contributions could be subdominant. Examples are models in which the only new particles are vector-like quarks (VLQs), where box diagrams with VLQ and Higgs exchanges generate $\Delta F = 2$ operators at one-loop level [666, 967], which were found in these papers to be larger than the Z contributions at tree-level. However, in [967] the new effects just listed have not been included. As shown in [666] for right-handed FC Z couplings these box contributions are dwarfed by the LR operator contributions mentioned in point **1**, whereas in B-mixing they are comparable. We will discuss VLQ models in Section 16.3.

15.5.3 Master Functions in Z-Models

$\Delta F = 2$ Master Functions

The $\Delta F = 2$ master functions for $M = K, B_q$ are given as follows

$$S(M) = S_0(x_t) + \Delta S(M) \equiv |S(M)|e^{i\theta_S^M}, \tag{15.147}$$

with $\Delta S(M)$ receiving contributions from various operators so that it is useful to write

$$\Delta S(M) = [\Delta S(M)]_{\rm VLL} + [\Delta S(M)]_{\rm VRR} + [\Delta S(M)]_{\rm LR} + \overline{[\Delta S(M)]}_{\rm VLL} + \overline{[\Delta S(M)]}_{\rm LR}. \tag{15.148}$$

The first three contributions are directly obtained from the previous section by making the substitutions listed earlier. They represent dimension-8 contributions coming from the simplified approach. The last two represent new dimension-6 contributions obtained by means of SMEFT as discussed earlier. Explicit formulas for them can be found in [766].

$\Delta F = 1$ Master Functions

These master functions can be directly obtained from the ones in Z' scenarios. They are given as follows

$$X_{\rm L}(K) = \eta_X X_0(x_t) + \frac{\Delta_L^{\nu\bar{\nu}}(Z)}{g_{\rm SM}^2 M_Z^2}\frac{\Delta_L^{sd}(Z)}{V_{ts}^* V_{td}}, \tag{15.149}$$

$$X_{\rm R}(K) = \frac{\Delta_L^{\nu\bar{\nu}}(Z)}{g_{\rm SM}^2 M_Z^2}\frac{\Delta_R^{sd}(Z)}{V_{ts}^* V_{td}}, \tag{15.150}$$

$$X_{\rm L}(B_q) = \eta_X X_0(x_t) + \left[\frac{\Delta_L^{\nu\nu}(Z)}{M_Z^2 g_{\rm SM}^2}\right]\frac{\Delta_L^{qb}(Z)}{V_{tq}^* V_{tb}}, \tag{15.151}$$

$$X_{\rm R}(B_q) = \left[\frac{\Delta_L^{\nu\nu}(Z)}{M_Z^2 g_{\rm SM}^2}\right]\frac{\Delta_R^{qb}(Z)}{V_{tq}^* V_{tb}}, \tag{15.152}$$

Downloaded from https://www.cambridge.org/core. UNIVERSIDAD AUTONOMA METROPOLITANA, on 17 Nov 2026 at 22:50:50, subject to the Cambridge Core terms of use, available at https://www.cambridge.org/core/terms. https://doi.org/10.1017/9781139524100.021

$$Y_{\rm A}(K) = \eta_Y Y_0(x_t) + \frac{\left[\Delta_A^{\mu\bar{\mu}}(Z)\right]}{M_Z^2 g_{\rm SM}^2}\left[\frac{\Delta_L^{sd}(Z) - \Delta_R^{sd}(Z)}{V_{ts}^\star V_{td}}\right] \equiv |Y_A(K)|e^{i\theta_Y^K}, \tag{15.153}$$

$$Y_{\rm A}(B_q) = \eta_Y Y_0(x_t) + \frac{\left[\Delta_A^{\mu\bar{\mu}}(Z)\right]}{M_Z^2 g_{\rm SM}^2}\left[\frac{\Delta_L^{qb}(Z) - \Delta_R^{qb}(Z)}{V_{tq}^\star V_{tb}}\right] \equiv |Y_A(B_q)|e^{i\theta_Y^{B_q}}. \tag{15.154}$$

Here $\eta_{X,Y}$ are QCD factors given in (15.79).

The Wilson coefficients (15.80) in Z-models read

$$\sin^2\vartheta_W C_9 = [\eta_Y Y_0(x_t) - 4\sin^2\vartheta_W Z_0(x_t)] - \frac{1}{g_{\rm SM}^2}\frac{1}{M_Z^2}\frac{\Delta_L^{sb}(Z)\Delta_V^{\mu\bar{\mu}}(Z)}{V_{ts}^* V_{tb}}, \tag{15.155}$$

$$\sin^2\vartheta_W C_{10} = -\eta_Y Y_0(x_t) - \frac{1}{g_{\rm SM}^2}\frac{1}{M_Z^2}\frac{\Delta_L^{sb}(Z)\Delta_A^{\mu\bar{\mu}}(Z)}{V_{ts}^* V_{tb}}, \tag{15.156}$$

$$\sin^2\vartheta_W C_9' = -\frac{1}{g_{\rm SM}^2}\frac{1}{M_Z^2}\frac{\Delta_R^{sb}(Z)\Delta_V^{\mu\bar{\mu}}(Z)}{V_{ts}^* V_{tb}}, \tag{15.157}$$

$$\sin^2\vartheta_W C_{10}' = -\frac{1}{g_{\rm SM}^2}\frac{1}{M_Z^2}\frac{\Delta_R^{sb}(Z)\Delta_A^{\mu\bar{\mu}}(Z)}{V_{ts}^* V_{tb}}. \tag{15.158}$$

Finally, in the case of $K_L \to \pi^0\mu^+\mu^-$ decays, one can use formulas of Section 15.4.5 with Z' replaced by Z. Note that the flavor-conserving couplings are SM ones.

15.5.4 Lessons on NP Patterns in Z Scenarios

A detailed phenomenology of tree-level Z exchanges has been presented in [601, 851] and in particular in [766]. We will now summarize the highlights of these papers in the form of lessons gained through these analyses. Numerous plots related to these lessons can be found in these papers.

We begin with the K-meson system and concentrate on the results obtained in [851] including the insights on $\Delta F = 2$ processes from [766]. The summary of the lessons is rather brief. On the other hand, the presentation in [851] is very detailed with numerous analytic expressions that could be useful for nonexperts who want to understand the details of the patterns of various effects. In the latter paper the main goal was to investigate, similar to the Z' case in Section 15.4, what are the implications of the ε'/ε anomaly discussed in Chapter 10 on rare decays $K^+ \to \pi^+\nu\bar{\nu}$ and $K_{\rm L} \to \pi^0\nu\bar{\nu}$ in various scenarios for the Z couplings to quarks: left-handed scenario (LHS) and right-handed scenario (RHS).

Lesson 1: In the LHS, a given request for the enhancement of ε'/ε determines the coupling $\mathrm{Im}\Delta_L^{sd}(Z)$. Similar in the RHS the coupling $\mathrm{Im}\Delta_R^{sd}(Z)$ is determined.

Lesson 2: In LHS there is a direct unique implication of an enhanced ε'/ε on $K_{\rm L} \to \pi^0\nu\bar{\nu}$: *suppression* of $\mathcal{B}(K_{\rm L} \to \pi^0\nu\bar{\nu})$. This property is known from NP scenarios in which NP to $K_{\rm L} \to \pi^0\nu\bar{\nu}$ and ε'/ε enters dominantly through the modification of Z-penguins. The known flavor-diagonal Z couplings to quarks and leptons and the sign

Downloaded from https://www.cambridge.org/core. UNIVERSIDAD AUTONOMA METROPOLITANA, on 17 Nov 2026 at 22:50:50, subject to the Cambridge Core terms of use, available at https://www.cambridge.org/core/terms. https://doi.org/10.1017/9781139524100.021

of the matrix element $\langle Q_8 \rangle_2$ determines this anticorrelation, which has been verified in all models with only LH flavor-violating Z couplings.

Lesson 3: The imposition of the $K_L \to \mu^+\mu^-$ constraint in LHS determines the range for $\mathrm{Re}\Delta_L^{sd}(Z)$, which with the already fixed $\mathrm{Im}\Delta_L^{sd}(Z)$ would allow to calculate the shifts in ε_K and ΔM_K if not for new contributions identified in [766], which were not included in [851]. There it was concluded that these shifts are very small for ε_K and negligible for ΔM_K. But this conclusion is not valid in the presence of these new contributions. Moreover, in concrete models new contributions beyond Z exchange are possible. For instance, in VLQ models box diagrams with VLQs can indeed provide contributions to ε_K and ΔM_K that are larger than coming from tree-level Z-exchange provided the masses of VLQs are far above 3 TeV [967]. We will discuss this in the context of the analysis in [666]. In any case $K_L \to \mu^+\mu^-$ determines the allowed range for $\mathrm{Re}\Delta_L^{sd}(Z)$.

Lesson 4: With fixed $\mathrm{Im}\Delta_L^{sd}(Z)$ and the allowed range for $\mathrm{Re}\Delta_L^{sd}(Z)$, the range for $\mathcal{B}(K^+ \to \pi^+\nu\bar{\nu})$ can be obtained. But in view of uncertainties in the $K_L \to \mu^+\mu^-$ constraint both an enhancement and a suppression of $\mathcal{B}(K^+ \to \pi^+\nu\bar{\nu})$ are possible, and no specific pattern of correlation between $\mathcal{B}(K_\mathrm{L} \to \pi^0\nu\bar{\nu})$ and $\mathcal{B}(K^+ \to \pi^+\nu\bar{\nu})$ is found. In the absence of a relevant ε_K constraint, this is consistent with the general analysis in [924]. $\mathcal{B}(K^+ \to \pi^+\nu\bar{\nu})$ can be enhanced by a factor of 2 at most if conservative bound on $K_L \to \mu^+\mu^-$ is used and only suppressed if stricter bound in (9.268) is used. See [766] and discussion at the end of Section 9.7.1.

Lesson 5: As far as the correlation of ε'/ε with $K_\mathrm{L} \to \pi^0\nu\bar{\nu}$ is concerned analogous pattern is found in RHS, although the numerics is different. See plots in [851]. But the new contributions from LR operators to ε_K found in [766] have dramatic impact on the results for $K^+ \to \pi^+\nu\bar{\nu}$ presented in [851]. Now not $K_L \to \mu^+\mu^-$ but the constraint from ε_K determines the allowed enhancement of $\mathcal{B}(K^+ \to \pi^+\nu\bar{\nu})$. While in [851] an enhancement of $\mathcal{B}(K^+ \to \pi^+\nu\bar{\nu})$ up to a factor of 5.7 was possible, now only an enhancement up to a factor of 1.5 is possible.

Lesson 6: In a general Z scenario in which the underling theory contains all the operators in (15.139) and (15.140) and simultaneously dimension-8 LR operators are present, the pattern of NP effects can change relative to LH and RH scenarios because of many parameters involved independent of whether new contributions considered in [766] are taken into account or not. As demonstrated in [851] the main virtue of the general scenario is the possibility of enhancing simultaneously ε'/ε, ε_K, $\mathcal{B}(K^+ \to \pi^+\nu\bar{\nu})$, and $\mathcal{B}(K_\mathrm{L} \to \pi^0\nu\bar{\nu})$, which is not possible in LHS and RHS. Thus the presence of both LH and RH flavor-violating currents is essential for obtaining simultaneously the enhancements in question when NP is dominated by tree-level Z exchanges. We refer to examples in [851]. Then the main message from this analysis is that in the presence of both LH and RH new flavour-violating couplings of Z to quarks, large departures from SM predictions for $K^+ \to \pi^+\nu\bar{\nu}$ and $K_\mathrm{L} \to \pi^0\nu\bar{\nu}$ are still possible. Similar conclusions have been reached in [799].

Concerning B physics observables we have the following lessons [766].

Lesson 7: In the $b \to s, d$ sector $\Delta F = 1$ constraints remain dominant, but allow still for sizable NP contributions, e.g., in $B_{d,s} \to \mu^+\mu^-$. In particular $B_d \to \mu^+\mu^-$ can be enhanced to the present upper bound. Nevertheless, the strong correlations in this scenario will allow for distinguishing it from other NP models with coming data from the LHC (LHCb, CMS, ATLAS) and Belle II.

Downloaded from https://www.cambridge.org/core. UNIVERSIDAD AUTONOMA METROPOLITANA, on 17 Nov 2026 at 22:50:50, subject to the Cambridge Core terms of use, available at https://www.cambridge.org/core/terms. https://doi.org/10.1017/9781139524100.021

Lesson 8: The correlations between R_K^ν and $R_{K^*}^\nu$ of Section 9.6 and between $\mathcal{B}(B_s \to \mu^+\mu^-)$ and $\mathcal{B}(B_d \to \mu^+\mu^-)$ allow to distinguish LH and RH scenarios for a large part of the parameter space. Because in the LH scenario the interference with the SM contribution is the same in $B \to K\nu\bar{\nu}$ and $B \to K^*\nu\bar{\nu}$, there is a very strict prediction $R_K^\nu/R_{K^*}^\nu \equiv 1$ [607]. An enhancement of each of the ratios is possible only up to $\sim 10\%$ in this scenario, but a strong suppression is possible, in contrast to RH models, where NP effects are tiny. For $\mathcal{B}(B_d \to \mu^+\mu^-)$ a moderate enhancement up to $\sim 2 \times 10^{-10}$ is possible, but also a strong suppression, in contrast with the RH case.

Lesson 9: Possible tensions in $\Delta M_{s,d}$ and ε_K can be successfully addressed in these NP scenarios.

Lesson 10: Very importantly this NP scenario fails in explaining the anomalies in $b \to s\ell^+\ell^-$ transitions like $R(K)$ and $R(K^*)$ and in $b \to c\tau\bar{\nu}_\tau$ like $R(D)$ and $R(D^*)$. In particular, due to small vector-couplings of Z to muons, the observed suppression of C_9 cannot be explained.

In summary, while the tree-level Z exchanges could be responsible for a hinted ε'/ε anomaly and could provide sizable departures from SM expectations in $K^+ \to \pi^+\nu\bar{\nu}$, $K_L \to \pi^0\nu\bar{\nu}$ and $B_{s,d} \to \mu^+\mu^-$, NP behind possible violation of lepton flavor universality must be different. Here Z' models of Section 15.4 in $b \to s\ell^+\ell^-$ transitions and leptoquark models of Section 16.4 in both $b \to s\ell^+\ell^-$ and $b \to c\tau\bar{\nu}_\tau$ transitions are performing much better.

Finally, let us mention that in models containing Z', FCNC processes mediated by the Z boson can be generated by $Z - Z'$ mixing. We will present the relevant expressions in the context of the presentation of 331 models in Section 16.2. FCNC processes mediated by the Z boson can also be generated in the process of EW symmetry breaking through mixing of the SM fermions with vector-like fermions. We will discuss this case in Section 16.3.

15.6 Beyond MFV: Right-Handed W'

A very important property of the SM regarding flavor-violating processes is the LH structure of the charged current interactions reflecting the maximal violation of parity observed in low-energy processes. LH charged currents encode at the level of the Lagrangian the full information about flavor mixing and CP violation represented compactly by the CKM matrix. As we have seen, due to the GIM [6] mechanism this structure has automatically profound implications for the pattern of FCNC processes that seems to be in remarkable accordance with the present data within theoretical and experimental uncertainties, bearing in mind the anomalies listed in Section 12.2.

As the SM is expected to be only the low-energy limit of a more fundamental theory, it is conceivable that at very short distance scales parity could be a good symmetry implying the existence of RH charged currents. Prominent examples of such fundamental theories are left-right (LR) symmetric models based on $\mathrm{SU}(2)_L \times \mathrm{SU}(2)_R \times \mathrm{U}(1)_{B-L}$ gauge group on which a rich literature exists.

Indeed, LR symmetric models were born 45 years ago [968–972]. Early papers mainly cover the examinations of two special cases, known as *manifest* scenario [972] and

Downloaded from https://www.cambridge.org/core. UNIVERSIDAD AUTONOMA METROPOLITANA, on 17 Nov 2026 at 22:50:50, subject to the Cambridge Core terms of use, available at https://www.cambridge.org/core/terms. https://doi.org/10.1017/9781139524100.021

pseudo-manifest scenario [842, 973–975], which are characterized by no spontaneous and fully spontaneous CP violation, respectively. The right-handed counterpart of the CKM matrix appears then in a special form being either identical to or the complex-conjugate of the CKM matrix up to certain phases as, e.g., summarized in [976]. The phenomenology of both scenarios has widely been studied in the literature [750, 977–979]. The book [7] contains a lot of information on these models as well.

By now in both scenarios strong constraints on the heavy charged gauge boson mass $M_{W_R} \geq 4\,\text{TeV}$ have been obtained [750, 980, 981] from the constraints on the $K_L - K_S$ mass difference, CP violation in kaon decays, and the neutron electric dipole moment, making these scenarios difficult to access in direct searches at the LHC. In addition the pseudo-manifest scenario has been ruled out by the correlation of ε_K and $\sin(2\beta)$ [982]. This means that the right-handed mixing matrix must be different from the CKM matrix to reach agreement with experiment. Motivated by this fact more general studies of CP violation have been performed in [976, 983, 984] and more recently in [772, 981, 985–988]. For a very recent analysis with many references see [989].

Moreover, the phenomenological interest in having another look at the RH currents in general originated from tensions between inclusive and exclusive determinations of the elements of the CKM matrix $|V_{ub}|$ and $|V_{cb}|$. In this context it has been pointed out in [990–992] that the presence of RH currents could either remove or significantly weaken some of these tensions, especially in the case of $|V_{ub}|$. The implications of these findings for many observables within an effective theory approach have been studied in [610].

As of 2019, it does not seem that RH currents play a significant role in the explanation of the tension between inclusive and exclusive determinations of $|V_{ub}|$. But they could still play a significant role in the flavor phenomenology, as in the presence of both LH currents in the SM and RH currents beyond it, new operators are generated, in particular LR operators with enhanced $K^0 - \bar{K}^0$ matrix elements. But also in rare decays they could be relevant.

It should also be stressed that in such models not only heavy charged gauge bosons with couplings to RH quarks and leptons are present but also charged and neutral scalars. The charged scalars are most important for $B \to X_s\gamma$ decays, while the neutral ones for $\Delta F = 2$ processes. We refer to [772] for a detailed analysis of these processes. In this paper also a list of Feynman rules for a general model with $\text{SU}(2)_L \times \text{SU}(2)_R \times U(1)_{B-L}$ gauge group is given.

Among recent studies let me just mention [861, 862, 993, 994], where further references can be found. While, until today, no clear signal of the presence of RH-charged currents have been identified, they could still play a significant role in the future. On the theoretical side, the study of FCNC at one-loop in the presence of RH-charged currents has recently been improved [136].

As a simple example let us write the effective Hamiltonian for the exchange of a charged gauge bosons W'^+ contributing to $B^+ \to \tau^+\nu_\tau$ as follows

$$\mathcal{H}_{\text{eff}} = C_L O_L + C_R O_R, \tag{15.159}$$

where

$$O_L = (\bar{b}\gamma_\mu P_L u)(\bar{\nu}_\tau \gamma^\mu P_L \tau^-), \quad O_R = (\bar{b}\gamma_\mu P_R u)(\bar{\nu}_\tau \gamma^\mu P_L \tau^-) \tag{15.160}$$

Downloaded from https://www.cambridge.org/core. UNIVERSIDAD AUTONOMA METROPOLITANA, on 17 Nov 2026 at 22:50:50, subject to the Cambridge Core terms of use, available at https://www.cambridge.org/core/terms. https://doi.org/10.1017/9781139524100.021

and

$$C_L = C_L^{\rm SM} + \frac{\Delta_L^{ub*}(W'^+)\Delta_L^{\tau\nu}(W'^+)}{M_{W'^+}^2}, \quad C_R = \frac{\Delta_R^{ub*}(W'^+)\Delta_L^{\tau\nu}(W'^+)}{M_{W'^+}^2}, \tag{15.161}$$

with $C_L^{\rm SM}$ having the same structure as the correction from W'^+ with $M_{W'^+}$ replaced $M_{W'}$, and

$$\Delta_L^{ub} = \frac{g}{\sqrt{2}} V_{ub}, \qquad \Delta_L^{\nu\tau} = \frac{g}{\sqrt{2}}, \qquad \Delta_R^{ub} = 0, \qquad ({\rm SM}). \tag{15.162}$$

The couplings $\Delta_{L,R}^{ub*}(W'^+)$ could be complex numbers and contain new sources of flavor violation. Then

$$\mathcal{B}(B^+ \to \tau^+\nu_\tau)_{W'^+} = \frac{1}{64\pi} m_{B^+} m_\tau^2 \left(1 - \frac{m_\tau^2}{m_{B^+}^2}\right)^2 F_{B^+}^2 \tau_{B^+} |C_R - C_L|^2. \tag{15.163}$$

Evidently in a model like this it is possible to improve the agreement with the data by choosing appropriately the couplings of W'^+.

15.7 Beyond MFV: Neutral Scalars and Pseudoscalars

15.7.1 Preliminaries

In BSM scenarios FCNC processes can be mediated by tree-level heavy neutral scalars and/or pseudoscalars $H^0(A^0)$.[6] This generally introduces new sources of flavor violation and CP violation as well as LH and RH *scalar* $(1 \mp \gamma_5)$ currents as opposed to vector LH and RH currents that we studied in previous sections in connection with tree-level Z' and Z exchanges.

As already mentioned in Section 15.1.4, there are ways to avoid such transitions at tree-level without fine-tuning through a special arrangement of the couplings of the Higgs system with two or more doublets to SM fermions [899, 900] so that there are no FCNC mediated by neutral scalars at tree-level. This is, for instance, the case of the MSSM and many 2HDM models in which one Higgs doublet is responsible for up-quark masses and a second for down-quark ones. An excellent review of 2HDMs discussing this topic is the review in [897], and some comments can also be found in Section 15.1.4.

However, even if in the SM and in many of its extensions there are no fundamental flavor-violating couplings of scalars to quarks and leptons, such couplings can be generated through loop corrections leading in the case of $\Delta F = 1$ transitions to Higgs-penguins (HP) and in $\Delta F = 2$ transitions to double Higgs-penguins (DHP). Yet, when the masses of the scalar particles are significantly lower than the heavy new particles exchanged in the loops, the HP and DHP look at the electroweak scale as flavor-violating tree diagrams with the couplings determined by the fundamental parameters of a given model.

[6] Unless otherwise specified, we will use the name *scalar* for both scalars and pseudoscalars.

Downloaded from https://www.cambridge.org/core. UNIVERSIDAD AUTONOMA METROPOLITANA, on 17 Nov 2026 at 22:50:50, subject to the Cambridge Core terms of use, available at https://www.cambridge.org/core/terms. https://doi.org/10.1017/9781139524100.021

But there exist models in which tree-level scalar exchanges take place at a fundamental level. That is, neutral scalar particles have flavor-violating couplings to quarks and leptons. Important examples are left-right symmetric models just discussed. From the point of view of low-energy theory there is no distinction between these possibilities as long as the vertices involving heavy particles in a HP cannot be resolved and to first approximation what really matters is the mass of the exchanged scalar and its flavor-violating couplings, either fundamental or generated at one-loop level.

Therefore, as the first step, similar to Z' scenarios presented in Section 15.4, we will study the patterns of NP contributions to FCNC processes that depend only on the couplings of $H^0(A^0)$ to fermions and on their masses. In situations in which a single H^0 or A^0 dominates NP contributions, we will find stringent correlations between $\Delta F = 2$ and $\Delta F = 1$ observables that will be markedly different from the ones caused by tree-level Z' and Z FCNC. This section is dominantly based on [504, 509].

Thus the goal of the present section is to analyze how SM predictions for FCNC processes are modified by tree-level scalar exchanges and to demonstrate that these modifications can be distinguished through correlations between quark flavor observables from the ones identified in Sections 15.4 and 15.5. Such a distinction would be crucial in case no new particles would be discovered directly at the LHC.

Before going into details, it will be useful to mention several differences between NP governed by Z' and scalar particles that are related to the existing lower bounds on their masses and the fact that these particle have different spins.

- The lower bounds on masses of Z' gauge bosons from the LHC are by now in the ballpark of 3 TeV in case their couplings to quarks are SM-like,[7] while new neutral scalars with masses below 1 TeV are not excluded.
- In the Z' scenarios in addition to new operators involving RH vector currents also SM operators with modified Wilson coefficients can be present. On the other hand in the case of tree-level scalar exchanges all effective low-energy operators are new.
- Even if after the inclusion of QCD corrections, there is some overlap between operators contributing to $\Delta F = 2$ processes in Z' and scalar scenarios, their Wilson coefficients are differently affected by QCD corrections. We will see this explicitly later. But in $\Delta F = 1$ transitions there is no overlap between the operators present in these two scenarios.
- We have seen that $\Delta F = 1$ FCNC can be significantly modified by Z exchanges still satisfying $\Delta F = 2$ constraints. On the other hand the smallness of the SM Higgs couplings to muons and electrons precludes any visible effects from tree-level Higgs exchanges in rare K and B_d decays with muon or electron pair in the final state once constraints from $\Delta F = 2$ processes are taken into account.
- It should be emphasized that the couplings of new scalars to neutrinos could be sizable if the masses of neutrinos are generated by a different mechanism than coupling to scalars, like in the case of the see-saw mechanism. We will assume that this is not the case so that NP effects of scalars in $K^+ \to \pi^+\nu\bar{\nu}$, $K_L \to \pi^0\nu\bar{\nu}$, and $b \to s\nu\bar{\nu}$ transitions will be negligible in contrast to Z' models, where NP effects in these decays can still be significant.

[7] In models in which Z' couples only to leptons Z' masses can be much lower.

Downloaded from https://www.cambridge.org/core. UNIVERSIDAD AUTONOMA METROPOLITANA, on 17 Nov 2026 at 22:50:50, subject to the Cambridge Core terms of use, available at https://www.cambridge.org/core/terms. https://doi.org/10.1017/9781139524100.021

Now comes a warning so that the readers are not disappointed at the end of this section. We will present many formulas that can be used for phenomenology but there is no space to present here numerical analysis. Such analysis with numerous plots can be found in [504, 509].

15.7.2 Model Assumptions and Notations

To proceed we have to specify our notations that will be analogous to the ones for Z' scenarios except that now we have to distinguish between a heavy neutral scalar and a heavy pseudoscalar. We will use a common name, H^0, for them unless otherwise specified. When a distinction will have to be made, we will either use H^0 and A^0 for scalar and pseudoscalar, respectively, or to distinguish SM Higgs from additional spin-0 particles we will use the familiar two-Higgs doublet model (2HDM) and MSSM notation: (H, A, h) with h denoting the SM Higgs particle.

Our strategy will be to consider in this section the simplest model in which the only new particle in the low-energy effective theory is a single neutral particle with spin-0, a scalar, or pseudoscalar. As in most specific extensions of the SM, like 2HDMs, of various sorts, and the MSSM, several spin-0 particles are present, the question arises of whether this minimal construction is possible from the point of view of an underlying fundamental theory.

The first question to be investigated are the transformation properties of this particle under the $SU(2)_L$ of the SM. If the scalar in question is not a $SU(2)_L$ singlet, then it must be placed in a complete $SU(2)_L$ multiplet, e.g., a second doublet, as is the case of 2HDM or the MSSM. However, this implies the existence of its $SU(2)_L$ partners in a given multiplet with masses close to the masses of our scalar. In fact, in the decoupling regime in 2HDM and MSSM the masses of $(H^{\pm}, H^0, A^0)$ are approximately the same. While $SU(2)_L$ breaking effects in the Higgs potential allow for mass splittings, they must be of $O(v)$ at most with $v = 246\,\text{GeV}$ being the electroweak symmetry breaking scale. Consequently we are lead to the conclusion that the case of the dominance of a single scalar with nontrivial transformations under $SU(2)_L$ is rather unlikely.

It follows then that our scalar should be a $SU(2)_L$ singlet. This does not preclude its couplings to SM fermions. For instance, the scalar-quark couplings of H to quarks can originate in the following low-energy effective operator

$$L = \lambda_L^{ij} \frac{H^0}{\Lambda} \bar{q}_R^i q_L^j h_{\text{SM}} + h.c., \tag{15.164}$$

with Λ denoting the cutoff scale of the low-energy theory and h_{SM} being the Higgs particle. After the spontaneous breakdown of $SU(2)_L$ the scalar left-handed coupling is given by

$$\Delta_L^{ij}(H^0) = \frac{1}{\sqrt{2}} \frac{v}{\Lambda} \lambda_L^{ij}, \tag{15.165}$$

with analogous expression for the right-handed coupling $\Delta_R^{ij}(H^0)$.

All the FCNC discussed in this section will be governed by the couplings $\Delta_{L,R}^{ij}(H^0)$ and the scalar mass M_H. The Feynman rule for the coupling of H^0 to quarks is shown

Downloaded from https://www.cambridge.org/core. UNIVERSIDAD AUTONOMA METROPOLITANA, on 17 Nov 2026 at 22:50:50, subject to the Cambridge Core terms of use, available at https://www.cambridge.org/core/terms. https://doi.org/10.1017/9781139524100.021

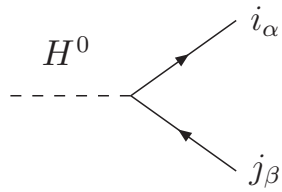


Figure 15.9 Feynman rules for a neutral colorless scalar particle H^0 with mass M_H, where i, j denote different quark flavors and α, β the colors. $P_{L,R} = (1 \mp \gamma_5)/2$.

in Figure 15.9 with (i, j) denoting quark flavors. But in contrast to the couplings of Z', for which there is generally no relation between LH and RH couplings, we have now the following important relation

$$\boxed{\Delta_L^{ij}(H^0) = [\Delta_R^{ji}(H^0)]^*.} \tag{15.166}$$

This difference is, of course, related to the fact that in the case at hand there is a chirality flip, while there is no chirality flip in the case of Z' and any gauge boson. In turn, as we will see later, the low-energy operators governing FCNC are quite different from the ones encountered in previous sections.

The couplings $\Delta_{L,R}^{ij}(H^0)$, as defined in Figure 15.9, are dimensionless quantities, but whereas in the case of gauge bosons they are built out of gauge couplings and some charges, in the present case we are used from the SM, 2HDM, and MSSM to deal with Yukawa couplings and eventually with the ratios of quark masses and the electroweak vacuum expectation value v or other mass scales. But it should be emphasized that the proportionality of the couplings in question to the masses of the participating quarks is not a general property. It applies only if the scalar and the SM Higgs, responsible for SU(2) breakdown, are in the same SU(2) multiplet or a multiplet of a larger gauge group G. Then after the breakdown of G to SU(2), the scalar appears as a singlet of SU(2) symmetry, with couplings to quarks involving their masses after SU(2) breakdown. While this is the case in several models, in our simple extension of the SM, we will assume that the involved scalar couplings are unrelated to the generation of quark masses and the couplings $\Delta_{L,R}^{ij}(H^0)$ are simply arbitrary complex numbers to be determined from experimental data or calculated from an explicit model. This will allow us to derive general expressions for FCNC observables that can be used in specific models constructed by the readers themselves.

15.7.3 Scalar versus Pseudoscalar

We will see in the next subsections that the pattern of flavor violations caused by the spin-0 particle in question depends, even at the qualitative level, on whether it is a scalar or pseudoscalar. This distinction is often made through the study of angular distributions in collider processes, but as we will demonstrate soon also flavor-violating processes can be helpful in distinguishing between a scalar and a pseudoscalar.

Downloaded from https://www.cambridge.org/core. UNIVERSIDAD AUTONOMA METROPOLITANA, on 17 Nov 2026 at 22:50:50, subject to the Cambridge Core terms of use, available at https://www.cambridge.org/core/terms. https://doi.org/10.1017/9781139524100.021

When listing the differences between the scalar and the pseudoscalar spin-0 particles, one should emphasize that in the presence of CP violation, the mass eigenstate H^0 propagating in a tree-diagram is not necessarily a CP eigenstate. Therefore, generally the coupling to $\mu^+\mu^-$ appearing at many places in this section can have the general structure

$$\boxed{L = \frac{1}{2}\bar{\mu}(\Delta_S^{\mu\bar{\mu}}(H) + \gamma_5\Delta_P^{\mu\bar{\mu}}(H))H\mu,} \tag{15.167}$$

with analogous expressions for other leptons and quarks. We drop the charge index as in this section only neutral scalars are present. The couplings $\Delta_{S,P}^{\mu\bar{\mu}}$ are defined in analogy to (15.54) by

$$\boxed{\Delta_S^{\mu\bar{\mu}}(H) = \Delta_R^{\mu\bar{\mu}}(H) + \Delta_L^{\mu\bar{\mu}}(H), \qquad \Delta_P^{\mu\bar{\mu}}(H) = \Delta_R^{\mu\bar{\mu}}(H) - \Delta_L^{\mu\bar{\mu}}(H).} \tag{15.168}$$

$\Delta_S^{\mu\bar{\mu}}$ is real and $\Delta_P^{\mu\bar{\mu}}$ purely imaginary as required by the hermiticity of the Hamiltonian, which can be verified by means of (15.166).

We will give the expressions for various observables in terms of the couplings $\Delta_{L,R}^{ij}(H)$ and $\Delta_{S,P}^{\mu\bar{\mu}}(H)$. They can be directly used in the case of the scalar particle being CP-even eigenstate, like (H^0, h) in 2HDM or MSSM setting $\Delta_P^{\mu\bar{\mu}}(H) = 0$. However, when the mass eigenstate is a pseudoscalar A, implying $\Delta_S^{\mu\bar{\mu}} = 0$, it will be useful to exhibit the i, which we illustrate here for the B_s^0 system:

$$\boxed{\Delta_L^{bs}(A) = -i\tilde{\Delta}_L^{bs}(A), \qquad \Delta_R^{bs}(A) = +i\tilde{\Delta}_R^{bs}(A), \qquad \Delta_P^{\mu\bar{\mu}}(A) = i\tilde{\Delta}_P^{\mu\bar{\mu}}(A).} \tag{15.169}$$

Here the flavor-violating couplings $\tilde{\Delta}_{L,R}^{bs}(A)$ are still complex, while $\tilde{\Delta}_P^{\mu\bar{\mu}}(A)$ is real.

The following useful relations follow from (15.166) and (15.169):

$$\boxed{\Delta_R^{sb}(A) = i[\tilde{\Delta}_L^{bs}(A)]^*, \qquad \Delta_L^{sb}(A) = -i[\tilde{\Delta}_R^{bs}(A)]^*.} \tag{15.170}$$

Interestingly, if the couplings defined here are treated as arbitrary complex numbers to be bounded by $\Delta F = 2$ observables, and there is only one particle contributing, it will not be possible to distinguish a scalar from a pseudoscalar on the basis of $\Delta F = 2$ transitions alone. On the other hand, when rare decays, in particular $B_{s,d} \to \mu^+\mu^-$, are considered, there is a difference between these two cases as the pseudoscalar contributions interfere with SM contribution, while the scalar ones do not. Consequently, the allowed values for $\tilde{\Delta}_P^{\mu\bar{\mu}}(A)$ and $\Delta_S^{\mu\bar{\mu}}(A)$ will differ from each other, and we will find other differences. But, if both scalar and pseudoscalar contribute to tree-level decays and have approximately the same mass as well as couplings related by symmetries, also their contributions to $\Delta F = 2$ processes differ.

After these introductory remarks we will present in the next subsections formulas for contributions of scalar particles to various flavor observables as functions of the preceding couplings. On several occasions the formulas will turn out to be very similar to the ones presented for Z', but the building blocks in these formulas will be different, and we will stress it whenever this will be necessary to avoid confusion.

Downloaded from https://www.cambridge.org/core. UNIVERSIDAD AUTONOMA METROPOLITANA, on 17 Nov 2026 at 22:50:50, subject to the Cambridge Core terms of use, available at https://www.cambridge.org/core/terms. https://doi.org/10.1017/9781139524100.021

15.7.4 $\Delta F = 2$ Processes

Master Functions Including *H* Contributions

In the presence of H tree-level contributions, similar to the Z' case, we will work with three different master functions

$$S(K), \qquad S(B_d), \qquad S(B_s), \tag{15.171}$$

for $K^0 - \bar{K}^0$ and $B^0_{s,d} - \bar{B}^0_{s,d}$ systems, respectively. In introducing these functions we will include in their definitions the contributions of all operators involved.

The derivation of the formulas listed soon proceeds as in Section 15.4 and is left as an exercise for the reader.

The $\Delta F = 2$ master functions for $M = K, B_q$ are then given as follows

$$S(M) = S_0(x_t) + \Delta S(M) \equiv |S(M)|e^{i\theta_S^M}, \tag{15.172}$$

with $\Delta S(M)$ receiving contributions from various operators so that it is useful to write

$$\Delta S(M) = [\Delta S(M)]_{\rm SLL} + [\Delta S(M)]_{\rm SRR} + [\Delta S(M)]_{\rm LR}. \tag{15.173}$$

We have encountered the contributing new operators already in Section 7.3 but we recall them here for convenience. For the K system we have [746, 749]

$$Q_1^{\rm LR} = \left(\bar{s}\gamma_\mu P_L d\right)\left(\bar{s}\gamma^\mu P_R d\right), \tag{15.174a}$$
$$Q_2^{\rm LR} = \left(\bar{s}P_L d\right)\left(\bar{s}P_R d\right). \tag{15.174b}$$

$$Q_1^{\rm SLL} = \left(\bar{s}P_L d\right)\left(\bar{s}P_L d\right), \tag{15.175a}$$
$$Q_1^{\rm SRR} = \left(\bar{s}P_R d\right)\left(\bar{s}P_R d\right), \tag{15.175b}$$
$$Q_2^{\rm SLL} = \left(\bar{s}\sigma_{\mu\nu}P_L d\right)\left(\bar{s}\sigma^{\mu\nu}P_L d\right), \tag{15.175c}$$
$$Q_2^{\rm SRR} = \left(\bar{s}\sigma_{\mu\nu}P_R d\right)\left(\bar{s}\sigma^{\mu\nu}P_R d\right), \tag{15.175d}$$

where $P_{R,L} = (1 \pm \gamma_5)/2$, and we suppressed color indices as they are summed up in each factor. For instance, $\bar{s}\gamma_\mu P_L d$ stands for $\bar{s}_\alpha \gamma_\mu P_L d_\alpha$ and similarly for other factors. For $B^0_q - \bar{B}^0_q$ mixing our conventions for new operators are

$$Q_1^{\rm LR} = \left(\bar{b}\gamma_\mu P_L q\right)\left(\bar{b}\gamma^\mu P_R q\right), \tag{15.176a}$$
$$Q_2^{\rm LR} = \left(\bar{b}P_L q\right)\left(\bar{b}P_R q\right), \tag{15.176b}$$

$$Q_1^{\rm SLL} = \left(\bar{b}P_L q\right)\left(\bar{b}P_L q\right), \tag{15.177a}$$
$$Q_1^{\rm SRR} = \left(\bar{b}P_R q\right)\left(\bar{b}P_R q\right), \tag{15.177b}$$

Downloaded from https://www.cambridge.org/core. UNIVERSIDAD AUTONOMA METROPOLITANA, on 17 Nov 2026 at 22:50:50, subject to the Cambridge Core terms of use, available at https://www.cambridge.org/core/terms. https://doi.org/10.1017/9781139524100.021

$$Q_2^{\rm SLL} = \left(\bar{b}\sigma_{\mu\nu}P_L q\right)\left(\bar{b}\sigma^{\mu\nu}P_L q\right), \tag{15.177c}$$

$$Q_2^{\rm SRR} = \left(\bar{b}\sigma_{\mu\nu}P_R q\right)\left(\bar{b}\sigma^{\mu\nu}P_R q\right). \tag{15.177d}$$

To calculate the SLL, SRR, and LR contributions to $\Delta S(M)$, we use again the expressions $T(B_q)$ and $T(K)$, which we recall here for convenience

$$T(B_q) = \frac{G_F^2}{12\pi^2}F_{B_q}^2\hat{B}_{B_q}m_{B_q}M_W^2\left(\lambda_t^{(q)}\right)^2\eta_B, \tag{15.178}$$

$$T(K) = \frac{G_F^2}{12\pi^2}F_K^2\hat{B}_K m_K M_W^2\left(\lambda_t^{(K)}\right)^2\eta_2, \tag{15.179}$$

with all entries defined in Sections 8.1 and 7.3. We have then

$$T(K)[\Delta S(K)]_{\rm SLL} = -\frac{(\Delta_L^{sd}(H))^2}{2M_H^2}\left[C_1^{\rm SLL}(\mu_H)\langle Q_1^{\rm SLL}(\mu_H,K)\rangle + C_2^{\rm SLL}(\mu_H)\langle Q_2^{\rm SLL}(\mu_H,K)\rangle,\right] \tag{15.180}$$

with the SRR contribution obtained by replacing L by R. Note that this replacement only affects the coupling $\Delta_L^{sd}(H)$ as the hadronic matrix elements being evaluated in QCD remain unchanged and the Wilson coefficients have been so defined that they also remain unchanged. See (15.182) and (15.183). For LR contributions we find

$$T(K)[\Delta S(K)]_{\rm LR} = -\frac{\Delta_L^{sd}(H)\Delta_R^{sd}(H)}{M_H^2}\left[C_1^{\rm LR}(\mu_H)\langle Q_1^{\rm LR}(\mu_H,K)\rangle + C_2^{\rm LR}(\mu_H)\langle Q_2^{\rm LR}(\mu_H,K)\rangle\right]. \tag{15.181}$$

Including NLO QCD corrections [749] the Wilson coefficients of the involved operators are given by

$$C_1^{\rm SLL}(\mu) = C_1^{\rm SRR}(\mu) = 1 + \frac{\alpha_s}{4\pi}\left(-3\log\frac{M_H^2}{\mu^2} + \frac{9}{2}\right), \tag{15.182}$$

$$C_2^{\rm SLL}(\mu) = C_2^{\rm SRR}(\mu) = \frac{\alpha_s}{4\pi}\left(-\frac{1}{12}\log\frac{M_H^2}{\mu^2} + \frac{1}{8}\right), \tag{15.183}$$

$$C_1^{\rm LR}(\mu) = -\frac{3}{2}\frac{\alpha_s}{4\pi}, \tag{15.184}$$

$$C_2^{\rm LR}(\mu) = 1 - \frac{\alpha_s}{4\pi}\frac{3}{N} = 1 - \frac{\alpha_s}{4\pi}. \tag{15.185}$$

It should be noticed that, similar to Z' case, also here the operators $Q_{1,2}^{\rm LR}$ contribute. But their Wilson coefficients are totally different. In particular, while in the Z' case the operator

Downloaded from https://www.cambridge.org/core. UNIVERSIDAD AUTONOMA METROPOLITANA, on 17 Nov 2026 at 22:50:50, subject to the Cambridge Core terms of use, available at https://www.cambridge.org/core/terms. https://doi.org/10.1017/9781139524100.021

$Q_1^{\rm LR}$ was the dominant one, it is $Q_2^{\rm LR}$ in the scalar case. Yet, as we will see in the context of our presentation also the operators $Q_1^{\rm SLL}$ and $Q_1^{\rm SRR}$ will play an important role, in particular when only one of the couplings $\Delta_L^{sd}(H)$ and $\Delta_R^{sd}(H)$ is nonvanishing as then LR operators do not contribute. Next

$$\boxed{\langle Q_i^a(\mu_H,K)\rangle \equiv \frac{m_K F_K^2}{3} P_i^a(\mu_H,K)} \tag{15.186}$$

are the matrix elements of operators evaluated at the matching scale $\mu_H = O(M_H)$, and P_i^a are the coefficients introduced and evaluated in [746]. The μ_H dependence of $P_i^a(\mu_H)$ cancels the one of $\Delta_{L,R}(H)$ and of $C_i^a(\mu_H)$ so that $S(K)$ does not depend on μ_H. It should be emphasized at this point that in contrast to gauge boson couplings $\Delta_{L,R}(Z')$ and $\Delta_{L,R}(Z)$ that are scale independent as far as leading QCD corrections are concerned, the couplings $\Delta_{L,R}(H)$ are scale dependent. Therefore consistent with (15.182) and (15.183), they are defined at $\mu_H = O(M_H)$. In numerical calculations one can simply set $\mu_H = M_H$. Similarly for B_q systems we have

$$T(B_q)[\Delta S(B_q)]_{\rm SLL} = -\frac{(\Delta_L^{bq}(H))^2}{2M_H^2}\left[C_1^{\rm SLL}(\mu_H)\langle Q_1^{\rm SLL}(\mu_H,B_q)\rangle + C_2^{\rm SLL}(\mu_H)\langle Q_2^{\rm SLL}(\mu_H,B_q)\rangle\right], \tag{15.187}$$

$$T(B_q)[\Delta S(B_q)]_{\rm LR} = -\frac{\Delta_L^{bq}(H)\Delta_R^{bq}(H)}{M_H^2}\left[C_1^{\rm LR}(\mu_H)\langle Q_1^{\rm LR}(\mu_H,B_q)\rangle + C_2^{\rm LR}(\mu_H)\langle Q_2^{\rm LR}(\mu_H,B_q)\rangle\right], \tag{15.188}$$

where the Wilson coefficients $C_i^a(\mu_H)$ are as in the K system, and the matrix elements are given by

$$\boxed{\langle Q_i^a(\mu_H,B_q)\rangle \equiv \frac{m_{B_q} F_{B_q}^2}{3} P_i^a(\mu_H,B_q).} \tag{15.189}$$

For SRR contributions one proceeds as in the K system.

The values of $\langle Q_i^a(\mu_H)\rangle$ obtained using the lattice results are collected in Table 13.3. They are given in the $\overline{\rm MS}$-NDR scheme. For simplicity we choose this scale to be M_H, but any scale of this order would give the same results for the physical quantities up to NNLO QCD corrections that are negligible at these high scales. The renormalization scheme dependence of the matrix elements is canceled by the one of the Wilson coefficients.

In the case of tree-level SM Higgs exchanges, we evaluate the matrix elements at $m_t(m_t)$ as the inclusion of NLO QCD corrections allows us to choose any scale of $O(M_H)$ without changing physical results. Then in the preceding formulas one should replace M_H by the SM Higgs mass and μ_H by $m_t(m_t)$. This also means that the flavor-violating couplings of

Downloaded from https://www.cambridge.org/core. UNIVERSIDAD AUTONOMA METROPOLITANA, on 17 Nov 2026 at 22:50:50, subject to the Cambridge Core terms of use, available at https://www.cambridge.org/core/terms. https://doi.org/10.1017/9781139524100.021

SM Higgs are defined here at $m_t(m_t)$. The values of hadronic matrix elements at $m_t(m_t)$ in the $\overline{\text{MS}}$-NDR scheme are given in Table 13.1.

We do not repeat the basic formulas for $\Delta F = 2$ Observables as they are identical to the ones in Section 15.4. Only the master functions in (15.171), given in (15.173) are now different.

15.7.5 Rare B Decays

These decays, in particular $B_{s,d} \to \mu^+\mu^-$, played already for many years a significant role in bounding scalar contributions in the framework of the MSSM and 2HDM. While the precise branching ratios of these two decays will constitute an important test of the SM and CMFV models and of several other extensions, in the future time-dependent studies proposed in [507] and analyzed in detail in [504, 509] will help in distinguishing between various NP scenarios. Indeed, the correlations between $B_{s,d} \to \mu^+\mu^-$ observables to be measured in time-dependent studies with the CP-asymmetries $S_{\psi\phi}$ and $S_{\psi K_S}$ will be helpful in this respect. General formulas for such time-dependent studies can be found in Section 9.2 and in the original papers.

Effective Hamiltonian for $b \to s\ell^+\ell^-$

To describe the decays $B_{d,s} \to \mu^+\mu^-$, $B \to K^*\ell^+\ell^-$, $B \to K\ell^+\ell^-$, and $B \to X_s\ell^+\ell^-$ and the related observables in scalar NP scenarios we begin with recalling the effective Hamiltonian that we already encountered in Section 9.1. We do it not only for convenience but also to assure the reader about the normalization of Wilson coefficients.

$$\mathcal{H}_{\text{eff}}(b \to s\ell\bar{\ell}) = \mathcal{H}_{\text{eff}}(b \to s\gamma) - \frac{4G_{\text{F}}}{\sqrt{2}}\frac{\alpha}{4\pi}V_{ts}^*V_{tb}\sum_{i=9,10,S,P}[C_i(\mu)Q_i(\mu) + C_i'(\mu)Q_i'(\mu)], \tag{15.190}$$

where

$$Q_9 = (\bar{s}\gamma_\mu P_L b)(\bar{\ell}\gamma^\mu \ell), \qquad Q_9' = (\bar{s}\gamma_\mu P_R b)(\bar{\ell}\gamma^\mu \ell), \tag{15.191a}$$

$$Q_{10} = (\bar{s}\gamma_\mu P_L b)(\bar{\ell}\gamma^\mu\gamma_5 \ell), \qquad Q_{10}' = (\bar{s}\gamma_\mu P_R b)(\bar{\ell}\gamma^\mu\gamma_5 \ell), \tag{15.191b}$$

$$Q_S = m_b(\bar{s}P_R b)(\bar{\ell}\ell), \qquad Q_S' = m_b(\bar{s}P_L b)(\bar{\ell}\ell), \tag{15.191c}$$

$$Q_P = m_b(\bar{s}P_R b)(\bar{\ell}\gamma_5 \ell), \qquad Q_P' = m_b(\bar{s}P_L b)(\bar{\ell}\gamma_5 \ell). \tag{15.191d}$$

Including the factors of m_b into the definition of scalar operators makes their matrix elements and their Wilson coefficients scale independent. $\mathcal{H}_{\text{eff}}(b \to s\gamma)$ stands for the effective Hamiltonian for the $b \to s\gamma$ transition that involves the dipole operators. As already mentioned in Section 15.4, Z' contributions to $b \to s\gamma$ can be neglected. We will

Downloaded from https://www.cambridge.org/core. UNIVERSIDAD AUTONOMA METROPOLITANA, on 17 Nov 2026 at 22:50:50, subject to the Cambridge Core terms of use, available at https://www.cambridge.org/core/terms. https://doi.org/10.1017/9781139524100.021

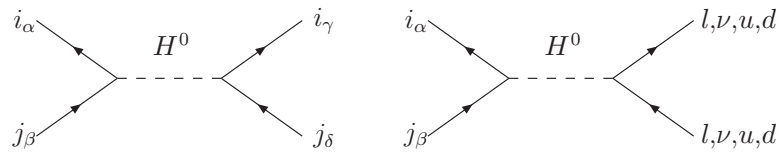


Figure 15.10 Tree-level H^0 contribution to $\Delta F = 2$ (left) and $\Delta F = 1$ (right) processes. Labels are explained in Figure 15.9.

comment on scalar contributions to this decay later, but for the time being we assume that they can be neglected as well.

It is important to notice the difference of ordering of flavors relatively to $\Delta F = 2$, which in view of the relation (15.166) implies the difference in the projections $P_{L,R}$ entering the operators $Q_{9,10}$ and $Q_{S,P}$. Therefore, the unprimed operators Q_S and Q_P represent the LHS scenario and the primed ones Q'_S and Q'_P the RHS scenario. We neglect effects proportional to m_s in each case but keep m_s and m_d different from zero when they are shown explicitly.

The Wilson coefficients C_9 and C_{10} do not receive any new contributions from scalar exchanges and take SM values as given in Section 9.1. A straightforward calculation of tree-level scalar exchanges in Figure 15.10 gives

$$m_b(\mu_H)\sin^2\theta_W C_S = \frac{1}{g^2_{\rm SM}}\frac{1}{M_H^2}\frac{\Delta_R^{sb}(H)\Delta_S^{\mu\bar{\mu}}(H)}{V_{ts}^*V_{tb}}, \tag{15.192}$$

$$m_b(\mu_H)\sin^2\theta_W C'_S = \frac{1}{g^2_{\rm SM}}\frac{1}{M_H^2}\frac{\Delta_L^{sb}(H)\Delta_S^{\mu\bar{\mu}}(H)}{V_{ts}^*V_{tb}}, \tag{15.193}$$

$$m_b(\mu_H)\sin^2\theta_W C_P = \frac{1}{g^2_{\rm SM}}\frac{1}{M_H^2}\frac{\Delta_R^{sb}(H)\Delta_P^{\mu\bar{\mu}}(H)}{V_{ts}^*V_{tb}}, \tag{15.194}$$

$$m_b(\mu_H)\sin^2\theta_W C'_P = \frac{1}{g^2_{\rm SM}}\frac{1}{M_H^2}\frac{\Delta_L^{sb}(H)\Delta_P^{\mu\bar{\mu}}(H)}{V_{ts}^*V_{tb}}, \tag{15.195}$$

where $\Delta^{\mu\bar{\mu}}_{S,P}(H)$ are defined in (15.168). It should be emphasized at this point that the couplings $\Delta^{sb}_{L,R}(H)$ extracted from ΔM_s and $S_{\psi\phi}$ are defined at $\mu_H = M_H$, therefore, as shown explicitly, m_b has to be evaluated also at this scale to keep these coefficients scale independent. In the case of the SM Higgs m_b has to be evaluated at $m_t(m_t)$ as at this scale the flavor-violating SM Higgs couplings in $\Delta F = 2$ processes are defined. In what follows we will not show this dependence explicitly. The values of m_b at different scales are collected in Table 4.2.

Next we recall that in terms of the couplings used in the analysis of $B^0_{s,d} - \bar{B}^0_{s,d}$ mixings we have according to (15.166)

$$\Delta_R^{sb}(H) = [\Delta_L^{bs}(H)]^*, \qquad \Delta_L^{sb}(H) = [\Delta_R^{bs}(H)]^*, \tag{15.196}$$

which should be kept in mind when studying correlations between $\Delta F = 1$ and $\Delta F = 2$ transitions. These relations can be directly used in the case of C_S and C'_S but in the case of

Downloaded from https://www.cambridge.org/core. UNIVERSIDAD AUTONOMA METROPOLITANA, on 17 Nov 2026 at 22:50:50, subject to the Cambridge Core terms of use, available at https://www.cambridge.org/core/terms. https://doi.org/10.1017/9781139524100.021

C_P and C'_P, as discussed in Section 15.7.3, it is useful to use in this context the following relations:

$$\Delta_R^{sb}\Delta_P^{\mu\bar{\mu}} = -[\tilde{\Delta}_L^{bs}]^*\tilde{\Delta}_P^{\mu\bar{\mu}}, \qquad \Delta_L^{sb}\Delta_P^{\mu\bar{\mu}} = [\tilde{\Delta}_R^{bs}]^*\tilde{\Delta}_P^{\mu\bar{\mu}}, \tag{15.197}$$

with $\Delta_P^{\mu\bar{\mu}}$ being imaginary but $\tilde{\Delta}_P^{\mu\bar{\mu}}$ real.

15.7.6 Rare *K* Decays

Effective Hamiltonian for $d \to s\ell^+\ell^-$

For the study of $K_{L,S} \to \mu^+\mu^-$ and $K_L \to \pi^0\ell\ell^-$ decays we will need the relevant effective Hamiltonian. It can be obtained from the formulas of subsection 15.4.4. For completeness we list here explicit formulas for operators and Wilson coefficients:

$$Q_9 = (\bar{s}\gamma_\mu P_L d)(\bar{\ell}\gamma^\mu \ell), \qquad Q'_9 = (\bar{s}\gamma_\mu P_R d)(\bar{\ell}\gamma^\mu \ell), \tag{15.198a}$$

$$Q_{10} = (\bar{s}\gamma_\mu P_L d)(\bar{\ell}\gamma^\mu\gamma_5 \ell), \qquad Q'_{10} = (\bar{s}\gamma_\mu P_R d)(\bar{\ell}\gamma^\mu\gamma_5 \ell), \tag{15.198b}$$

$$Q_S = m_s(\bar{s}P_L d)(\bar{\ell}\ell), \qquad Q'_S = m_s(\bar{s}P_R d)(\bar{\ell}\ell), \tag{15.198c}$$

$$Q_P = m_s(\bar{s}P_L d)(\bar{\ell}\gamma_5 \ell), \qquad Q'_P = m_s(\bar{s}P_R d)(\bar{\ell}\gamma_5 \ell). \tag{15.198d}$$

Note that because of the sd ordering instead of qb, scalar operators have L and R interchanged with respect to $b \to s, d$ transitions.

The Wilson coefficients C_9 and C_{10} do not receive any new contributions from scalar exchange and take SM values as given in (6.334). However, to include charm component in $K_L \to \mu^+\mu^-$ we make replacement:

$$\eta_Y Y_0(x_t) \longrightarrow \eta_Y Y_0(x_t) + \frac{V_{cs}^* V_{cd}}{V_{ts}^* V_{td}} Y_{\rm NNL}, \tag{15.199}$$

where at NNLO [625]

$$Y_{\rm NNL} = \lambda^4 P_c(Y), \qquad P_c(Y) = 0.115 \pm 0.017\,. \tag{15.200}$$

The coefficients of scalar operators are

$$m_s \sin^2\vartheta_W C_S = \frac{1}{g_{\rm SM}^2}\frac{1}{M_H^2}\frac{\Delta_L^{sd}(H)\Delta_S^{\mu\bar{\mu}}(H)}{V_{ts}^* V_{td}}, \tag{15.201}$$

$$m_s \sin^2\vartheta_W C'_S = \frac{1}{g_{\rm SM}^2}\frac{1}{M_H^2}\frac{\Delta_R^{sd}(H)\Delta_S^{\mu\bar{\mu}}(H)}{V_{ts}^* V_{td}}, \tag{15.202}$$

$$m_s \sin^2\vartheta_W C_P = \frac{1}{g_{\rm SM}^2}\frac{1}{M_H^2}\frac{\Delta_L^{sd}(H)\Delta_P^{\mu\bar{\mu}}(H)}{V_{ts}^* V_{td}}, \tag{15.203}$$

$$m_s \sin^2\vartheta_W C'_P = \frac{1}{g_{\rm SM}^2}\frac{1}{M_H^2}\frac{\Delta_R^{sd}(H)\Delta_P^{\mu\bar{\mu}}(H)}{V_{ts}^* V_{td}}. \tag{15.204}$$

Downloaded from https://www.cambridge.org/core. UNIVERSIDAD AUTONOMA METROPOLITANA, on 17 Nov 2026 at 22:50:50, subject to the Cambridge Core terms of use, available at https://www.cambridge.org/core/terms. https://doi.org/10.1017/9781139524100.021

$K_L \to \mu^+\mu^-$ and $K_S \to \mu^+\mu^-$

We know from previous material that only the so-called short-distance (SD) part to a dispersive contribution to $K_L \to \mu^+\mu^-$ can be reliably calculated. Therefore, in what follows, as in other NP scenarios, this decay can be presently only treated as an additional constraint with the rough upper bound given in (9.268).

The relevant branching ratio can be obtained by first introducing:

$$\hat{P}(K) \equiv C_{10} - C'_{10} + \frac{m_K^2}{2m_\mu}\frac{m_s}{m_d + m_s}(C_P - C'_P) \tag{15.205}$$

and

$$\hat{S}(K) \equiv \sqrt{1 - \frac{4m_\mu^2}{m_K^2}}\frac{m_K^2}{2m_\mu}\frac{m_s}{m_d + m_s}(C_S - C'_S). \tag{15.206}$$

We then find [504]

$$\begin{aligned}\mathcal{B}(K_L \to \mu^+\mu^-)_{\rm SD} = &\frac{G_F^4 M_W^4}{4\pi^5} F_K^2 m_K \tau_{K_L} m_\mu^2 \sqrt{1 - \frac{4m_\mu^2}{m_K^2}} \sin^4\vartheta_W \\ &\times \left\{\left[\mathrm{Re}\left(V_{ts}^* V_{td}\hat{P}\right)\right]^2 + \left[\mathrm{Im}\left(V_{ts}^* V_{td}\hat{S}\right)\right]^2\right\}.\end{aligned} \tag{15.207}$$

We recall that C_{10} does not receive any contribution from scalar exchanges and includes also SM charm contribution as given in (15.199). $C'_{10} = 0$ for scalar exchanges.

Equivalently we can write

$$\mathcal{B}(K_L \to \mu^+\mu^-)_{\rm SD} = \kappa_\mu \left\{\left[\mathrm{Re}\left(V_{ts}^* V_{td}\hat{P}\right)\right]^2 + \left[\mathrm{Im}\left(V_{ts}^* V_{td}\hat{S}\right)\right]^2\right\}, \tag{15.208}$$

where

$$\kappa_\mu = \frac{\alpha^2 \mathcal{B}(K^+ \to \mu^+\nu)}{\lambda^2\pi^2}\frac{\tau(K_L)}{\tau(K^+)}. \tag{15.209}$$

Finally, for $K_S \to \mu^+\mu^-$ decay, we just interchange Re and Im in all preceding expressions so that

$$\mathcal{B}(K_S \to \mu^+\mu^-)_{\rm SD} = \kappa_\mu \left\{\left[\mathrm{Im}\left(V_{ts}^* V_{td}\hat{P}\right)\right]^2 + \left[\mathrm{Re}\left(V_{ts}^* V_{td}\hat{S}\right)\right]^2\right\}. \tag{15.210}$$

$K_L \to \pi^0\ell^+\ell^-$

While in the case of Z' models large enhancements of branching ratios were not possible due to constraints from data on $K^+ \to \pi^+\nu\bar{\nu}$ [611], this constraint is absent in the case of scalar contributions, and it is of interest to see by how much the branching ratios can be

Downloaded from https://www.cambridge.org/core. UNIVERSIDAD AUTONOMA METROPOLITANA, on 17 Nov 2026 at 22:50:50, subject to the Cambridge Core terms of use, available at https://www.cambridge.org/core/terms. https://doi.org/10.1017/9781139524100.021

enhanced in the models considered here still being consistent with all data, in particular with the bound on $K_L \to \mu^+\mu^-$ in (9.268).

Probably the most extensive model independent analysis of decays in question has been performed in [637], where formulas for branching ratios for both decays in the presence of new operators have been presented. We have already elaborated on these formulas in the case of Z' exchanges in Section 15.4.5. The case of scalar contributions is more involved.

To use the formulas of [637] for scalar contributions, we introduce the following quantities [504]:

$$\omega_{7A} = -\frac{1}{2\pi}\frac{\eta_Y Y_0(x_t)}{\sin^2\vartheta_W}\frac{\mathrm{Im}(\lambda_t^{(K)})}{1.4\cdot 10^{-4}}, \tag{15.211}$$

$$\bar{y}_P = \frac{y_P + y_P'}{2}, \qquad \bar{y}_S = \frac{y_S + y_S'}{2}, \tag{15.212}$$

with y_i related to the Wilson coefficients $C_{P,S}$ as follows:

$$y_P = -\frac{M_W^2 \sin^2\vartheta_W}{m_l} V_{ts}^* V_{td} C_P, \qquad y_S = -\frac{M_W^2 \sin^2\vartheta_W}{m_l} V_{ts}^* V_{td} C_S, \tag{15.213}$$

with analogous formulas for primed coefficients. Here m_l stands for m_e and m_μ as the authors of [637] anticipating helicity suppression included these masses already in the effective Hamiltonian.

Using [637] the authors of [504] find then corrections from tree-level A^0 and H^0 exchanges to the branching ratios that should be added directly to SM results in (9.282) and (9.283):

$$\Delta\mathcal{B}_P^{e^+e^-} = \left(1.9\ \omega_{7A}\mathrm{Im}(\bar{y}_P) + 0.038\ (\mathrm{Im}(\bar{y}_P))^2\right)\cdot 10^{-17}, \tag{15.214}$$

$$\Delta\mathcal{B}_P^{\mu^+\mu^-} = \left(0.26\ \omega_{7A}\mathrm{Im}(\bar{y}_P) + 0.0085\ (\mathrm{Im}(\bar{y}_P))^2\right)\cdot 10^{-12}, \tag{15.215}$$

$$\Delta\mathcal{B}_S^{e^+e^-} = \left(1.5\ \mathrm{Re}(\bar{y}_S) + 0.0039\ (\mathrm{Re}(\bar{y}_S))^2\right)\cdot 10^{-16}, \tag{15.216}$$

$$\Delta\mathcal{B}_S^{\mu^+\mu^-} = \left(0.04\ \mathrm{Re}(\bar{y}_S) + 0.0041\ (\mathrm{Re}(\bar{y}_S))^2\right)\cdot 10^{-12}. \tag{15.217}$$

Note that in the absence of helicity suppression, the large suppression factors are canceled by the conversion factors in (15.213). The numerical results for these new contributions can be found in [504].

15.7.7 ε'/ε

To get an idea of the impact of tree-level neutral scalar exchange on ε'/ε, it is useful to return to the master formula for ε'/ε in Section 14.7. The effective Hamiltonian for $K \to \pi\pi$ obtained from tree-level neutral scalar exchange in Figure 15.10 reads

$$\mathcal{H}_{\mathrm{eff}} = -\frac{1}{M_H^2}\sum_i \sum_{A,B=L,R} \Delta_A^{sd}(H)\Delta_B^{ii}(H)(\bar{s}P_A d)(\bar{q}_i P_B q_i), \tag{15.218}$$

with $i = d, s, b, u, c$.

Downloaded from https://www.cambridge.org/core. UNIVERSIDAD AUTONOMA METROPOLITANA, on 17 Nov 2026 at 22:50:50, subject to the Cambridge Core terms of use, available at https://www.cambridge.org/core/terms. https://doi.org/10.1017/9781139524100.021

The contributing scalar-scalar operators can be compactly denoted by

$$O^q_{SAB} = (\bar{s}P_A d)(\bar{q}P_B q), \qquad q = d, s, b, u, c \tag{15.219}$$

and, with the definition (14.83), their coefficients and P_i factors in (14.84) are given by

$$C^q_{SAB} = \frac{1}{M_H^2}\Delta_A^{sd}(H)\Delta_B^{qq}(H), \qquad P^q_{SLR} = -P^q_{SRL}, \qquad P^q_{SLL} = -P^q_{SRR}. \tag{15.220}$$

It should be noted that generally C^q_{SLL} and C^q_{SRR} differ from each other, and this is also the case of C^q_{SLR} and C^q_{SRL} .

From the tables in the appendix of [798] one finds then the largest values of P^q_{SAB}. These are

$$\boxed{P^u_{SLR} = -266 \pm 20, \quad P^d_{SLR} = 214 \pm 18, \quad P^d_{SLL} = -87 \pm 16, \quad P^u_{SLL} = 74 \pm 16.} \tag{15.221}$$

All other P_i factors are below 1, and the corresponding contributions can be neglected, unless there is a strong enhancement of the corresponding Wilson coefficients.

In the latter context, it should be emphasized, that these results, as they stand, cannot be used for phenomenology because the P_i factors, representing hadronic matrix elements, have been calculated at the electroweak scale, while the Wilson coefficients are evaluated at a much higher scale $O(M_H)$. To complete the analysis the gap between these two scales has to be closed by including RG effects between these scales in the framework of the SMEFT. Here contributions from top Yukawa couplings could turn out to be important. Such an analysis should be available in the literature when this book is published.

15.8 Beyond MFV: Charged Scalar Exchanges

We have already mentioned charged scalars at various places in this book. They naturally are present in 2HDM and in supersymmetric models, which we decided not to discuss in detail in this book as there is a very rich literature on them. In particular I recommend strongly the general review in [897] and the review of flavor-phenomenology of 2HDM models with generic Yukawa structure in [995].

Even before $R(D)$ and $R(D^*)$ anomalies became popular, the role of charged Higgs bosons in $B^+ \to D^0\tau^+\nu$ decays has been studied. A thorough analysis of this decay is presented in [996], where further references to older papers can be found. However, the $R(D)$ and $R(D^*)$ anomalies gave motivation for several newer theoretical analyses of which we just quote four. First, the study of these decays in 2HDM of type III [995, 997] and in NP models with general flavor structure in [775]. Moreover, in [998] 2HDM and 3HDM models with the nonminimal flavor violations originating from flavor-dependent gauge interactions have been analyzed. A recent summary of the situation can be found in

Downloaded from https://www.cambridge.org/core. UNIVERSIDAD AUTONOMA METROPOLITANA, on 17 Nov 2026 at 22:50:50, subject to the Cambridge Core terms of use, available at https://www.cambridge.org/core/terms. https://doi.org/10.1017/9781139524100.021

[999]. In particular 2HDM of type II cannot simultaneously describe the data on $\mathcal{R}(D)$ and $\mathcal{R}(D^*)$, but this is possible in 2HDM of type III.

It is evident that $B^+ \to \tau^+\nu_\tau$, $\bar{B} \to D\tau\nu$, and $\bar{B} \to D^*\tau\nu$ can play a potential role in constraining the charged scalar contributions. Yet, due to the fact that the data in the case of $B^+ \to \tau^+\nu_\tau$ moved significantly toward the SM and because of large uncertainty in $|V_{ub}|$, the identification of a concrete NP in this decay appears to us presently as a big challenge. The decays $B \to D\tau\nu$ and $B \to D^*\tau\nu$ seem to be more promising, and new insight in their role in charged scalar physics will be gained in the Belle II era.

15.9 Beyond MFV: Colored Gauge Bosons and Scalars

15.9.1 Colored Neutral Gauge Bosons G'

In various NP scenarios neutral gauge bosons with color (G') are present. One of the prominent examples of this type are Kaluza–Klein gluons in Randal–Sundrum scenarios that belong to the adjoint representation of the color $\mathrm{SU}(3)_C$. In what follows we will assume that these gauge bosons carry a common mass $M_{G'}$ and being in the octet representation of $\mathrm{SU}(3)_C$ couple to fermions in the same manner as gluons do. However, we will allow for different values of their left-handed and right-handed couplings. Therefore, up to the color matrix t^a, the couplings to quarks will be again parametrized by:

$$\boxed{\Delta_L^{sd}(G'), \qquad \Delta_R^{sd}(G'), \qquad \Delta_L^{qq}(G'), \qquad \Delta_R^{qq}(G').} \tag{15.222}$$

General couplings are defined in the Feynman rules in Figure 15.11. Calculating then the tree-diagrams with G' gauge boson exchanges and expressing the result in terms of the operators encountered in previous sections, we find that the initial conditions at $\mu = M_{G'}$ are modified. As G' do not couple to leptons, they can only influence $\Delta F = 2$ and non-leptonic decays. Therefore, we collect here only the initial conditions for these two classes of processes.

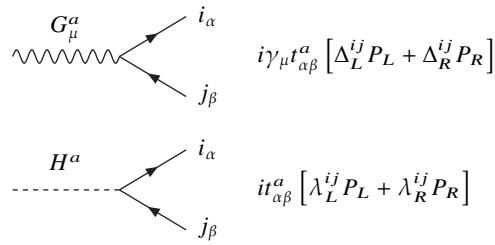


Figure 15.11 Feynman rules for the colored neutral gauge boson G_μ with mass M_G and colored neutral scalar particle H with mass M_H, where i, j denote down-type quarks.

Downloaded from https://www.cambridge.org/core. UNIVERSIDAD AUTONOMA METROPOLITANA, on 17 Nov 2026 at 22:50:50, subject to the Cambridge Core terms of use, available at https://www.cambridge.org/core/terms. https://doi.org/10.1017/9781139524100.021

$\Delta F = 2$ Transitions

The initial conditions for $\Delta F = 2$ transition change relative to Z' case. In LO they are given as follows [1007]

$$C_1^{\rm VLL}(M_{G'}) = \left[\frac{1}{3}\right]\frac{\Delta_L^{sd}(G')^2}{2M_{G'}^2}, \qquad C_1^{\rm VRR}(M_{G'}) = \left[\frac{1}{3}\right]\frac{\Delta_R^{sd}(G')^2}{2M_{G'}^2}, \tag{15.223}$$

$$C_1^{\rm LR}(M_{G'}) = \left[-\frac{1}{6}\right]\frac{\Delta_L^{sd}(G')\Delta_R^{sd}(G')}{M_{G'}^2}, \qquad C_2^{\rm LR}(M_{G'}) = [-1]\frac{\Delta_L^{sd}(G')\Delta_R^{sd}(G')}{M_{G'}^2}. \tag{15.224}$$

In particular we note that the coefficient $C_2^{\rm LR}(M_{G'})$ is now the largest as opposed to Z' case, where it was vanishing. As the matrix element of $Q_2^{\rm LR}$ is large, Kaluza–Klein gluons were problematic ten years ago in the context of RS scenarios. Deriving the preceding conditions is a good exercise. One will then notice that these coefficients are not normalized to unity and are not dimensionless. They are just coefficients of the operators in the relevant effective Hamiltonian.

The NLO QCD corrections to tree-level colored gauge boson exchanges at $\mu = M_{G'}$ to $\Delta S = 2$ are not known. They are expected to be small due to small QCD coupling at this high scale and serve mainly to remove certain renormalization scheme and matching scale uncertainties. More important is the RG evolution from low-energy scales to $\mu = M_{G'}$ necessary to evaluate $\langle Q_1^{\rm VLL}(M_{G'})\rangle$ and $\langle Q_{1,2}^{\rm LR}(M_{G'})\rangle$. Here NLO QCD corrections can be included using the technology in [746].

$K \to \pi\pi$ Decays

The new initial conditions for the operators entering $K \to \pi\pi$ read now at LO as follows [271]

$$C_3(M_{G'}) = \left[-\frac{1}{6}\right]\frac{\Delta_L^{sd}(G')\Delta_L^{qq}(G')}{4M_{G'}^2}, \qquad C_3'(M_{G'}) = \left[-\frac{1}{6}\right]\frac{\Delta_R^{sd}(G')\Delta_R^{qq}(G')}{4M_{G'}^2}, \tag{15.225}$$

$$C_4(M_{G'}) = \left[\frac{1}{2}\right]\frac{\Delta_L^{sd}(G')\Delta_L^{qq}(G')}{4M_{G'}^2}, \qquad C_4'(M_{G'}) = \left[\frac{1}{2}\right]\frac{\Delta_R^{sd}(G')\Delta_R^{qq}(G')}{4M_{G'}^2}, \tag{15.226}$$

$$C_5(M_{G'}) = \left[-\frac{1}{6}\right]\frac{\Delta_L^{sd}(G')\Delta_R^{qq}(G')}{4M_{G'}^2}, \qquad C_5'(M_{G'}) = \left[-\frac{1}{6}\right]\frac{\Delta_R^{sd}(G')\Delta_L^{qq}(G')}{4M_{G'}^2}, \tag{15.227}$$

$$C_6(M_{G'}) = \left[\frac{1}{2}\right]\frac{\Delta_L^{sd}(G')\Delta_R^{qq}(G')}{4M_{G'}^2}, \qquad C_6'(M_{G'}) = \left[\frac{1}{2}\right]\frac{\Delta_R^{sd}(G')\Delta_L^{qq}(G')}{4M_{G'}^2}. \tag{15.228}$$

Due the nonvanishing value of $C_6(M_{G'})$ the dominance of the operator Q_6 is more pronounced than in the case of a colorless Z'.

Phenomenology of ε_K, ε'/ε, ΔM_K, and $\Delta I = 1/2$ rule in this scenario can be found in [271].

Downloaded from https://www.cambridge.org/core. UNIVERSIDAD AUTONOMA METROPOLITANA, on 17 Nov 2026 at 22:50:50, subject to the Cambridge Core terms of use, available at https://www.cambridge.org/core/terms. https://doi.org/10.1017/9781139524100.021

15.9.2 Colored Neutral Scalars (H^c)

$\Delta F = 2$ Transitions

Denoting the couplings to quarks by $\lambda^{ij}_{L,R}$, we find for $\Delta F = 2$ transitions

$$C_1^{\rm SLL}(M_{H^c}) = \left[\frac{5}{12}\right]\frac{\lambda_L^{sd}(H^c)^2}{2M_{H^c}^2}, \qquad C_2^{\rm SLL}(M_{H^c}) = \left[-\frac{1}{16}\right]\frac{\lambda_L^{sd}(H^c)^2}{2M_{H^c}^2}, \quad (15.229)$$

$$C_1^{\rm SRR}(M_{H^c}) = \left[\frac{5}{12}\right]\frac{\lambda_R^{sd}(H^c)^2}{2M_{H^c}^2}, \qquad C_2^{\rm SRR}(M_{H^c}) = \left[-\frac{1}{16}\right]\frac{\lambda_R^{sd}(H^c)^2}{2M_{H^c}^2}, \quad (15.230)$$

$$C_1^{\rm LR}(M_{H^c}) = \left[\frac{1}{4}\right]\frac{\lambda_L^{sd}(H^c)\lambda_R^{sd}(H^c)}{M_{H^c}^2}, \qquad C_2^{\rm LR}(M_{H^c}) = \left[\frac{1}{6}\right]\frac{\lambda_L^{sd}(H^c)\lambda_R^{sd}(H^c)}{M_{H^c}^2}. \quad (15.231)$$

In fact, these results have been obtained in collaboration with Jennifer Girrbach-Noe.

ε'/ε

Here we proceed as in the case of the colorless neutral scalar but including appropriate color factors. The effective Hamiltonian for $K \to \pi\pi$ obtained from tree-level neutral scalar exchange in Figure 15.11 reads

$$\mathcal{H}_{\rm eff} = -\frac{1}{M_H^2}\sum_i \sum_{A,B=L,R} \lambda_A^{sd}(H)\lambda_B^{ii}(H)(\bar{s}_\alpha P_A t^a_{\alpha\beta} d_\beta)((\bar{q}_i)_\gamma P_B t^a_{\gamma\delta}(q_i)_\delta), \quad (15.232)$$

with $i = d, s, b, u, c$ and $\alpha, \beta, \gamma, \delta$ being color indices.

The contributing scalar-scalar operators can be compactly denoted by

$$[O^q_{SAB}]^c = (\bar{s}_\alpha P_A t^a_{\alpha\beta} d_\beta)(\bar{q}_\gamma P_B t^a_{\gamma\delta} q_\delta), \qquad q = d, s, b, u, c \quad (15.233)$$

and their coefficients and P_i factors in (14.84) by

$$[C^q_{SAB}]^c = \frac{1}{M_{H^c}^2}\lambda_A^{sd}(H^c)\lambda_B^{qq}(H^c), \qquad [P^q_{SLR}]^c = -[P^q_{SRL}]^c, \qquad [P^q_{SLL}]^c = -[P^q_{SRR}]^c, \quad (15.234)$$

with the superscript "c" denoting the special color structure. Again it should be noted that generally $[C^q_{SLL}]^c$ and $[C^q_{SRR}]^c$ differ from each other and this is also the case of $[C^q_{SLR}]^c$ and $[C^q_{SRL}]^c$.

To use (14.84) and calculate colored Higgs contribution to ε'/ε we need the factors $[P^q_{SAB}]^c$. But the operators in (15.233) do not belong to the operator basis used in [798], and these factors cannot be found in the tables of that paper.

To find $[P^q_{SAB}]^c$ we have to express the operators in (15.233) in terms of the ones used in [798]. To this end we use the relation (5.145):

$$\mathbf{\Pi} = \frac{1}{2}\left[\tilde{\mathbf{1}} - \frac{1}{N}\mathbf{1}\right], \quad (15.235)$$

Downloaded from https://www.cambridge.org/core. UNIVERSIDAD AUTONOMA METROPOLITANA, on 17 Nov 2026 at 22:50:50, subject to the Cambridge Core terms of use, available at https://www.cambridge.org/core/terms. https://doi.org/10.1017/9781139524100.021

where

$$\mathbf{\Pi}_{\alpha\beta,\gamma\delta} = (t^a)_{\alpha\beta} \otimes (t^a)_{\gamma\delta}, \quad \tilde{\mathbf{1}}_{\alpha\beta,\gamma\delta} = \delta_{\alpha\delta} \otimes \delta_{\gamma\beta}, \quad \mathbf{1}_{\alpha\beta,\gamma\delta} = \delta_{\alpha\beta} \otimes \delta_{\gamma\delta}. \tag{15.236}$$

This allows one to write

$$\boxed{[P^q_{SAB}]^c = \frac{1}{2}\left[\tilde{P}^q_{SAB} - \frac{1}{N} P^q_{SAB}\right], \qquad q = u, c, b,} \tag{15.237}$$

and using tables in [798], to calculate $[P^q_{SAB}]^c$ for $q = u, c, b$. But for $q = d, s$ we have to use in addition the following relations obtained by means of Fierz transformations

$$\widetilde{O}^{d,s}_{SLR} = -\frac{1}{2} O^{d,s}_{VRL}, \qquad \widetilde{O}^{d,s}_{SLL} = -\frac{1}{2} O^{d,s}_{SLL} - \frac{1}{8} O^{d,s}_{TLL} \tag{15.238}$$

and likewise for their chirality-flipped counterparts. $\tilde{P}^q_{SAB}$ for $q = d, s$ can now be expressed it terms of those found in the tables of [798],

$$\tilde{P}^{d,s}_{SLR} = -\frac{1}{2} P^{d,s}_{VRL}, \qquad \tilde{P}^{d,s}_{SLL} = -\frac{1}{2} P^{d,s}_{SLL} - \frac{1}{8} P^{d,s}_{TLL}. \tag{15.239}$$

We find finally for $N = 3$

$$\boxed{[P^{d,s}_{SLR}]^c = -\frac{1}{4} P^{d,s}_{VRL} - \frac{1}{6} P^{d,s}_{SLR}, \qquad [P^{d,s}_{SLL}]^c = -\frac{5}{12} P^{d,s}_{SLL} - \frac{1}{16} P^{d,s}_{TLL}.} \tag{15.240}$$

Having all these expressions at hand and using the tables in the appendix of [798], we find then the largest values of $[P^q_{SAB}]^c$. These are[8]

$$\boxed{[P^u_{SLR}]^c = 14 \pm 4, \qquad [P^d_{SLR}]^c = -5 \pm 4 \qquad [P^d_{SLL}]^c = 24 \pm 7, \qquad [P^u_{SLL}]^c = -20 \pm 3} \tag{15.241}$$

All other P_i factors are far below 1, and the corresponding contributions can be neglected, unless there is a strong enhancement of the corresponding Wilson coefficients. Comparing these P_i factors with the ones for a colorless scalar in (15.221), we observe that they are much lower. But the fate of these contributions depends also on the size of the couplings, and without an analysis in a concrete model it is not possible to decide whether colorless scalars or colored one will be more relevant for ε'/ε. Yet, for colored scalars to be able to compete with the colorless ones, their couplings must be sufficiently larger or their masses smaller. This could in principle be forbidden by the bounds on other processes.

Finally, as in the case of colorless scalars, RG effects between scales $O(M_{H^c})$ and the electroweak scale have to be taken into account in the framework of the SMEFT. Such analysis should be available in the literature when this book is published.

[8] The large errors result from cancellations between the two terms in (15.240).

Downloaded from https://www.cambridge.org/core. UNIVERSIDAD AUTONOMA METROPOLITANA, on 17 Nov 2026 at 22:50:50, subject to the Cambridge Core terms of use, available at https://www.cambridge.org/core/terms. https://doi.org/10.1017/9781139524100.021